MECHANISMS OF ASPHALT MIXTURE RUTTING FAILURE IN THE HAMBURG WHEEL TRACKING TEST AND THE POTENTIAL FOR REPLACING THE FLOW NUMBER TEST

BY

PREEDA CHATURABONG

A dissertation submitted in partial fulfillment of

the requirements for the degree of

Doctor of Philosophy

(Civil & Environmental Engineering)

UNIVERSITY OF WISCONSIN-MADISON

2016

Date of Final Oral Examination: 07/27/2016

The dissertation is approved by the following members of the Final Oral Committee:
Hussain U. Bahia, Professor, Civil and Environmental Engineering
William Likos, Professor, Civil and Environmental Engineering
James M Tinjum, Associate Professor, Civil and Environmental Engineering
Brock Hedegaard, Assistant Professor, Civil and Environmental Engineering
Robert E Rowlands, Professor, Mechanical Engineering

ACKNOWLEDGEMENTS

I would like to express my sincere gratitude to my advisor Prof. Hussain Bahia for supporting of my Ph.D. study, for his patience, motivation, and knowledge. His guidance helped me in all the time of research and writing of this thesis.

Besides, I would like to thank my thesis committees: Prof. William Likos, Prof. James Tinjum, Prof. Brock Hedegaard, and Prof. Robert Rowlands for their intuitive comments and encouragement.

I also thank Dr. Pouya Teymourpour and Mr. Dan Swiertz who commented and revised my thesis document, Dr. Andrew Hanz who motivated me to achieve the beginning of my goal since I have joined in this group, and provided me the mix designs and raw material for this project. Without their valuable support it would not be possible to conduct this research.

I would like to thank my MARC fellows for the stimulating discussions, for the projects we worked on together before deadlines, and for all the fun we have had in the last four years. Also, I thank my Thai friends in Wisconsin and Thailand to support my ideal. In particular, I am grateful to Dr. Kunnawee Kanitpong for enlightening me the first glance of research.

Last but not the least, I would like to thank my family: my parents and Utchariya Mongkoladisai and my sister for supporting me spiritually throughout writing this thesis and my life in general.

ABSTRACT

Rutting is one of the most prevalent failure occurring in Hot Mix Asphalt (HMA) especially in the summer season and slow moving traffic areas. Rutting is a structural failure compromising the safety of traveling and thus needs to be accurately evaluated in a laboratory before use on the field. Although the Flow Number (FN) testing is commonly used for evaluating the rutting resistance of HMA in a laboratory, there are some shortcomings in using FN testing such as the confining pressure value to be used, and the costly and complicated equipment. Another potential test that is likely to be more advantageous than the FN testing for evaluating the rutting resistance is the Hamburg Wheel Tracking (HWT) test. However, the HWT is typically conducted in wet conditions, which can confound rutting with moisture damage effects. HWT test can be used in dry condition to avoid the moisture confounding effects, but to date not enough studies of HWT test in the dry condition have been reported. The objective of this study is to optimize the HWT test by conducting it in a dry conditions as a rational rutting test in the laboratory. Fitting response of HWT and FN tests using the power law and the Francken model were applied to determine the tertiary points of HWT and FN tests' results. In addition, Image Processing and Analysis Software version 2(IPAS2) was used to define the mechanisms of rutting occurring while testing by the HWT device. The validity of the Dry HWT testing for characterization of rutting of asphalt mixtures was verified by comparing its results to those from the confined Flow Number (FN) test and the Wet HWT test.

Results indicate that Dry HWT test is an effective tool for quantifying rutting potential with better simulation of typical field behavior. Very good correlations of creep slopes measured by the confined FN, unconfined FN, with the Dry HWT confirm that the HWT test could be a better test than the FN in terms of cost, simplicity of equipment and field simulation in the

laboratory. It was also concluded that the Wet HWT currently used in the AASHTO 324 can be used as a substitute to the Dry HWT test in the creep stage (before the Stripping Inflection Point) since the difference in creep slope estimated for both conditions is within the experimental error. The Wet HWT results after the creep slope remain useful for detecting the moisture sensitivity, and the measured cohesion/adhesion of mastics from the mixtures confirm this value of the test.

TABLE OF CONTENTS

LIST OF FIGURES

LIST OF TABLES

LIST OF EQUATIONS

1. INTRODUCTION

1.1 Background

Rutting, often referred to as permanent deformation, is the surface depression in the wheel path. Figure 1-1 shows a diagram of rutting in an asphalt pavement. Ruts primarily occur in warm climate areas. They can often be found in slow moving traffic areas, especially at intersections or the lanes of a bus stop. However, ruts also can occur in high-speed traffic due to weak asphalt mixtures or excessive truck loading. Typically, there are two basic types of rutting namely: asphalt mix rutting and subgrade rutting. Mix rutting occurs when the subgrade does not rut yet and surface presents wheel-path depression due to compaction and mix design problems. Subgrade rutting happens due to deformation of the subgrade due to loading. In this case, the surface settles into subgrade ruts causing wheel-path depression.

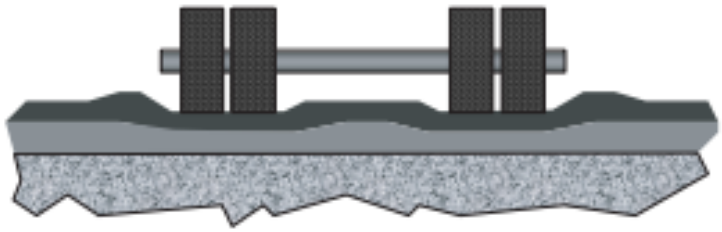

Figure 1-1. Diagram of Rutting in an Asphalt Pavement.

The two primary mechanisms of rutting have been identified, including shear failure (lateral movement) and densification (volume reduction). Shear failure (lateral movement) of the HMA courses occurs in the top 100 mm of the pavement surface (Yildirim, et al., 2007); however, if the material is unsatisfactory, shear failure can occur deeper. Permanent Deformation in pavement is usually created gradually with increasing numbers of load applications. Typically, it appears as longitudinal depressions in the wheel paths and sometimes occurs in conjunction with upheavals on the sides. It is caused by a combination of densification (decrease in volume

and, hence, increase in density) and shear deformation and can occur in any one or more of the HMA layers as well as in the unbound materials underneath the HMA. Eisenmann and Hilmer (Lu, et al., 2006a) also found that rutting was mainly caused by deformation flow rather than volume change. However, significant challenges have been realized in developing a cost effective laboratory test that can accurately simulate how rutting occurs in the field. This problem raises both policy issues within the agency and economic issues within the industry. Two tests that are widely used in the United States to determine the rutting in the laboratory are Flow Number Test and Hamburg Wheel Tracking Test (HWT).

The flow number test is the most popular test in the US to determine rutting resistance. This test can be carried out using with two conditions: unconfined and confined pressure specified in AASHTO TP79. However, it has a shortcoming in simulating the field behavior. In addition, the cost of this device is one disadvantage for determining rutting performance in the laboratory.

The HWT is gaining popularity due to being simple and reliable for testing of HMA mixes (Yildrim et al. 2007; Liddle and Choi 2007; Lu and Harvey 2006a; Lu and Harvey 2006b). Esso, A. G. of Helmut-Wind Inc., Hamburg, Germany, originally manufactured the HWT in the 1970s. The HWT test was intended to measure rutting performance and moisture damage of asphalt mixture. In the early 1990s, the device was initially introduced to the United States by pavement engineers and officials, after a European asphalt study tour (European Asphalt Study Tour 1991; Yildrim and Kennedy 2001). Studies began to emerge that evaluate HWT device to characterize moisture sensitivity of asphalt mixtures and to predict field performance (Liddle and Choi 2007; Lu and Harvey 2006a; Lu and Harvey 2006b; Aschenbrenner 1995; Aschenbrenner 1994; Aschenbrenner and Far 1994). Aschenbrener 1994; Aschenbrener 1995; and Aschenbrener

and Far 1994 found that HWT device was sensitive to aggregate quality, asphalt cement stiffness, short-term aging duration, asphalt source or refining processes, antistripping treatments, and compaction temperatures.

While HWT device is the preferred equipment to determine the moisture damage of asphalt mixtures, one main purpose of the HWT device is to evaluate permanent deformation in asphalt mixtures. All research studies pertaining to HWT testing have reported measuring rut depth in wet condition, which confound moisture effects in asphalt mixtures with the rutting behavior. This confounding effect is the main challenge in how HWT device can be used to distinguish rut depth at high temperatures without confounding it with rutting due to moisture damage.

1.2 Problem Statement

Currently, the Hamburg Wheel Tracking (HWT) test (AASHTO 324) is one prominent laboratory method to test rutting resistance of an asphalt mixture as it can represent the cyclic loading using actual wheel loads and it is less expensive than Flow Number Test device (AASHTP TP 79). However, the current HWT test is conducted using wet conditions and there is still no significant research done using the dry condition of the test. The problem with using the wet condition is it confounds the effect of moisture damage with rutting resistance of mixtures. In addition, the use of Flow number (which is a dry test) requires defining the confining pressure of the sample, which can vary depending on the thickness of layer and type of pavement structure. The use of confined Flow number can also make the test more costly and complicated.

Loaded Wheel Testers currently used in the United States include the Georgia Loaded Wheel Tester (GLWT), Asphalt Pavement Analyzer (APA), Hamburg Wheel Tracking Device

(HWTD), LCPC (French) Wheel Tracker, Purdue University Laboratory Wheel Tracking Device (PURWheel), and one-third scale Model Mobile Load Simulator (MMLS3) (Cooley Jr., et al., 2000). Although some of these devices are used for research, the Hamburg Wheel Tracking Test is prominently used nowadays for rutting resistance by Highway Agencies. The standard of the test for the HWT device (AASHTP 324) is conducted in water and thus cannot be considered a reliable method to measure rutting resistance due to repeated traffic loading cycle in dry conditions. Water conditioning may result in stripping the asphalt film from the aggregates and reduction of cohesion strength of binder or mastic in the mix. Such effects create a higher creep rate and possible a tertiary phase that is distinct from the permanent deformation occurring in dry wheel tracking tests. In wet Hamburg wheel tracking test, specimens are cured in the test temperature water for 30 minutes to equalize test temperature to specimens. Two failure mechanisms that can occur in the test are the cohesive and adhesive failure in HMA, and may be due to two factors: the diffusion of water into bitumen weakening of the mastic and the migration of water through mastic to the interface of mastic and aggregate.

Recently, Cox and Sons manufactured HWT device that is capable of conducting the test in a dry condition, but very limited data had been published using this device.

Williams (1999) proposed that HWT test is the most robust equipment among other wheel tracking tests, i.e. APA and FPRT, to quantify rut depth of Hot Mix Asphalt. However, moisture in asphalt mixture, in some tests, may confound the result of rutting performance. Therefore, the resolution of the moisture effect problem in HWT device is needed.

1.3 Hypothesis

Hamburg Wheel Tracking Test is a practical rut depth test in which confinement of the loaded area is easily achieved and can represent field conditions. However, the use of wet

conditioning is problematic as it can create moisture damage. Using the Hamburg Wheel Test in dry condition can be a better representation of permanent deformation behavior of asphalt mixtures in the field and can be used as a reliable performance test.

1.4 Objectives

1. Evaluate the trends of rutting of asphalt mixtures in the flow number (FN) test and the HWT test to determine if they can give same information. The power law and the Francken models are used in this evaluation.

2. Aggregate packing in asphalt mixture changes with an increasing number of cycles (Roohi, 2014) in both uniaxial loading cycle test (Unconfined Flow Number Test) and in confined FN. To compare the HWT to FN rutting mechanisms, the aggregate structure of asphalt mixtures changes in the HWT test need to be evaluated.

3. Since FN test gives good results in correlating with the field performance, it can be used as the reference for the HWT validity. Therefore, comparing results from FN test to results from Dry Hamburg Wheel Test is one of the objectives of this study.

4. Since rut depth in wet HWT results is confounded by moisture damage effects, the correlation between wet and dry condition testing in HWT test will be used as one of the objectives of this thesis to evaluate relative effect of moisture. In addition use the pull-off test to determine the cause of the difference between wet and dry HAT testing.

1.5 Research Methodology

The objectives of this research will be met through completion of the following tasks.

- Task 1: Literature Review
    - Overview of Permanent Deformation Mechanisms

  - Overview of Permanent Deformation Performance laboratory testing in use.
  - The Rational Use of Confined Pressure Testing
  - Overview of Image Processing and Analysis System (IPAS)
- Task 2: Experimental Design and Testing
- Task 3: Data Analysis
  - Analysis of using Francken model and Power Law Model to fit the HWT curve
  - Evaluation of the aggregate packing of HWT samples tested in dry condition
  - Analysis of the comparison of the strain behavior in dry HWT testing and the confined flow number testing
  - Analysis of correlation of HWT results between different testing condition at the same temperature
- Task 4: Development of Recommendations for Implementation.

2 LITERATURE REVIEW

2.1 Permanent Deformation

Permanent deformation, or rutting, has been a continuing problem in hot mix asphalt (HMA) performance (KanDhal, 2003). Rutting is defined as an accumulation of unrecoverable strain resulting from applied standing or slow moving loads along the asphalt pavement. The cause of deformation can be either the consolidation (densification) or a lateral movement (shear failure) of HMA under traffic or both. Shear failure of HMA pavement usually occurs in the top 10 cm of the pavement's surface (Solaimanian, 2003). Permanent deformation not only creates a safety hazard for the vehicle traveling along the pavement, but also reduces the service life of the pavement. Recently, the permanent deformation potential has increased due to higher traffic volumes (equivalent single axle loads [ESALs]) and an increasing use of radial tires, which typically exhibit higher inflation pressures. Therefore, an effective laboratory test needed to predict HMA rutting potential that is inexpensive and easy to use for quality control and quality assurance (QC/QA) would be of excellent benefit. Nowadays, the most common types of the standardized laboratory test of this nature are the loaded wheel tester (LWT) and flow number (FN) test. These two methods can simulate the field performance of rutting if run in a confined condition as confined testing better simulates the rate of deformation in the field (Kalou et al., 2002).

Many researchers have studied the practicality of devices to measure rutting resistance in HMA in the laboratory. There are some advantages to supporting the devices, resulting in good correlation with the field performance. However, some disadvantages of each device prevent their widespread usage. Witczak (2002) studied the development of test protocols, criteria, and guidelines for the simple performance test (SPT) in the laboratory to understand the Superpave volumetric mix design procedure. Table 2-1 summarizes the results showing the ranking of high-

priority SPT candidates for permanent deformation in the laboratory; the top three potential tests for determining permanent deformation included the dynamic modulus (E*), the flow number, and the flow time. Consequently, these results indicated three testing and parameter combinations as performance tests for permanent deformation: 1) the dynamic modulus, E*, determined using the triaxial dynamic modulus test; 2) the flow number, Fn, determined using the triaxial repeated load test; and 3) the flow time, FT, determined using the triaxial static creep test. Witczak (2005) later summarized the theory behind the three validated tests and briefly described the test methods.

Table 2-1. Ranking Summary of the High-Priority SPT Candidates for Permanent Deformation. (Witczak, 2005)

Test	Individual Team Rankings*									Total Score
$E^*/\sin\phi$ Stiffness	1	1	1	3	2	2	2	6	2	*20*
Triaxial Flow Time (F_T)	5	3	2	2	1	1	1	3	4	*22*
Triaxial Reated Load (F_N)	2	2	4	1	4	4	3	2	1	*23*
Repeated Shear γ_p-N	3	6	3	5	3	3	5	4	3	*35*
Triaxial Repeated Load ε_p-N	4	5	5	4	5	5	4	1	5	*38*
G^* Stiffness	6	4	6	6	6	6	6	5	6	*51*

* 1 for high priority, 6 for low priority.

Although some test methods yield a good correlation results to field performance, such as unconfined flow number, many studies have not considered a wide variety of mixture types, particularly high traffic mixtures. This indicates that the disadvantage of those devices is related to simulating field conditions. As shown in Figure 2-1, the correlations between laboratory results (i.e., flow number and flow time) and rut depths from the field display an excellent relationship with four mixtures, excluding two outliers. These two outliers are mixtures for high traffic volume that give less than 10 mm in rut depth for 1.5 million ESALs in the field test;

however, laboratory results from flow number and flow time are minuscule (premature failure).

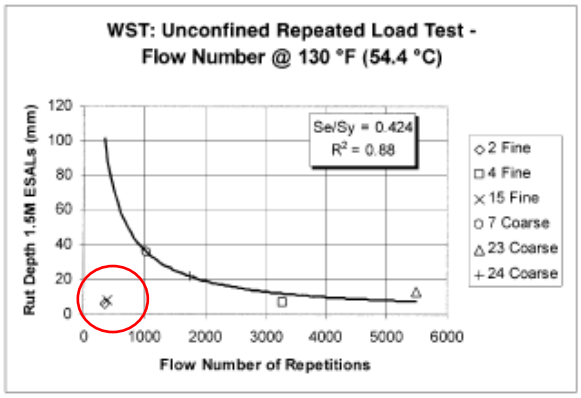

NOTE: Sections 2 and 15 were excluded from the analysis.

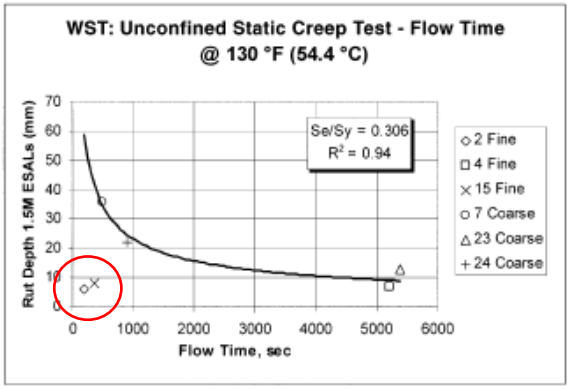

NOTE: Sections 2 and 15 treated as outliers and are not included in statistical analysis.

(a) **(b)**

Figure 2-1. Neglected High Traffic Mixture Samples in (a) Unconfined Flow Number and (b) Unconfined Static Creep Test–Flow Time. (Witczak, 2005)

Zhang et al. (2005) overviewed fundamental and simulative performance tests of permanent deformation for HMA, presenting the summary of advantages and disadvantages of permanent deformation testing in a laboratory, as shown in Table 2-2.

Table 2-2. Summary of Advantages and Disadvantages of Permanent Deformation Resistance Testing in a Laboratory. (Zhang, 2005)

Test Methods	Sample Dimension	Advantages	Disadvantages
Fundamental Test			
Diametral test	4 in. diameter × 2.5 in. height	• Test is easy to perform • Equipment is generally available in most labs • Specimen is easy to fabricate	• State of stress is non-uniform and strongly dependent on the shape of the specimen • May be inappropriate for estimating

			permanent deformation • High temperature (load) changes in the specimen shape significantly affect the state of stress and the test measurement • Were found to overestimate rutting • For the dynamic test, the equipment is complex
Uniaxial Static (Creep)	4 in. diameter × 8 in. height and others	• Easy to perform • Test equipment is simple and generally available • Widespread, well known • More technical information	• Ability to predict performance is questionable • Restricted test temperature and load levels do not simulate field conditions • Does not simulate field dynamic phenomena • Difficult to obtain 2:1 ratio specimens in lab
Uniaxial Repeated Load		• Better simulates traffic conditions	• Equipment is more complex • Restricted test temperature and load levels do not simulate field conditions • Difficult to obtain 2:1 ratio specimens in lab
Uniaxial Dynamic Modulus		• Non-destructive tests	• Equipment is more complex • Difficult to obtain 2:1 ratio specimens in lab
Uniaxial Strength Test		• Easy to perform • Test equipment is simple and generally available • Minimum test time	• Questionable ability to predict permanent deformation

Triaxial Static (creep confined)	4 in. diameter × 8 in. height and others	• Relatively simple test and equipment • Test temperature and load levels better simulate field conditions than unconfined • Potentially inexpensive	• Requires a triaxial chamber • Confinement increases complexity of the test
Triaxial Repeated Load		• Test temperature and load levels better simulate field conditions than unconfined • Better expresses traffic conditions • Can accommodate varied specimen sizes • Criteria available	• Equipment is relatively complex and expensive • Requires a triaxial chamber
Triaxial Dynamic Modulus		• Provides necessary input for structural analysis • Non-destructive test	• At high temperature it is a complex test system (small deformation measurement sensitivity is needed at high temperature) • Some possible minor problem due to stud, LVDT arrangement • Equipment is more complex and expensive • Requires a triaxial chamber
Triaxial Strength		• Relatively simple test and equipment • Minimum test time	• Ability to predict permanent deformation is questionable • Requires a triaxial chamber
Simulative Tests			
Hamburg Wheel Tracking Device	10.2 in. × 12.6 in. × 1.6 in.	• Widely used in Germany	• Less potential to be accepted widely in the United States

		• Capable of evaluating moisture-induced damage • 2 samples tested at the same time	
Asphalt Pavement Analyzer	Cylindrical 6 in. × 3.5 or 4.5 in. or beam	• Simulates field traffic and temperature conditions • Simple to perform • 3 to 6 samples can be tested at the same time	• Relatively expensive
Other Loaded Wheel Tracking Test Devices	Varied	• Simulates field traffic and temperature conditions • Uses SGC sample	• Not widely available in the U.S. • Very little data available

Table 2-2 shows that the triaxial flow number test can yield a good correlation to field performance. The concept of using the triaxial flow number test is applying sinusoidal load on a specimen with a specific load and rest period, as shown in Figure 2-2.

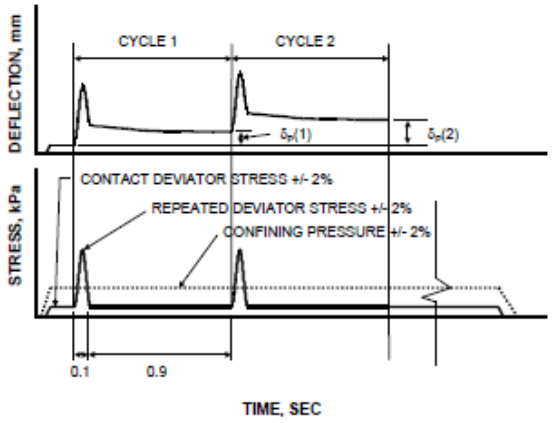

Figure 2-2. Loading in the Flow Number Test.

Figure 2-2 shows a schematic of the repeated loading used in the FN test. Haversine axial compressive-load pulses are applied to the specimen. The duration of the load pulse is 0.1 sec, followed by a rest period of 0.9 sec. However, Hajj (2010) studied the equivalent deviator stress

pulse experienced in the pavement. The study found that typical equivalent deviator stress pulses were less than 0.1 sec applied in the FN test in the case of 20 to 60 mph non-braking speeds and 20 mph braking speed. As a result, the standard load pulse of 0.1 sec does not simulate actual traffic-induced deviator stress pulse duration.

A simulative device that has become increasingly popular in the United States is the Hamburg wheel tracking (HWT) test as it can be conducted on both wet and dry conditions to address the moisture damage and rutting performance in asphalt mixtures and is also an inexpensive device relative to other tests. The original history of the HWT test in the United States emerged in 1990. A group of individuals representing AASHTO, FHWA, National Asphalt Pavement Association (NAPA), Strategic Highway Research Program (SHRP), Asphalt Institute (Al), and TRB participated in a tour of six European countries in September 1990. They found that Germany had a large centralized research facility: the Bundesanstalt fur Strassenwesen—the Federal Highway Research Center in Germany (BAST). The lab included a full-scale pavement testing device to provide wheel tracking tests for rutting (Euro tour, 1990). Later, Aschenbrener (1994, 1995) and Aschenbrener et al. (1994) studied the evaluation of the HWT device to predict moisture damage in HMA and found that the HWT device was sensitive to aggregate quality, asphalt cement stiffness, short-term aging duration, asphalt source or refining processes, antistripping treatments, and compaction temperatures. During the Federal Highway Administration's (FHWA) 1993 to 2001 Superpave Validation Study, pavement and laboratory tests were performed on five surface course mixtures. The pavement and laboratory tests also provided a good correlation between the rut depth in the asphalt pavement layer at 58°C and several laboratory mixture properties (one of those properties was the creep slopes from the HWT device at 50°C). Later, Stuart (2002) studied the evaluation of the rutting resistance for mixtures

containing polymer-modified asphalt binders with identical high-temperature PGs, but varied chemistries. As the HWT was one of the performance tests in this study, which found a moderate correlation between creep slopes from HWT at 58°C and rut depth from the French pavement rutting tester (French PRT) at 70°C. After the study of FHWA, the HWT device gained popularity because of its fast and reliable testing of HMA mixes. Many researchers tried to conduct further study on the evaluation of HWT device to characterize the moisture sensitivity of asphalt mixtures and to predict field performance (Lu and Harvey, 2006a; Lu and Harvey, 2006b; Yildirim et al., 2007; Liddle and Choi, 2007).

Although the HWT device is a promising device for determining permanent deformation and moisture damage in the laboratory, a dry condition test is needed to quantify only permanent deformation without moisture confounding and compare directly with the confined FN, which yields excellent results in permanent deformation performance prediction.

Two promising test methods were identified through a thorough literature review and are summarized in Table 2-3. Detailed herein is the literature review for the performance test methods of high-temperature resistance.

Table 2-3. Summary of Proposed Test Protocols for Permanent Deformation.

Performance	**Performance HMA Test**
Permanent Deformation	Flow Number Test (AASHTO TP79), Hamburg Wheel Tracking Test (AASHTO T324)

2.2 Hamburg Wheel Tracking Test

Many types of LWT equipment are available, such as the Georgia LWT, the asphalt pavement analyzer (APA), the Superfos Construction rut tester, the HWT device, and the French Laboratoire Central des Ponts et Chaussées (LCPC) wheel tracker. In order for LWT devices to be used with a significant level of confidence, there needs to be an acceptable correlation of actual field rutting to those values predicted by LWTs in the laboratory. The most common LWT used in many states in the US is the HWT test.

The HWT test is used to measure the effects of rutting and moisture damage performance; it has been gaining popularity because it offers reliable and rapid testing of various HMA mixes (Yildirim et al., 2007; Lu et al., 2006a). The HWT test displays sensitivity to the premature failure of HMA mixtures due to binder stiffness, weak aggregate packing, moisture damage, and insufficient adhesion between the aggregate and binder. The HWT used steel rather than the rubber wheels utilized in British devices. The procedures for using HWT and preparing a specimen are specified in AASHTO T324. Based on the standard, the device is operated by moving a steel wheel backward and forward across the surface of HMA specimens (cylindrical or slab/cubical) submerged in a constant temperature water bath specified in AASHTO T324 as 50±1°C. The equipment is capable of testing a pair of specimens simultaneously. The steel wheels have a diameter of 203 mm (8 inches) and a width of 47 mm (1.85 inches). Each steel wheel weighs 158 lbs. The typical setup of a HWT device, specimen preparation, and failure specimens are shown in Figure 2-3. The result for HWT is rut depth measured by linear variable differential transformers (LVDTs) on deformation at 11 points along the length of each specimen at an accuracy of 0.01 mm. The device automatically ends the test when either the preset number of wheel passes is reached or a rut depth of 20 mm (0.8 inches) is measured. The test duration

when considering 20,000 passes including a curing time of 30 minutes is approximately 7 hours. However, in some tests the specimens fail early, and test times are shorter.

Figure 2-3. (Clockwise) Final Test Setup of Hamburg Wheel Tracking Device, Specimens under the Wheel Load, Specimens Ready for Testing in HWT Device, and Failed Specimens with High Rut Depth (Rahman and Hossain 2014).

The HWT device outputs are rut depth versus the number of wheel passes. Figure 2-4 shows a curve between rut depth and number of wheel passes, including post-compaction consolidation, creep slope, stripping slope, and stripping inflection point. Post-compaction consolidation is deformation (mm) at 1,000 wheel passes. It is assumed that the wheel densifies the mixture within the first 1,000 passes; consequently, this is called post-compaction consolidation. Creep slope is the inverse linear line between post-compaction and stripping inflection if stripping occurs. Creep slope relates primarily to rutting as a result of plastic flow, and it is the number of wheel passes required to create 1 mm of rut depth. After creep slope, one point and one line are related to the moisture resistance of HMA, which is stripping inflection point and stripping slope, respectively. The stripping inflection point is the number of wheel passes at the intercept of creep slope and stripping slope. Stripping slope is the inverse linear rate of deformation after the stripping point. Stripping slope relates to the moisture damage of HMA,

and it is the number of wheel passes required to create 1 mm of rut depth after the stripping inflection point (Yildirim, et al., 2007).

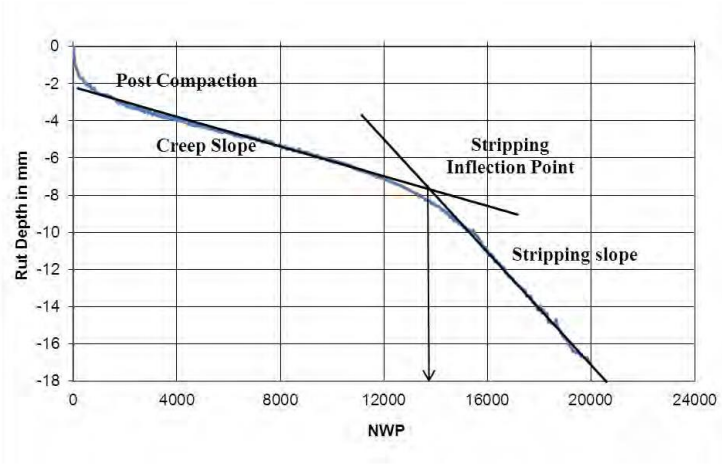

Figure 2-4. Typical Hamburg Wheel Tracking Device Test Results.

Some states such as TxDOT, CDOT, KDOT, WSDOT, and MDT adopted the AASHTO standard, with some changes depending on the mixture type. For example, Hamburg, Germany, specifies allowable rut depth of less than 4 mm at 20,000 passes. The Colorado Department of Transportation (CDOT) uses a test temperature according to the site and specifies a rut depth of less than 10 mm after 20,000 passes (Izzo and Tahmoressi 1999). The TxDOT follows their TEX-242-F procedure. Requirements for results of TEX-242-F tests are listed in Table 2-4.

Table 2-4. Hamburg Wheel Tracking Device Test Criteria.

High-Temperature Binder Grade	**Number of Wheel Passes**	**Maximum Rut Depth (mm.)**
PG 64	10,000	12.5
PG 70	15,000	12.5
PG 76	20,000	12.5

(Source: Zhou et al. 2005)

In past research studies, Aschenbrener (1995) evaluated factors that affect HWT results. The stripping performance of 20 different mixtures was compared with the field performance. These two sets of data obtained an excellent correlation. The study concluded that HWT results are sensitive to the quality of aggregate, asphalt cement stiffness, short-term aging duration, refining processes, liquid anti-stripping agents, hydrated lime additives, and compaction temperatures. Izzo and Tahmoressi (1999) evaluated the HWT and its capability to assess the moisture susceptibility of HMA in Texas. Six different mixtures prepared with and without antistripping additives were tested at 40°C and 50°C. Mixtures were modified with hydrated lime and liquid antistripping additives. All mixtures used the same asphalt binder. For mixtures tested at 40°C, the use of anti-stripping additives improved mix performance. Mixtures with hydrated lime performed better than the mixtures modified with a liquid anti-stripping additive. For mixtures tested at 50°C, results were inconsistent (Izzo, et al., 1999). Gogula et al. (2003) studied the effect of PG binder, including PG 52-28, PG 64-22, PG 58-28, and PG 70-28, and air voids on HWT. The result showed that the mixture with PG 70-28 performed better than the mixtures with any other binder types. Their study also indicated that mixtures with lower air voids (7%) performed better compared to mixtures compacted to 2% higher air voids (9%) (Bonaquist, 2008).

2.3 Flow number Test

The flow number is another approach to measure the rutting performance of asphalt concrete mixtures (Mclean and Monismith, 1974). It is the prevalent approach correlating laboratory results to the field performance. Flow number is defined as the number of load pulses when the rate of change in permanent strain happens during the repeated load test. This can be determined by taking the derivative of the permanent strain and number of load cycle curves

(Bonaquist, 2012). The device used for testing flow number can be either uniaxial loading cycle testing or triaxial testing. The widely used device in the US for flow number is called the asphalt mixture performance tester (AMPT), which is a small servo-hydraulic testing device (Figure 2-5) developed specifically for testing asphalt concrete mixtures

Figure 2-5. Photograph of the IPC Global Asphalt Mixture Performance Tester.

In NCHRP Project 9-19, the flow number data were found to correlate well with observed rutting in the field pavements (Witczak et al., 2002). The additional development and testing work for the AMPT was completed in NCHRP Project 9-29 (Bonaquist, 2011). It included ruggedness testing, AASHTO standard draft, and an interlaboratory study to establish the precision of the flow number test. The test can be carried out with or without confining pressure. If confining pressure is used, it remains constant during the test. The typical permanent axial strain response and the determination of the flow number are represented in Figure 2-6.

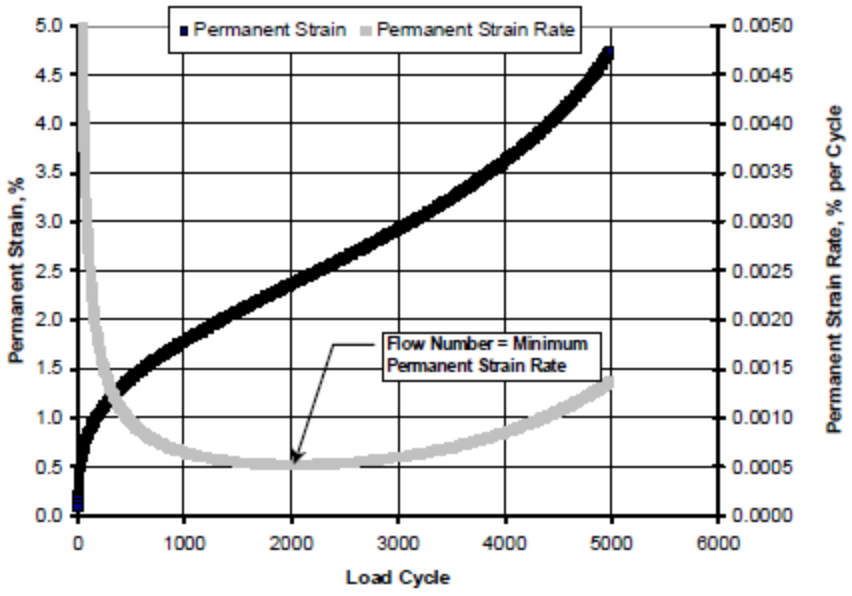

Figure 2-6. Example of Flow Number Test Data. (R. Bonaquist, Evaluation of Flow Number (Fn) as a Discriminating HMA Mixture Property 2012)

The flow number can be determined by using Francken's (1977) model to fit the permanent strain versus number of loading cycle curves and then performing the differentiation on the fitted curve (Biligiri et al., 2007). Flow number can be tested in two conditions of confining stress: a uniaxial loading cycle test (unconfined pressure test) and a triaxial test (confined pressure test).

2.3.1 Uniaxial Loading Cycle Test (Unconfined Pressure Test)

The good correlations of flow number and rutting resistance of mixtures used in experimental sections at the FHWA Pavement Testing Facility, MNRoad, and WesTrack (Witczak et al., 2002) are shown in NCHRP Project 9-19. The example of the relationship between flow number and rut depth is shown in Figure 2-7.

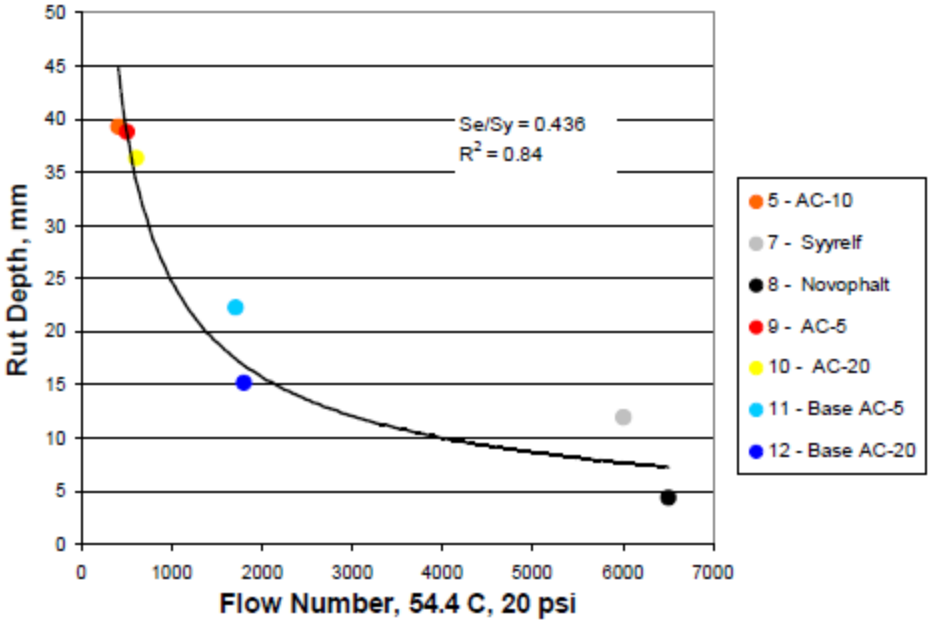

Figure 2-7. Relationship between Flow Number and Rut Depth for the FHWA Pavement Testing Facility Sections (Witczak et al., 2002)

NCHRP Project 9-33 developed tentative criteria for the flow number test. These are based on flow number experimental data collected by the FHWA on several field projects and a relationship between mixture volumetric properties and rutting resistance developed in NCHRP Projects 9-25, 9-31, and 9-33 (Advanced Asphalt Technologies, 2011). The air void content of the specimens is 7.0%±0.5%. The temperature used for testing the flow number was conducted at 50% reliability performance grade temperature obtained from LTPPBind 3.1 at a depth of 20 mm without making traffic volume or speed adjustments. Moreover, the flow number test was determined without confinement using an axial stress of 87 psi (600 kPa). The minimum flow number for an average rut depth is 7 mm, which is consistent with 95% reliability of 12 mm, as shown in Table 2-5.

Table 2-5. NCHRP 9-33 Recommended Minimum Flow Number Requirements (Bonaquist, 2008).

Traffic Level (*Million ESALs)*	**Minimum Flow Number** *(Cycles)*
< 3	---
3 to < 10	53
10 to < 30	190
≥30	740

In a previous WHRP project on flow number, conditioning was shown to have a major effect on the flow number. WHRP Projects 0092-08-06 and 0092-09-01 found a reasonable relationship between the flow number and estimated rutting resistance from the NCHRP Project 9-33. The relationship was best when mixtures were conditioned for 4 hours at 135°C. The unconfined flow number testing was recommended with the following conditions:

- Unconfined tests using a repeated deviatoric stress of 87 psi (600 kPa);
- Testing at the 50% reliability high pavement temperature from LTPPBind 3.1; and
- Air void content of 7.0%±0.5%.

The current WHRP project studied the potential test for testing permanent deformation. It was found that an unconfined FN test gives premature failure, resulting in an FN of 60 and 65 at 10 million traffic level mixes. These results show that FNs are less than the minimum value specified in the specification.

.

2.3.2 Triaxial Test (Confined Pressure Test)

Kaloush et al. (2002) showed a good relationship between the field and laboratory slope parameter, as shown in Figure 2-8. Although the unconfined results in the research yielded better correlation with field rut depth, this figure indicates that the rate of deformation in the field is better simulated by the confined repeated load tests.

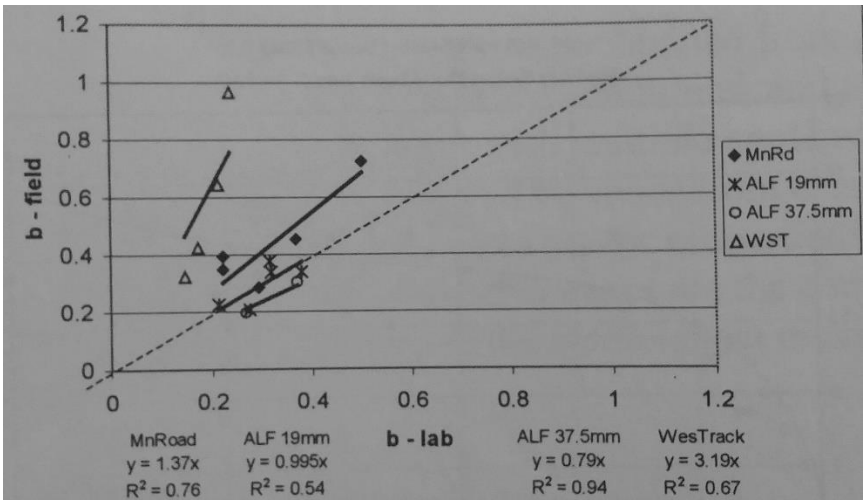

Figure 2-8. Comparison of the Slope Parameter for Field and Laboratory Test-Confined Laboratory Tests. (Kaloush, 2002)

Moreover, Table 2-6 summarizes the general project information for the verification mixtures along with the testing conditions and the resulting FN (Ulloa, 2013). The results showed that the field rut depth and measured flow number are strongly correlated.

Table 2-6. General Project Information for Validation and Testing Results. (Ulloa, 2013)

Mixture ID	Location	20-Year MESALs	Traffic Speed (mph)	$T_{effective}$ (°C)	Construction Date/Initial In-Place Air Voids	Field Rut Depth	Deviator/ Confining Stresses (psi)	Pulse Duration/ Rest Period (s)	Measured Mean Flow Number[a]	$FN_{critical}$
BA-6428	Mount Lombo Street to Ramsey Way, Reno, Nev.	1	25	36.8 (for RD < 0.25 in.)	2008/6%	≤0.05 in. after 4 years of service	78/39	0.05/0.70	>20,000	5,000
ML-6428	Moana Lane Extension: from Neil Road to Louie Lane, Reno	6	40	36.0 (for RD < 0.25 in.)	2006/6%	≤0.09 in. after 6 years of service	77/44	0.03/0.50	>20,000	7,000
US95-6428	US-95: 2.5 mi South of Searchlight, Las Vegas	18	50	44.7 (for RD < 0.25 in.)	2007/7%	No visible rutting	78/38	0.02/0.20	>20,000	13,000
NV55-6422	WesTrack Nevada Automotive Test Center, Silver Springs	30 (0.58[b])	40	43.6 (for RD < 0.50 in.)	June 1997/4%	0.87 in. after 5 months	77/40	0.03/0.30	8,395	13,000
NV19-6422	WesTrack Nevada Automotive Test Center, Silver Springs	30 (4.8[b])	40	38.6 (for RD < 0.50 in.)	March 1996/8%	0.52 in. after 2.5 years	76/45	0.03/0.30	5,895	13,000

[a]Determined with Francken model.
[b]Actual test track traffic.

The condition using a confined flow number in WHRP Project 0092-08-06 was used in NCHRP Project 9-30A in the development of an improved rutting model for asphalt concrete. The confined flow number condition uses a confining pressure of 69 kPa and a repeated deviatoric stress of 483 kPa. Air void and temperature use the same criteria condition as the unconfined flow number.

2.3.2.1 The Rational Use Confined Pressure Testing

Characterizing the flexible pavement stresses under wheel loads can be simply considered as a homogeneous half-space. The half-space has an infinitely large area and infinite depth with a top plane where the loads are applied. Boussinesq (1885) originated the linear theory to analyze a nonlinear half-space based on a concentrated load applied on an elastic half-space. After that, some researchers modified Boussinesq's theory, including the Kansas State Highway Commission (1947), Foster and Ahlvin (1954), Ahlvin and Ulery (1962), and Huang (1968). However, flexible pavements are a layered system where the top layer generally contains higher quality materials and cannot be represented by a homogeneous mass (Burmister, 1943). Therefore, Burmister developed solutions for a two-layered system in 1943 and then extended it

to a three-layered system (Burmister, 1945). Later, Huang developed a multilayer system using a computer-based solution called KENLAYER (Huang, 1967, 1968a). KENLAYER is the elastic multilayered system under the circular loaded area, where each layer has linear elasticity and is homogeneous, isotropic, and infinite in area extent. The results obtained by KENLAYER compare well with those from other layer system programs, such as ELSYM5, VESYS, DAMA, and MICH-PAVE, which are also used for determining the behavior of flexible pavements. Brown and Bell suggested the use of stress invariants as the most appropriate method of comparing the stress states affecting material behavior and characterization. A recent study from Ulloa et al. (2009) used the mathematical model to determine the stress invariants in pavement. The concept for calculating the model is that the octahedral normal and shear stresses are used to convert the stress tensor observed in the HMA layer under dynamic loads to deviator and confining stresses in FN test setup. In the laboratory, the condition of confinement and deviator stress are achieved by applying a static confining pressure all around a sample using compressed air and a repeated deviator vertical stress using an axial actuator to a 100 mm in diameter by 150 mm height cylindrical HMA sample, respectively. The deviator stress, σd, and confining stress (i.e., σc = σ2 = σ3) under triaxial conditions can be written as a function of the octahedral stress components as represented in Equations 2-1 and 2-2:

$$\sigma_d = \frac{3}{\sqrt{2}}|\tau_{oct}| \qquad (2\text{-}1)$$

$$\boldsymbol{\sigma_c = \sigma_3 = \sigma_2 = \sigma_{oct} - \frac{\sigma_d}{3}} \qquad (2\text{-}2)$$

Where: $\sigma_{oct} = \frac{1}{3}(\sigma_1 + \sigma_2 + \sigma_3) = \frac{1}{3}\bar{I}_1$

$$|\tau_{oct}| = \frac{1}{3}\sqrt{(\sigma_1 - \sigma_2)^2 + (\sigma_2 - \sigma_3)^2 + (\sigma_3 - \sigma_1)^2} = \sqrt{\frac{2}{3}\bar{I}_{2D}}$$

In the study, they considered the non-braking and braking conditions with the range of deviator stress from 69 to 132 psi and ended up with a range of equivalent confining stresses from 27 to 47 psi at 2 inches below the pavement surface with a 4- to 8-inch thick HMA layer. The results of the confining stress from each method with the same condition of contact pressure (87 psi) and asphalt are summarized in Table 2-7.

Table 2-7. Summary of Confining Stress at Two Inches Below the Surface Using Different Methods.

Methods	**Confining Stress (psi)**
Boussinesq (Solution at axis of Symmetry)	36.6
Foster and Ahlvin	30.4
KENLAYER	30.78
Ulloa	34

Different methods of determining confining stress show close results within a range of 30–36 psi with a contact pressure of 87 psi and a 6-inch asphalt layer. In addition, the confining stress used in NCHRP 719 and the WHRP report was 10 psi for the FN test program. NCHRP 719 implemented various confining stresses to determine the range of confining stress that should be applied in the FN test program. Based on Figure 2-9, a small confining stress of 10 psi substantially reduces the plastic strains throughout the test program and can retain a sample without failure through 10,000 cycles for all tests. Increasing the confining pressure to 20 psi only caused a slight additional reduction in plastic strains (NCHRP 719). Therefore, a confining stress of 10 psi is adequate for use in the FN test program.

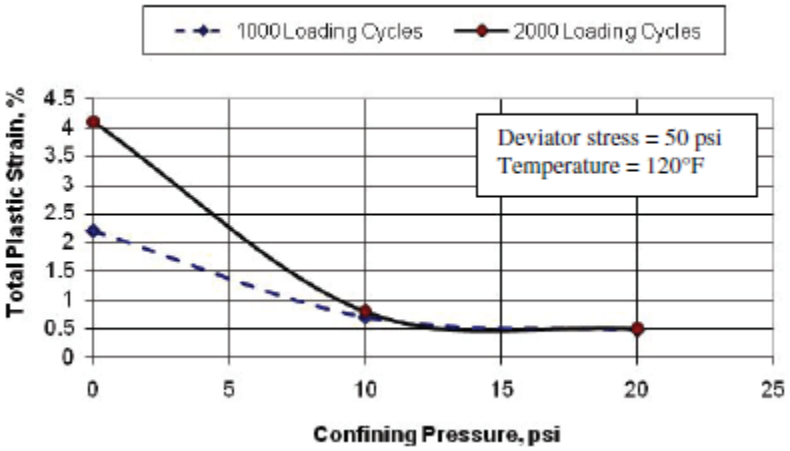

Figure 2-9. Influence of Confining Pressure on Total Plastic Strain. (NCHRP 719)

2.4 Image Processing and Analysis System (IPAS)

In this study, one of the objectives was to determine the aggregate packing of the HMA tested in dry HWT; thus, the image processing and analysis were tools for determining the internal aggregate structure of asphalt mixtures. The image processing and analysis software—namely, Image Processing and Analysis System (IPAS)—applied in this dissertation was initiated by Coenen (2011). Afterward, Roohi (2012) developed the software to analyze the contact length of the aggregate to determine the effect of the aggregate structure on permanent deformation results. Many researchers currently use this imaging analysis software to analyze internal aggregate structure in asphalt mixtures. The overview of IPAS is presented below.

Two main functions are considered in the software, which is a function of image processing and a function of microstructure analysis. The details of both the functions and implementation of the initial IPAS version is more understandable in Coenen (2011) and Coenen et al. (2011). This chapter presents an overview of IPAS 1 and the evolution of IPAS 2.

2.4.1 Image Processing and Analysis System Overview

A scanned picture of a cut asphalt mixture, as illustrated in Figure 2-10, is processed by a digital imaging processor (DIP) algorithm to convert a color image (i.e., red-green-blue [RGB]) into a binary image (i.e., black and white). Then the binary color can be calculated by the matrix shown in Figure 2-11 in MATLAB to obtain internal structure parameters, such as a number of contact zones and aggregate segregation (Coenen, 2011; Coenen et al., 2011). The color of a scanned image is a RGB considered as a three-dimensional matrix in MATLAB. Each component of the matrix shows the intensity of each color at the specific pixel. However, the geometry of each phase (i.e., aggregate and mastic) needs to be determined; therefore, a gray color image was used to analyze and distinguish aggregate and mastic because colors of these two phases show a significant difference in a gray scale image in terms of color intensity. The matrix of the gray scale is a two-dimensional matrix in MATLAB (Figure 2-11). Finally, a gray-scale image is converted to a binary color (i.e., black and white) image used for microstructure analysis. To obtain the most appropriate binary image relative to the actual image, some filters are needed to enhance the image quality for separating different phases of material. The image filters include median, region maxima (i.e., Hmax), watershed filtering, threshold filtering, and erosion techniques.

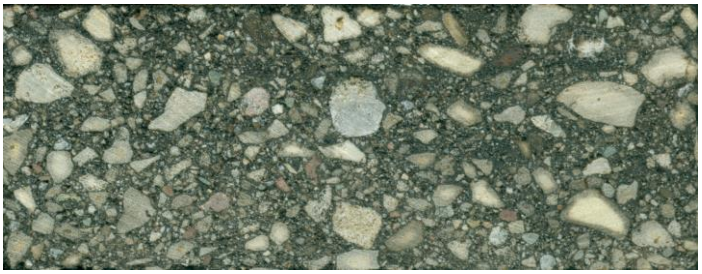

Figure 2-10. A Scanned Picture of a Cut Asphalt Mixture Sample.

There is also the step to quantify the orientation of the aggregate. The orientation feature of IPAS calculates the angles of the major axis of each aggregate from the horizontal axis and a radial axis.

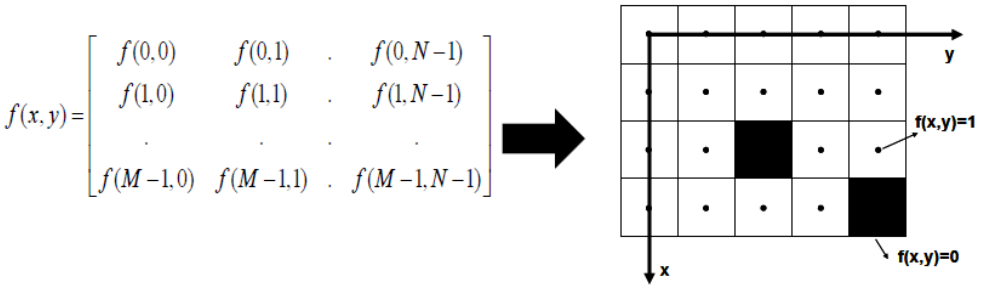

Figure 2-11. A Digital Image in MATLAB Using a Matrix. (Roohi, 2012)

2.4.2 Image Processing and Analysis System Development (IPAS^2)

In this development, Roohi (2012) developed the software to quantify the aggregate internal structure that contains many indices based on image analysis. Aggregate internal structure indices can potentially dictate the rutting resistance of asphalt mixture. The indices in IPAS^2 are presented in Table 2-8.

Table 2-8. The New Aggregate Internal Structure Indices in IPAS^2

Aggregate Internal Structure Indices
• Number of aggregate proximity zones
• Proximity zone length (i.e., representation of proximity area in 2-dimesional analysis)
• Normal to proximity zone plane orientation

First, the number of aggregate proximity zones in the asphalt mixture represents the internal aggregate structure packing—that is, how many contact points are in the aggregate structure. An increasing number of proximity zone gives rise to a better stress distribution. Second, the proximity zone length can represent the degree of interlock in an asphalt mixture. If

the proximity zone length increases, the interlock between the aggregate will increase as well. The proximity zone is defined as the length of distance between 2 adjacent aggregates between which the distance is equal or less than 0.10 mm as detected from the image using pixels of the size of less than 0.020 mm. The software convert the image into aggregates into white colored pixels and the mastic into black colored pixels. The software then searches for all areas where the number of black pixels between the white aggregates is less than the 0.10 mm threshold and mark it as proximity zone. The total length of these zones is called the Total Proximity Length (TPL). Finally, the normal to proximity zone plane orientation represents the orientation of loading direction. Roohi (2012) showed that proximity zone length was related to rutting resistance in the asphalt mixture as it showed a linear regression (R^2) of 0.9 in the total proximity zone and flow number in uniaxial loading cycle testing, as presented in Figure 2-12.

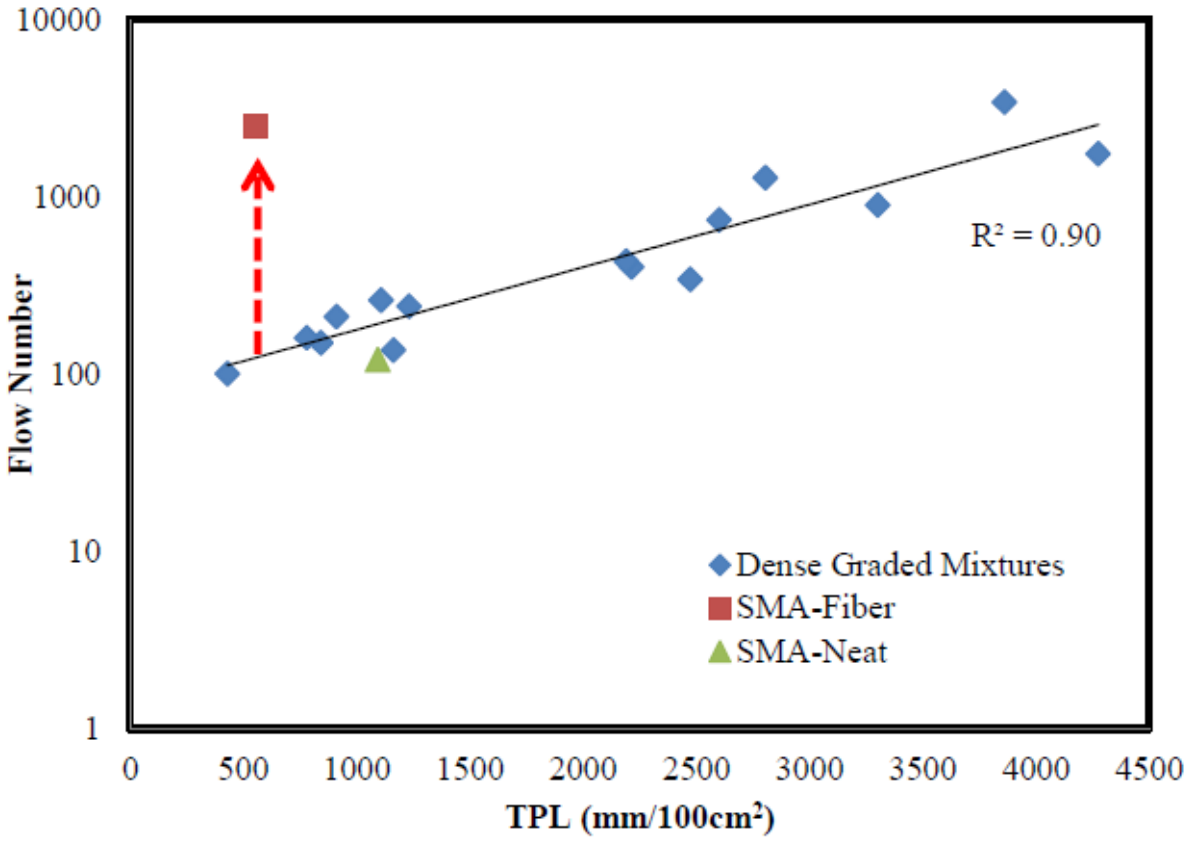

Figure 2-12. Comparing SMA Flow Number Results and Aggregate Packing with Dense Graded Mixtures. (Roohi, 2014)

Furthermore, using the total proximity length to determine aggregate structure in asphalt mixture in each cycle zone was evaluated, as shown in Figure 2-13. The results showed that total proximity lengths (TPLs) increase in the primary zone, but after the primary zone (i.e., during the secondary and tertiary zones), the TPLs reduced with increasing loading cycles. The dilation (bulge in asphalt mixture) of the asphalt mixture occurred after testing the uniaxial loading cycle as a no confinement, stress-encompassing sample, as shown in Figure 2-14.

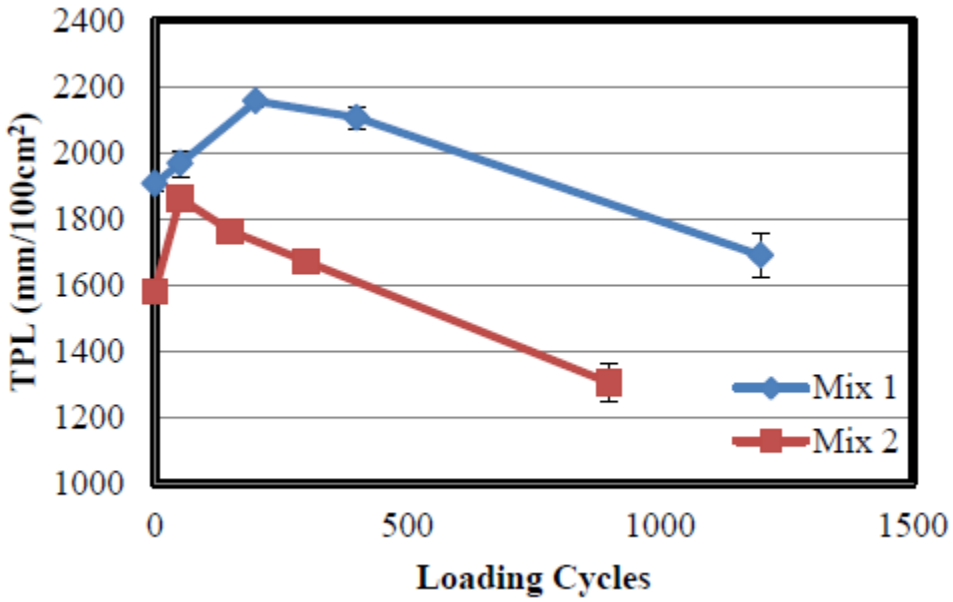

Figure 2-13. Evolution in Aggregate Packing during Loading in the FN Test. (Roohi, 2014)

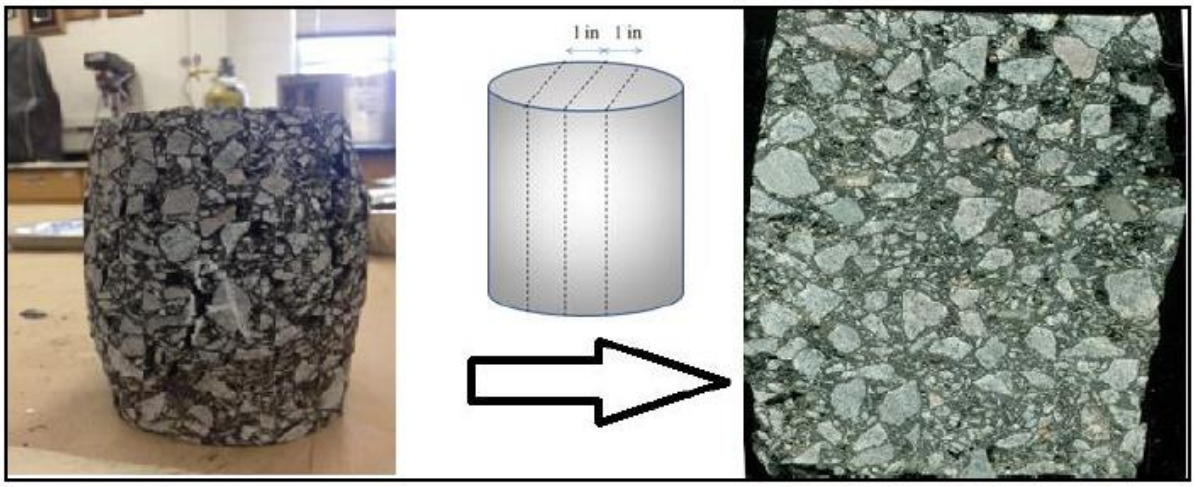

Figure 2-14. Cutting Section of a Failed Sample in the FN Test. (Roohi, 2014)

These results from uniaxial loading cycle testing in previous study could indicate that the main mechanism of deformation in the primary creep zone of rutting is the densification of the asphalt mixture. The aggregate packing (as measured by TPLs) increases during the primary zone. However, TPLs start decreasing when the loading cycles increase during the secondary creep zone, as observed by the dilation of the aggregate structure. In addition, the failure and tertiary flow in mixtures mainly happened due to the instability of the aggregate structure. The instability happens as a result of the aggregate skeleton bulging (dilation) in mixture samples—in particular, the portion of the aggregate skeleton close to the outer side of samples, as the confining stress is lower. To verify the concept of aggregate skeleton bulging as the main mechanism controlling tertiary flow, asphalt mixtures were prepared for testing in a confined condition using PVC, as shown in Figure 2-15.

Figure 2-15. Confined Flow Number Sample by PVC. (Roohi, 2014)

These results were also confirmed by the mechanisms shown in Confined FN test during which the inception of TPL reduction took much more cycles.

3 EXPERIMENTAL PLAN AND INTRODUCTION OF TEST METHODS

3.1 Experimental Plan

The goal in designing this experiment was to examine the preliminary result of dry HWT to be potentially used in a laboratory to quantify permanent deformation in Wisconsin. Therefore, the selected mixes would provide meaningful results while representing the aggregates commonly used in Wisconsin mix designs. Loose mixes were obtained from Mathy Construction Company in Wisconsin to evaluate the results. The two mix designs acquired were E-3 and E-10. E-3 represents the mixture for a low traffic volume of 3 million ESAL while E-10 is the mixture for 10 million ESAL.

The experimental design was classified into two phases to determine the aggregate packing of dry HWT and to correlate with confined FN and HWT testing results. The mix designs were evaluated with a different gradation of aggregate and asphalt content. The mix designs used in these experiments are summarized in Table 3-1.

Table 3-1. Summary of Hot Mix Asphalt Mix Designs.

Mix Designs	Binder Type	Asphalt Content (%AC)	AV (%)	VMA (%)
E-3	58-28	5.4	4.0	14.6
E-10	58-28	5.1	3.4	13.3

All mix designs presented in Table 3-1 were designed to compact and test in the HWT test and flow number test to determine Experiments 1 and 2.

Experiment 1: Determination of Aggregate Packing of HWT Sample before and after Testing

HWT samples were prepared to evaluate the aggregate packing and orientation angle of the aggregate for this phase. All samples targeted the air void at 7%±0.5. The samples' height and cutting processes followed AASHTO T324. The other factors and number of levels for conducting this study are shown in Table 3-2.

Table 3-2. Summary of Factors to Determine Aggregate Packing of HWT Samples.

Factors	**Level**	**Description**
Mixture	2	Loose mixes from Wisconsin(E-3 , E-10)
Points of cycles to analyze	5	Initial mixture, primary zone, secondary zone, onset tertiary zone, and failure
Replicates	2	

After testing, each sample was cut into 6 pieces, as shown in Figure 3-1, to analyze the aggregate structure and orientation angle. Scanning each face of each piece with a high resolution scanner (i.e., HP Scanjet G3110 used) was done after cutting. Finally, the IPAS^2 software was used to analyze aggregate packing and orientation angle in asphalt mixtures.

(a)

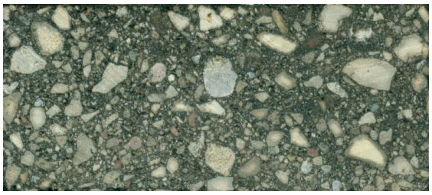

(b) **(c)**

Figure 3-1. Cut Samples for Analyzing Contact Lengths and Orientation Angles a) 6 pieces each sample b) Scanned Sample before Loading c) Scanned Sample after Loading.

Experiment 2: Determination of Correlation between Dry HWT Test and Confined FN Test

Two methods of testing, including dry HWT test and confined flow number, were used to determine HMA's permanent deformation performance. All samples targeted an air void at 7%±0.5. The sample procedure to make dry HWT and confined FN samples was specified in AASHTO T324 and AASHTO TP79. A representative sample was obtained by using the following types of aggregate sources from varying regions in Wisconsin:

- Granite: Cisler (north central Wisconsin)
- Limestone: Waukesha (southeast Wisconsin)

These two types of aggregate were selected as they are widely used in the United States. Almost all states in the United States can provide either of them. According to the information from USGS, shown in Figure 3-2, limestone is mostly found in the central and eastern regions of the United States. A few Midwestern states can find limestone too. For granite, most resources are found in the eastern and western regions, and some are in the north (i.e., Minnesota and Wisconsin).

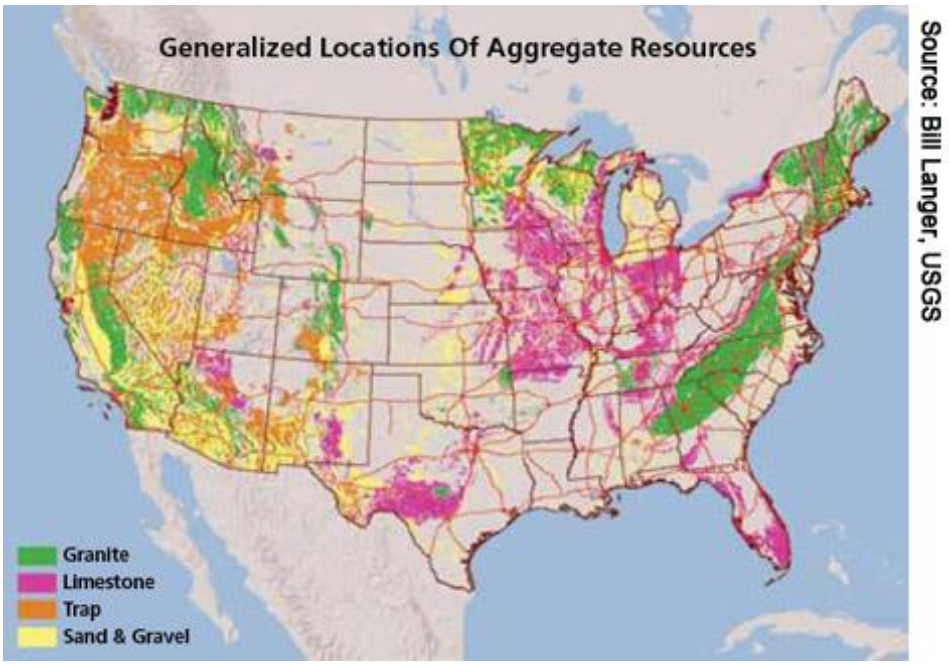

Figure 3-2. Locations of Aggregate Resources (USGS)

The factors and level considered in this phase are shown in Table 3-3.

Table 3-3. Summary of Factors to Correlation between Dry HWT Test and Confined FN Test.

Factors	Level	Description
Methods	2	Dry HWT, Confined FN
Aggregate Types	2	Cisler-Granite, Waukesha-Limestone
Binder Types	2	S-28, V-28
Mixture Types	2	MT and HT

Experiment 3: Determination of the Correlation between Wet and Dry Condition Testing in HWT Test

The goal in designing this experiment was to quantify the correlation of failure stages occurring in the wet and dry HWT samples; therefore, two conditions of the HWT were carried out in this experiment.

Mixes ranging from permanent deformation resistant to permanent deformation susceptibility were selected to allow for evaluation and analysis of the HWT in dry and wet conditions at a wide range of sensitivities. The use of mixes with a wide range of behaviors provides a valid means of comparison by ensuring that the results of the test would not be confounded with the variability inherent in the test method. The mix selection process was produced based on the WisDOT mix design specification for medium and heavy traffic from aggregate sources that have a variety of angularities resisting and susceptible to permanent deformation. To identify the mix design susceptible to moisture and permanent deformation, the results of this analysis provided four mix designs with different aggregate gradations and aggregate sources. The experimental matrix is provided in Table 3-4.

Table 3-4. Summary of Factors to Determine the Correlation between Wet and Dry Condition Testing in HWT Test.

Factors	Level	Description
Methods	2	Dry HWT, Wet HWT
Aggregate Types	2	Cisler, Waukesha
Binder Types	2	S-28, V-28
Mixture Types	2	MT and HT

The experimental plan involves two types of binders and mixtures procured from the company in Wisconsin (Mathy Construction), including S-28 and V-28, where S and V represent the binder used for the standard and very heavy traffic, respectively. The mixture types included

MT and HT, which represent the gradation design used for medium and high traffic. To verify the properties of the supplied binder, the binder properties measured in this study included complex modulus (G*), phase angle (δ), and G*/Sin(δ). All binder properties were measured using the dynamic shear rheometer (DSR). Temperature testing and binder properties are provided in Table 3-5.

Table 3-5. Summary of Binder Testing

Binder Types	Performance Grade (˚C)	Complex Modulus [G*(kPa)]	Phase Angle [δ(˚)]	G*/Sin(δ)
Original Binder				
S-28	58	1275	72.9	1275
V-28	64	1658	86.9	1735.33
RTFO Binder				
S-28	58	3719	82.9	3748
V-28	70	2315	68.4	2492

The performance grade (PG) at a high temperature for these two binders can be evaluated based on the PG standard. The PG for these two binders are 58°C and 64°C for S-28 and V-28, respectively. The multiple stress creep recovery (MSCR) analysis, also as specified in AASHTO TP-70, and MP-19 were carried out to quantify the non-recoverable creep compliance (J_{nr}) and the recovery of each binder, both original and rolling thin film oven (RTFO) binders. Because the temperature to conduct the HWT testing was 50°C, 50°C was used in the MSCR testing. The summary results of each binder are presented in Table 3-6.

Table 3-6. The MSCR Analysis Summary

Binder Types	Parameters	Average	STD	COV
Original Binder				
S-28	Average % Recovery (3.2 kPa)	0.89	0.056	6%
	Average Jnr (3.2 kPa)	2.29	0.223	10%
V-28	Average % Recovery (3.2 kPa)	34.64	1.151	3%
	Average Jnr (3.2 kPa)	0.51	0.014	3%
Rolling Thin Film Oven (RTFO) Binder				
S-28	Average % Recovery (3.2 kPa)	0.81	0.296	8%
	Average Jnr (3.2 kPa)	2.38	0.018	1%
V-28	Average % Recovery (3.2 kPa)	30.80	1.219	4%
	Average Jnr (3.2 kPa)	0.96	0.009	1%

Non-recoverable creep compliance (Jnr) at 3.2 kPa and the percent of recovery at Jnr 3.2kPa results were reported for both original and RTFO binders. The results show that the Jnr of the V-28 binder is less than that of the S-28 binder. This means that, at the same traffic level, the V-28 binder can be more resistant to creep behavior than the S-28 binder. The percent of binder recovery also shows that the V-28 binder's capability to recover was greater than that of the S-28. As seen in Table 3-6, after releasing the constant load, almost fully permanent deformation was observed in the S-28 binder.

The mix designs were evaluated using a different gradation of aggregate and binder replacement. The mix designs used in this study are provided in Table 3-7.

Table 3-7. Summary of Hot Mix Asphalt Mix Designs.

Aggregate Types	Mixture Types	Binder Type	Binder Replacement (%)	N_{design}	AV (%)	VMA (%)	VFA (%)
Granite (Cisler)	MT	S-28	18.2	115	3.76	15.84	76.24
	MT	V-28	18.2	115	3.38	15.36	77.98
	HT	S-28	7.1	160	4.84	17.46	72.27
	HT	V-28	7.1	160	3.99	16.25	75.43
Limestone (Waukesha)	MT	S-28	16.1	115	3.92	16.35	74.36
	MT	V-28	16.1	115	4.10	16.39	74.97
	HT	S-28	9.8	160	4.02	14.97	73.11
	HT	V-28	9.8	160	4.48	15.24	70.59

All mixes presented in Table 3-7 were designed to compact and test in the HWT test to determine the correlation between dry and wet HWT indices. Mix gradations are provided in Appendix A.

The subsequent sections of this chapter are dedicated to presenting the general concepts and procedures of the tests developed in the experimental plan. The test results and detailed analyses will be addressed in Chapter 4.

3.2 Mechanical Testing of Asphalt Mixtures

According to the experimental design, three mechanical tests were selected for this study. Experiments 1 through 3 aimed to determine aggregate packing of the dry HWT samples, correlate the results between the dry HWT and confined FN test, and correlate the parameter indices of the failure curve between wet and dry HWT tests. Therefore, two mechanical laboratory tests were used to test the samples: HWT device and confined flow number test.

3.2.1 Hamburg Wheel Tracking Testing

3.2.1.1 Wet Hamburg Wheel Tracking Test

The HWT test was used to measure the effects of rutting and moisture damage performance. The HWT test displays sensitivity to the premature failure of the HMA mixtures due to improper binder stiffness, weak aggregate packing, moisture damage, and insufficient adhesion between the aggregate and binder. The HWT uses a steel wheel rather than a rubber wheel, which was utilized in the British device. The procedures for using HWT and preparing specimens are specified in AASHTO T324. Based on the standard, the device is operated by moving a steel wheel backward and forward across the surface of HMA specimens (cylindrical or slab/cubical) submerged in a constant temperature water bath specified in AASHTO T324 as 50±1°C. The equipment is capable of testing a pair of specimens simultaneously. The steel wheels have a diameter of 203 mm (8 inches) and a width of 47 mm (1.85 inches) and oscillate at 52±2 passes per minute. Each steel wheel weighs 158 lbs. The typical setup of the HWT device, specimen preparation, and failure specimens are shown in Figure 2-3. The rut depth data were recorded by the LVDTs at the side of the wheel. The deflection of the LVDTs collected begins at 0 mm. As the wheel runs over the specimen, the LVDTs record the rut depth of each cycle, with a maximum of 11 points along the test specimen at an accuracy of 0.01 mm, as shown in Figure 3-3. The device automatically ends the test when either the preset number of wheel passes or a rut depth of 20 mm (0.8 inches) is reached. The test duration when considering 20,000 passes including a curing time of 30 minutes in the water with a specified temperature is approximately 7 hours. However, in some tests the specimens fail early, and test times are shorter.

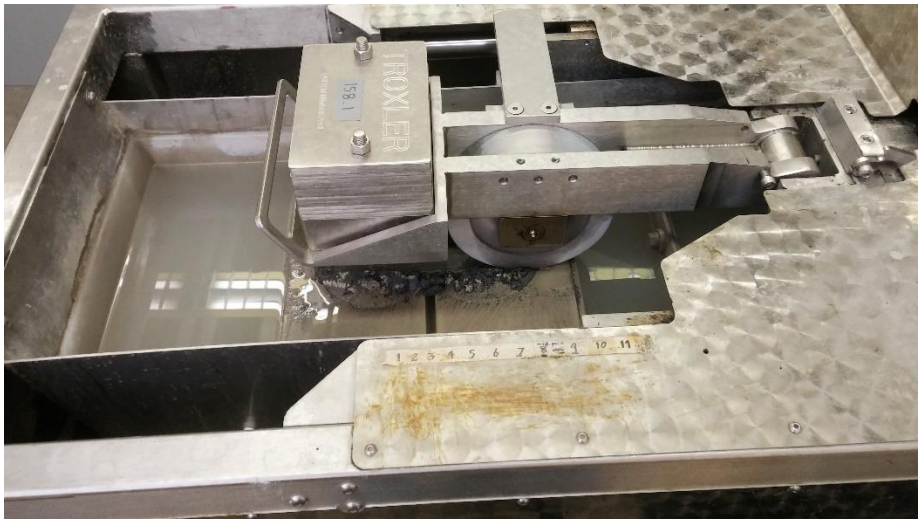

Figure 3-3. The Position of 11 Points Recorded Along the Test Specimen.

3.2.1.2 Dry Hamburg Wheel Tracking Test

The device used to conduct the experiment was the same as a wet HWT. The load of the wheel was 705±4.5 N (158 ± 1.0 lb). The wheel reciprocates over the specimen with the position varying sinusoidally over time. However, this study used the test in the dry condition with the specified temperature. The HWT device used in this study is manufactured by Troxler with a single wheel, as shown in Figure 3-4. The conditions for conducting the tests in this study followed the same as specified in AASHTO T324 in the wet HWT test as follows:

Conditions

- Temperature: 50°C±1°C
- Speed of the wheel test: 52±2 passes/minute

Figure 3-4. Photograph of the Hamburg Wheel Tracking Device.

The rationale behind using the specified conditions of speed, wheel loading, and sample thickness in the HWT test can be addressed as follows:

1. The wheel moves reciprocally across the top of the specimens at 52 passes per minute, with a total travel of 280 mm in one direction; the average speed can be approximated as 1.1 km/h (Stuart, 2002). The speed was based on an empirical test (Aschenbrener, 1994).

2. The load applied on a specimen is 703 N (158 lbs), where a steel wheel 47 mm (1.85 inches) wide rolls 230 mm before reversing direction. The average contact stress of 730 kPa or 105 psi is approximated as the stress by one rear tire of a double-axle truck. (Beecrof, 2014). The manufacturer results produced a load of 158 lbs because tandem- and single-axle vertical stress with a braking condition and a non-braking condition are in the 69–132 psi range (Hajj, 2010), which corresponds to the average contact stress applied to a specimen (105 psi) in HWT.

3. In the field, the minimum lift thickness of a specimen should be at least three times the nominal maximum aggregate size (NMAS) to ensure that the aggregate can be oriented during compaction to achieve the required density and to ensure that the mix is impermeable. Also, a WesTrack Forensic Team (1998) study indicated that a laboratory rut depth of 14 mm would be expected in a field rut depth of 12.5 mm. Therefore, the average thickness of 62 mm is thick enough to observe the rut depth and corresponds to a nominal maximum aggregate size.

3.2.2 Confined Flow Number Testing

Confined flow number testing was conducted in an AMPT, as shown in Figure 3-5. Nowadays, WisDOT uses this device to carry out the lab test. The confined flow number procedure has not yet been standardized as of the time of this writing. However, many researchers use a confined flow number test to determine the permanent deformation of the asphalt mixture. It is believed that confining pressure is needed to differentiate the difference in rutting resistance for various mixture types as it can eliminate the premature failure of tertiary flow (Quintus et al., 2012). In fact, the AMPT equipment is able to test dynamic modulus, flow time, and flow number of the asphalt mixture. The temperature, deviator stress, and confining pressure condition can be controlled inside an environmentally controlled chamber using AMPT software. The conditions to conduct the tests were in accordance with NCHRP 719 and WHRP 0092-08-06, as follows:

Conditions

- Temperature: 50% reliability high-performance grade temperature, without traffic or speed adjustments, from LTPPBind3.1 at a depth of 20 mm for surface courses and the top of the layer for intermediate and base courses.
- Air Void Content: 7.0%± 0.5%

- Confining Pressure: 69 kPa
- Repeated Deviator Stress: 483 kPa

Figure 3-5. Photograph of the AMPT

Why these conditions were used in the confined pressure testing in laboratory were addressed in Chapter 2.

3.3 Image Processing and Analysis System 2 (IPAS^2)

IPAS2 is a tool to analyze aggregate structure in asphalt mixture in this study. The analysis in IPAS2 gives the contact length and orientation angle results. These parameters were used to determine the aggregate structure in HWT and confined FN samples. The software interface shown during data analysis is shown in Figure 3-6. After image processing is completed, the contact length data is obtained from a text file. For orientation analysis, there is a separate analysis which as shown in Figure 3-7. Results for orientation angle are given as both text file and the bar charts as shown in Figure 3-8.

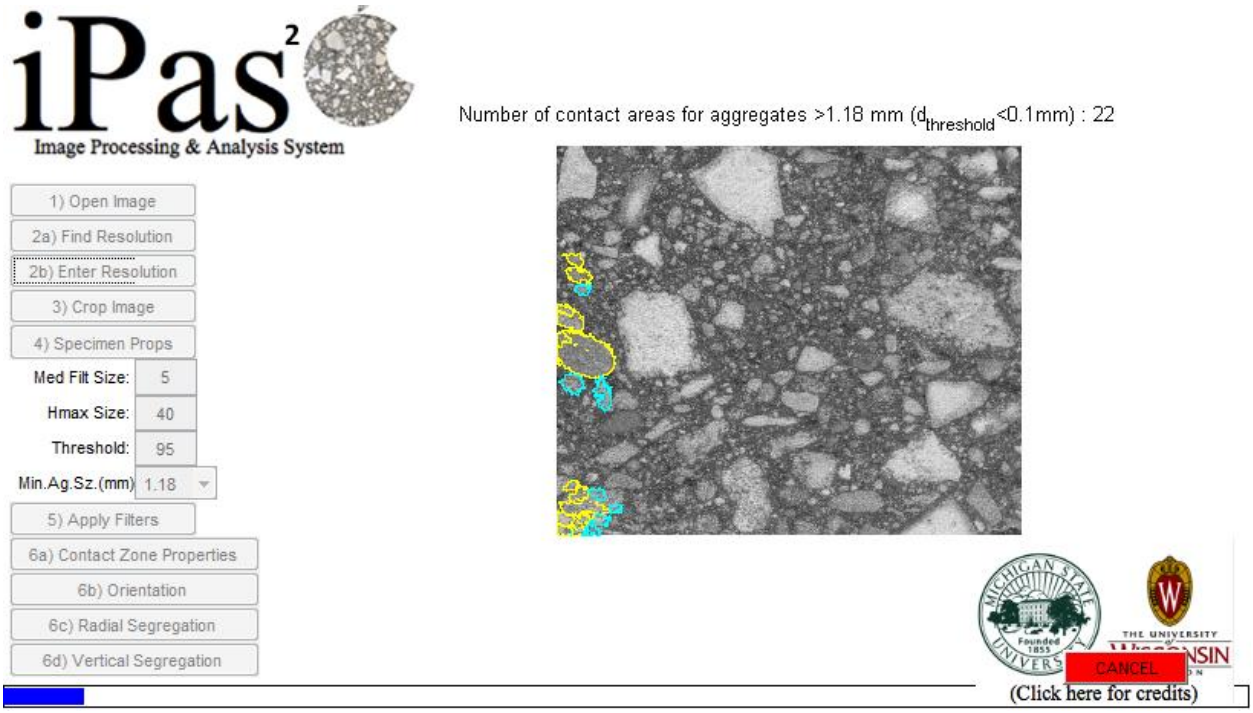

Figure 3-6. The Contact Zone Properties Analysis Part in IPAS^2

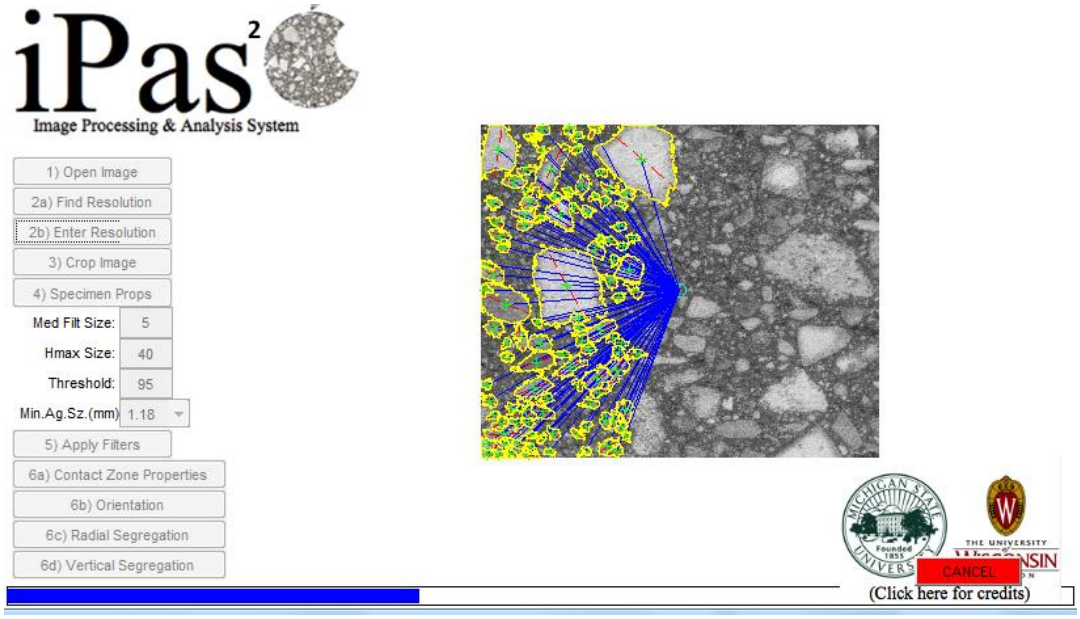

Figure 3-7. The Orientation Analysis Part in IPAS^2

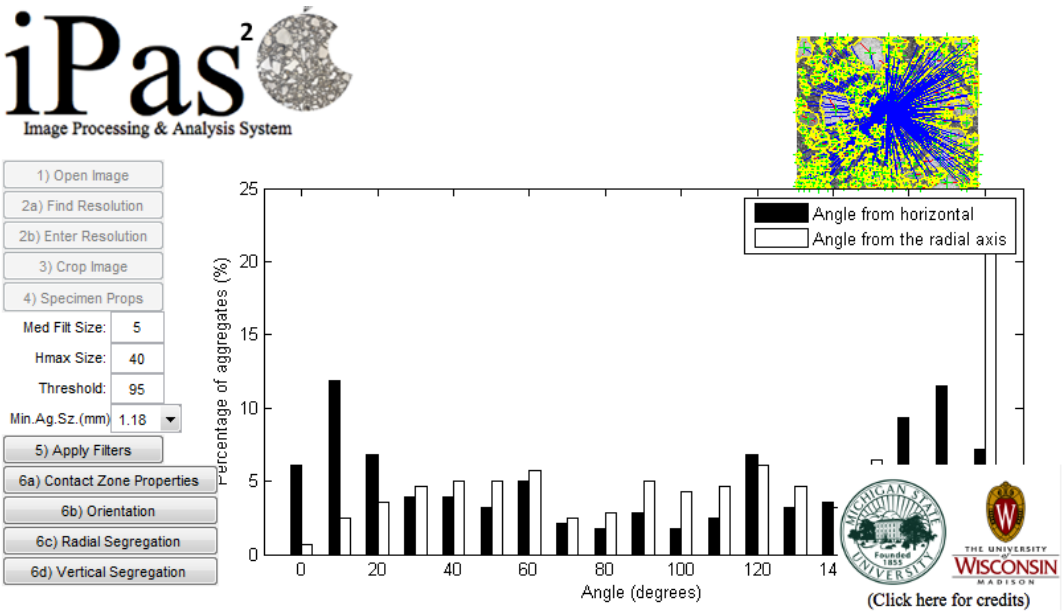

Figure 3-8. The Orientation Angle Bar Chart Showing The Percentage of Aggregate in Each Angle Part in IPAS^2.

4 TEST RESULTS AND DATA ANALYSIS

The results of previously described test methods and statistical analysis are presented in this chapter to show the condition of aggregate packing after dry HWT testing, the correlation between HWT and confined as well as unconfined FN test data, and the correlation between dry and wet HWT parameter indices. Furthermore, multiple replicates for each mix were tested, allowing for the examination of the reliability of each test method. The statistical method of analysis of variance is also used to examine further if relevant controlled factors influence the rutting measurements from the HWT testing.

4.1 Evaluation of Rutting Mechanism by Hamburg Wheel Tracking Test

The mechanisms of permanent deformation measured in this study need to be evaluated during each failure stage prior to analyzing the aggregate packing in the mixtures. In the following sections the method to determine the tertiary point, deemed to be the instability point in the FN test, is first explained. Then, the aggregate structure analysis of asphalt mixture in each stage of the rutting measurements is presented.

4.1.1 The Tertiary Point in Dry Hamburg Wheel Tracking Test

The output of HWT includes the permanent deformation accumulation as a function of loading passes. The typical output includes three main zones: (1) initial consolidation, (2) creep slope, and (3) stripping (or tertiary) slope. In case of wet condition, the stripping slope is generally related to the effect of stripping of binder from aggregate surface or the weakening of the mastic due to water diffusion (also called moisture damage). In case of the dry Hamburg, the tertiary slope is generally related to the point of mixture instability and it also called the flow number at which there is a rapid increase in rutting rate (slope) of sample response. The points of change in rate are called Stripping Inflection Point, or Tertiary Point in the wet and dry

condition, respectively. The stripping inflection point is indicative of the intersected point of creep slope and stripping slope at the failure by moisture. Similarly the Tertiary Point is the intercept point of the creep slope and tertiary slope.

As specified in many research studies, the flow number test is the prevalent approach to correlate the laboratory permanent deformation testing results to the field performance. Several models have been tried to fit the flow number curve as illustrated in Figure 4-1. Biligiri et.al (2001) concluded that Francken model is the best method to determine the curve fitting and calculate the flow number (the tertiary point). Therefore, to define the output of the dry HWT test, Francken model was first utilized.

The typical results of the dry HWT are illustrated in Figure 4-2. In the plot, the y-axis shows the rut depth increasing with number of passes. The rut depth drastically increases at the beginning of passes, then exhibits a relatively constant slope until finally exhibiting a somewhat steeper slope. Considering the curve shape, it is observed however that the tertiary slope is not clearly observed and thus the use of the Francken model should be carefully validated before applying it to the dry Hamburg test results. Similar to dry Hamburg test, the wet HWT results show 3 stages of the rutting as shown in Figure 4-3. However, the output of the wet test shows a very clear increase in slope as the moisture effects could weaken the sample. Therefore, it is commonly acknowledged that different definitions should be used to describe the failure mechanisms; since the wet HWT is tested in water and shows the premature rut changed on the curve, the final stage of rutting is described as the stripping slope.

In addition to the Francken model, the power law has been used in many studies for prediction of pavement rutting in the field. The power law does not consider the tertiary stage

and instead focus on the primary and secondary creep stages as the main pavement distress mechanism (Witczak et. Al. 2002).

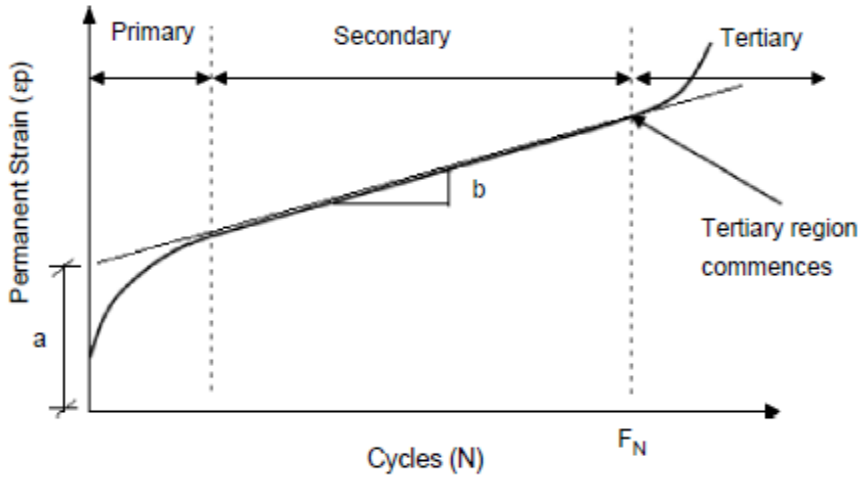

Figure 4-1. Typical Relationship between Permanent Strain and Number of Cycles in Repeated Load Permanent Deformation Test. (Biligiri et, al. 2001)

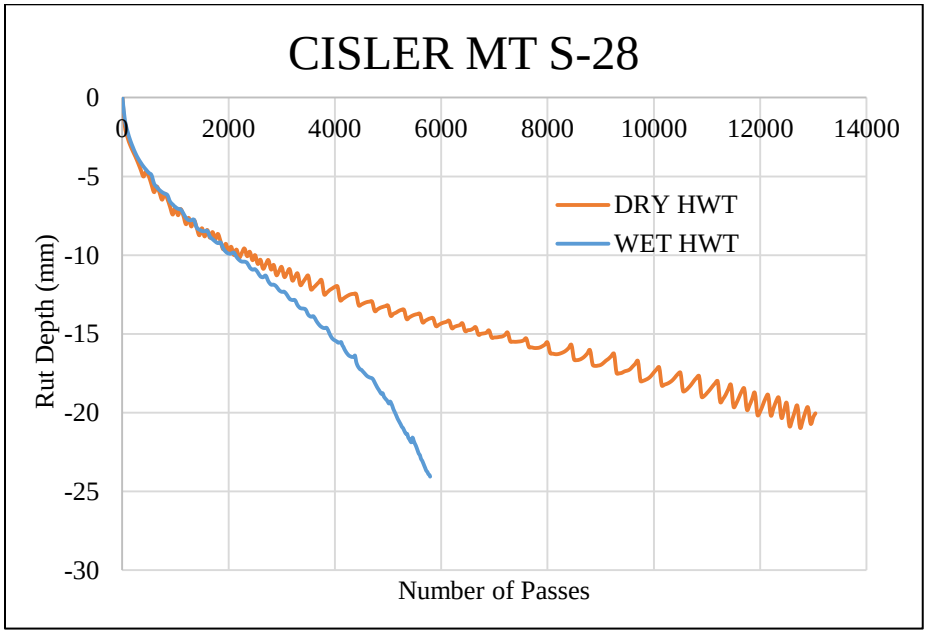

Figure 4-2. Typical results for Rut Depth vs. Number of Passes in the Dry and Wet Hamburg Wheel Test

4.1.1.1 Francken Model Data Analysis

The data analysis conducted using the Francken composite model to fit the results is presented in this section. The steps used to determine the tertiary point values were as follows:

Step 1: Invert the curve to a positive value. The values on the y-axis need to be positive and be converted from rut depth to strain as shown in Figure 4-3.

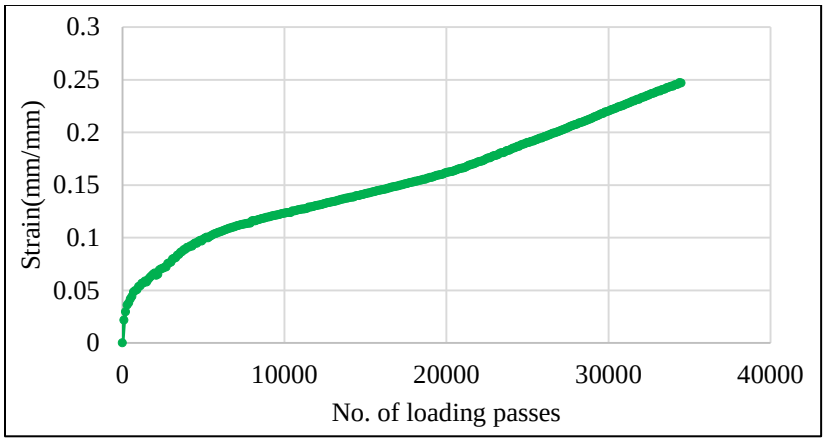

Figure 4-3. Inverting the HWT plot to positive value and Converting the rut depth on y-axis to Strain

Step 2: Use the Francken model equation to fit the curve.

$$\epsilon_p(N) = AN^B + C(e^{DN} - 1) \qquad 4\text{-}1$$

Where:

$\varepsilon_p(N)$ = permanent deformation or permanent strain;

N = number of loading cycles or passes; and

A, B, C, and D = regression constants.

Step 3: The first derivative of the Francken model on number of loading passes would produce the strain rate of change (composite model) as described in Equation 4-2. This equation represents the strain slope. These two steps are illustrated in Figure 4-4.

$$\frac{d\epsilon_p}{dN} = (A \times B \times N^{(B-1)}) + (C \times D \times e^{DN}) \qquad 4\text{-}2$$

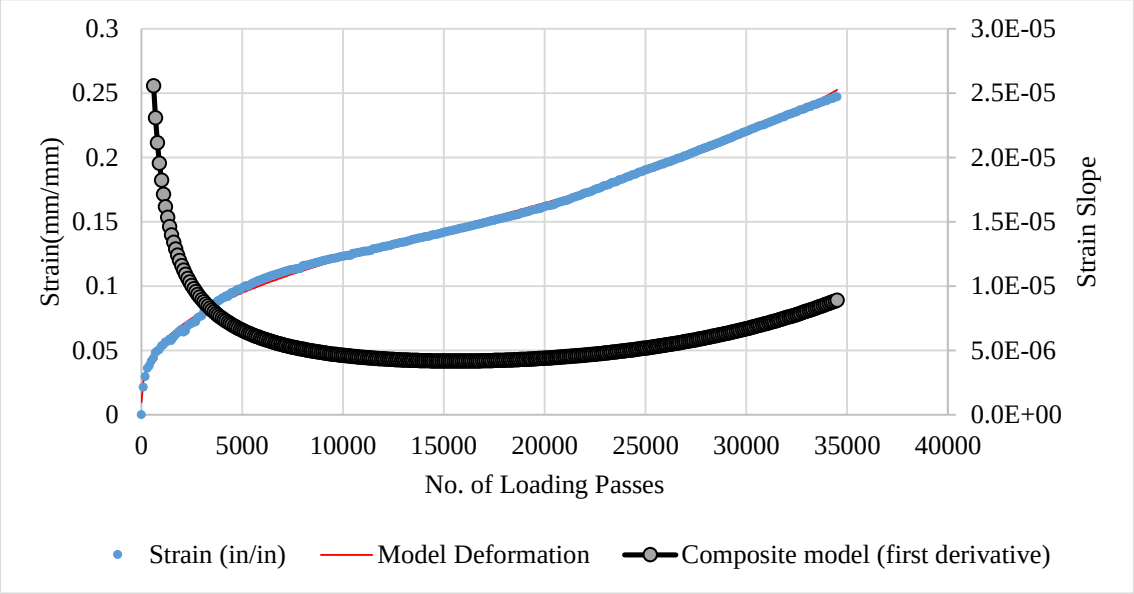

Figure 4-4. Fitted Curve and Strain Rate on HWT Output.

Step 4: The tertiary point is mathematically calculated by the second derivative of Francken model using Equation 4-3. This would yield the lowest point of the second-degree polynomial curve (strain slope) plotted against number of loading passes. The tertiary points are illustrated in Figure 4-5.

$$\frac{\partial^2 \epsilon_p}{dN^2} = (A \times B \times (B-1) \times N^{(B-2)}) + (C \times D^2 \times e^{DN}) \qquad 4\text{-}3$$

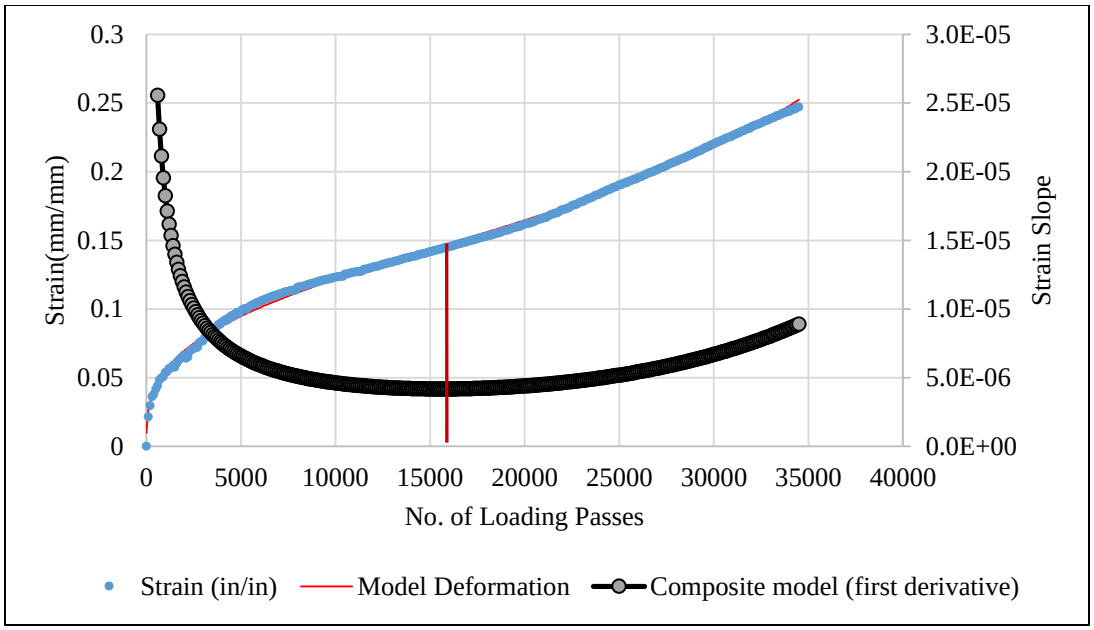

(a)

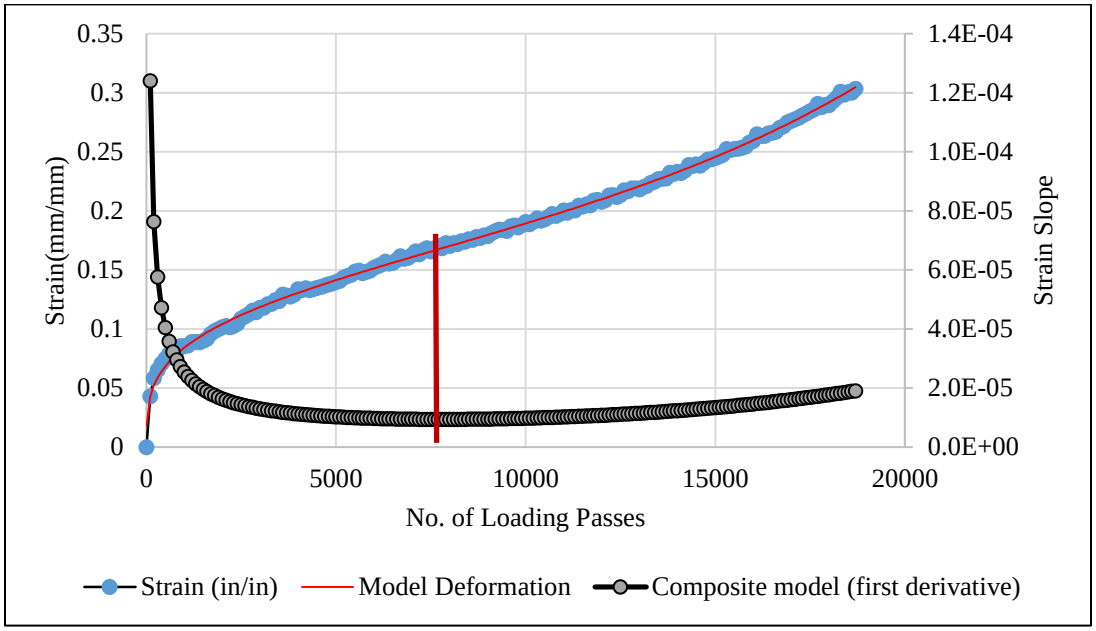

(b)

Figure 4-5. The Tertiary Point Determined by Francken Model for (a) E-10 Mixture (b) E-3 Mixture.

4.1.1.2 Power Law Model Data Analysis

Another widely used model does not recognize the Tertiary zone in the rutting mechanism and assumes that the main stages are the initial consolidation and the secondary creep. The concept behind this model is that tertiary stage represents the ultimate failure and thus need not to be modeled.

As shown in Figure 4-1 , the Power Law model can be fitted such that a slope is determined from the power factor (b) in the equation of $\varepsilon = (aN)^b$. The creep slopes of Confined FN test and Dry HWT can be determined and compared to evaluate if using the 2 tests can give same information.

4.1.2 The Mechanisms of Permanent Deformation of Asphalt Mixtures in the Hamburg Wheel Tracking Test Using IPAS2 Imaging software

Permanent deformation can be caused by either shear deformation failure or densification, or by the combination of shear failure and densification. Roohi (2014) showed the correlation between the total proximity lengths (TPLs) of aggregates estimated from image analysis and loading cycles in uniaxial loading testing. The results indicate that the main mechanism of permanent deformation is densification in the primary zone. The material mainly loses some air voids rapidly which increases aggregate packing due to the proximity of more aggregates. The stiffening of mixtures after the primary stage is due to the higher packed aggregates as compared to the initial stage of mixture densification.

In secondary zone, the aggregate skeleton starts deformation due to shearing. Since the aggregate contacts are not perfectly oriented in the axial loading direction, the aggregate skeleton begins deformation along the directions. However, since the aggregate skeleton is still stable at most of the proximity zones, there is no rapid deformation or failure of the specimen. In the

tertiary zone, the deformation occurs via a loss of load bearing capacity in some parts. When some parts of the aggregate skeleton as the main paths of stress in the material are highly deformed (i.e. localized bulging of a sample), the whole skeleton becomes statically instable due to the loss of load bearing capacity in some parts. Therefore, a drastic deformation starts after a cycle of loading which is designated as flow number (FN). In some samples localized bulging is sufficient for the failure to start; however, other samples may bulge under cyclic loading in symmetric shape due to these localized failures. If the stress level is not high enough or the mixture aggregate skeleton is highly packed, the mixture may never experience the tertiary zone (Low-stress level and highly packed aggregate skeleton reduce the plastic deformation in the aggregate skeleton and asphalt binder).

Since the pavement in the field is confined, using confined testing to determine the aggregate packing in asphalt mixture should better predict the permanent deformation mechanism in the field.

The permanent deformation mechanisms can be considered in three failure stages. Flow number curve presenting permanent strain against load cycle can show the changing of slopes in strain which represents each failure stage in permanent deformation. Figure 4-6 shows the typical FN permanent strain against load cycle.

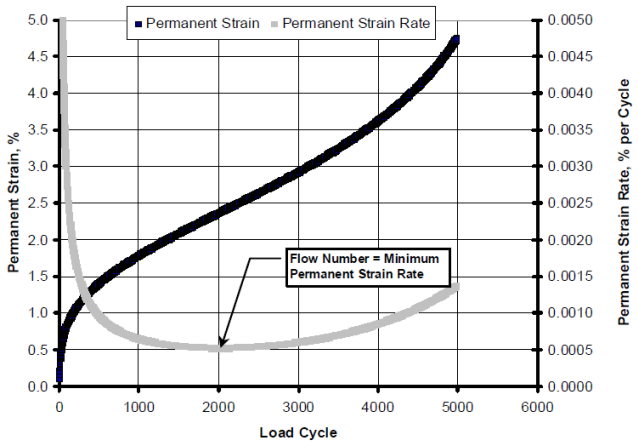

Figure 4-6. The Typical FN Permanent Strain and Permanent Strain Rate Curve against Load Cycle.

The cumulative permanent strain (εp) curve in flow number testing can be divided into three stages: primary, secondary and tertiary. The definitions of the failure occurring in each stage are as follows:

Primary stage – Permanent strain rapidly increases creating an initial high level of rutting with a decreasing permanent strain rate. This is because of a rearrangement of the mix structure with a final concentration of stresses at the surface of contact between the loading plate and sample due to small irregularities (Archilla, 2007), mainly associated with volume change (densification).

Secondary stage – Permanent strain gradually increases with a gradually decreasing (almost constant) permanent strain rate that is also related to volume change (densification); however, shear deformation increases when the permanent strain rate start increasing (Flow Point). Lower rates of deformation during the secondary stage of the uniaxial repeated loading test evoke a more stable mix after initial densification has been achieved, and the structure of the mixture has finished its relocation due to initial traffic compaction (Archilla, 2007).

Tertiary stage – Permanent strain quickly increase with increasing of permanent strain rate. High level of permanent axial strain mainly associated with plastic or shear deformations subjected to ideal no volume change conditions (Witczak,2002).

In this study, two mixes were prepared to quantify the tertiary flow that is adapted from the methodology from the previous section. The objective is to track the change in aggregate packing during cyclic loading process until failure of the mixtures in HWT testing. The target air void for all samples was 7%±0.5%. Two replicate samples were tested for each mixture type to determine the tertiary point, and capture the different zones of behavior (i.e. primary, secondary, and tertiary zone). The test temperature was controlled in the stable temperature of 50°C in dry condition with a wheel load of 158 lbs. Five numbers of loading passes were selected based upon the obtained tertiary point in each mixture to represent untested sample, primary zone, secondary zone, tertiary point, and tertiary zone. These results were compared with the aggregate packing for the untested and the failed samples.

Each failure stage was conducted to analyze the aggregate structure inside the mixed sample. Two mix designs (i.e. E-3 and E-10) were used for evaluating the aggregate contact length at each stage. From the evaluation of flow number curve by Francken model method, the loading pass that represented at each failure stage (i.e. original stage, primary stage, secondary stage and tertiary stage) of two mix designs are presented in Table 4-1.

Table 4-1. Loading Passes of Each Failure Stage for E-3 and E-10 Mix Designs.

Failure Stage	Loading Passes	
	E-3	**E-10**
Original	0	0
Primary	1,000	4,000
Secondary	4,000	10,000
Tertiary	8,000	15,600
Failure Sample (25 mm)	21,169	50,000

Samples after testing exhibited characteristic deformation in the center of the sample as illustrated in Figure 4-7.

(a) Primary stage

(b) Secondary stage

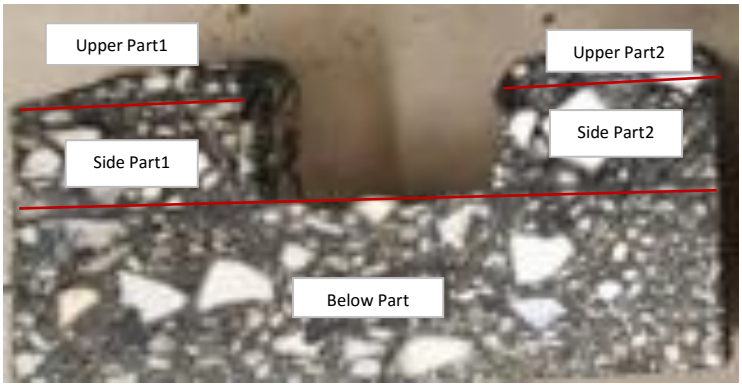

(c) Tertiary stage

Figure 4-7. The Examples of Sample Side image during Testing in HWT and Definition of Each Part for Area Analysis.

As shown in Figure 4-7, only the areas of asphalt mixture were analyzed for the Total Proximity Lengths (TPLs). The cross section areas in each stage for E-3 and E-10 are presented in Table 4-2. Considering to the volume of asphalt mixture in each stage, a width and a thickness change with increasing number of passes, but no change appears in the length. Hence, the area change can be considered as the volume change in each stage. Results show that the cross section area reduces with shifting from one stage to another; however, the tertiary stage and failure stage show minor changes in the cross section area. These results are in agreement with the mechanisms of rutting in each stage of failure in which the volume change occurs in primary and secondary stage (Archilla, 2007), but ideal no volume change occurs after tertiary stage (Witczak,2002).

Table 4-2. The Cross Section Areas of HMA in Failure Stage.

Dimension						
E-3 Secondary	Width (mm)	Height (mm)	Width (mm)	Height (mm)	Area (mm^2)	Area (cm^2)
Below Part	145	43			6235	
	Left		Right			
Side Part	45	18	49	21.5	1864	
					8099	**81.0**
E-3 Tertiary	Width (mm)	Height (mm)	Width (mm)	Height (mm)	Area (mm^2)	Area (cm^2)
Below Part	145	37			5365	
	Left		Right			
Side Parts	44	25	42	27	2234	
Upper Parts	44	8	42	6	302	
					7901	**79.0**
E-3 Failure	Width (mm)	Height (mm)	Width (mm)	Height (mm)	Area (mm^2)	Area (cm^2)
Below Part	145	38			5510	
	Left		Right			
Side Parts	40	21	40	27	1920	
Upper Parts	40	12	40	10	440	
					7870	**78.7**
E-3 Secondary	Width (mm)	Height (mm)	Width (mm)	Height (mm)	Area (mm^2)	Area (cm^2)
Below Part	145	46			6670	
	Left		Right			
Side Parts	48	15	48	15	1440	
					8110	**81.1**
E-3 Tertiary	Width (mm)	Height (mm)	Width (mm)	Height (mm)	Area (mm^2)	Area (cm^2)
Below Part	145	37.5			5438	
	Left		Right			
Side Parts	46	24	43	24	2136	
Upper Parts	46	6	43	6	396	
					7970	**79.7**
E-3 Failure	Width (mm)	Height (mm)	Width (mm)	Height (mm)	Area (mm^2)	Area (cm^2)
Below Part	145	35			5075	
	Left		Right			
Side Parts	40	30	48	27	2496	
Upper Parts	40	7	48	10	380	
					7951	**79.5**

4.1.2.1 Total Proximity Lengths (TPLs) Analysis

The TPLs of samples were estimated by analyzing two parts of the sample during testing. The first part is the section under the wheel loading and the second is the average of two parts on the sides of the loading wheel. The results of the TPLs at various loading passes at the middle point of the sample, under the wheel loading, are shown in Figure 4-8 while those on both sides of the wheel are shown in Figure 4-9.

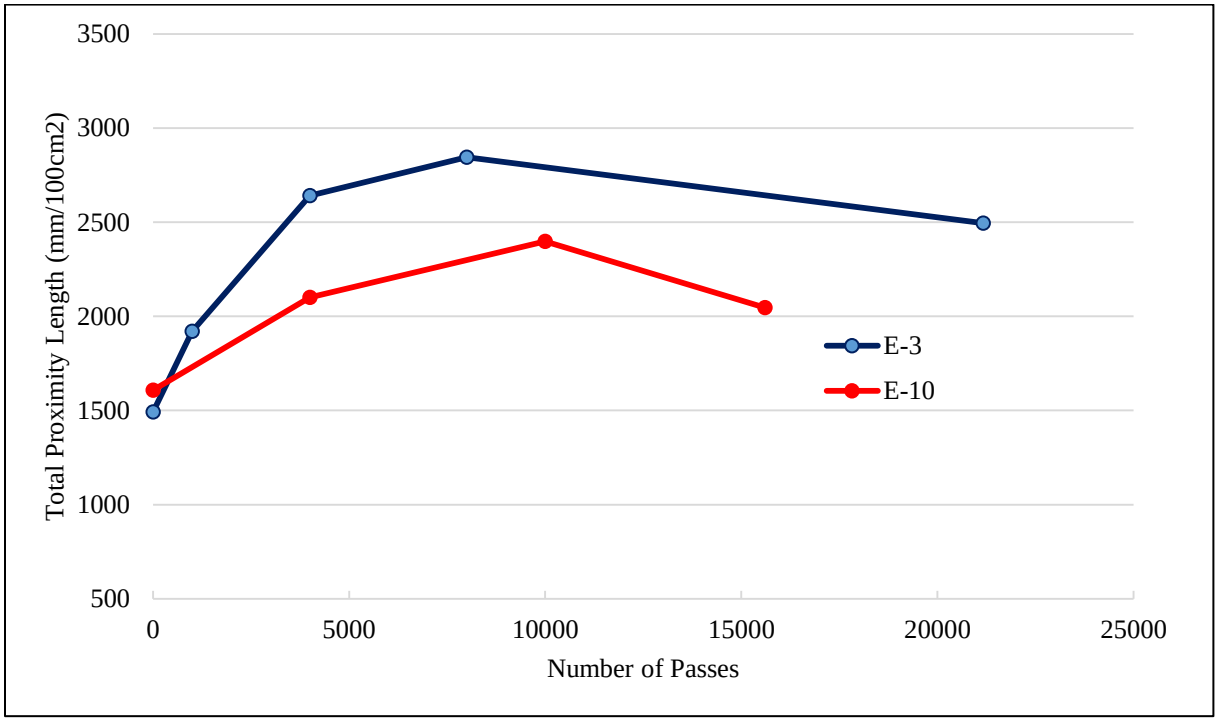

Figure 4-8. The Relationship between TPL for the section below The Loading Wheel in HMA Sample and Number of Passes.

Figure 4-8 shows two mix designs of HMA labeled as E-3 and E-10. The results of TPLs for both mix designs illustrates the same trend in which TPL increases with number of loading pass until a maximum is reached at approximately 8000-10000 passes, then TPLs begins to decrease. The steeper slope in the initial failure zone changes to flatter slope when the number of loading pass increases. This indicates that at primary and secondary zone, the mechanism to the

permanent deformation in HMA is densification under the wheel load followed by better packing of aggregates. However after reaching the peak, dilation and loss of packing of aggregates is dominating the rutting mechanism. It is clear from the images that there is a shear deformation during which the surface of sample on the sides of the wheel are heaving (upward movement). These results are consistent with the mechanisms of permanent deformation in the FN test under confined and unconfined that were reported by Roohi in 2012.

To best describe the mechanism of rutting in the HWT it can be stated that the aggregates are compacted by the steel wheel at the initial stage, thus aggregate skeleton is becoming more packed. In the secondary stage, mixes are in the steady stage during which the aggregate skeleton becomes more packed but at a lower rate. After reaching a maximum packed condition, the skeleton begins deforming along the lateral directions and shifted to the sides of the sample mixes as observed by dilation of aggregate structure. In the last tertiary stage however, the aggregate skeleton deforms rapidly and aggregates move to the sides of the samples, as shown in Figure 4-7 (c). The two sides of the samples are obviously observed to show reoriented aggregate skeleton which is an indication of shear failure. The instability happens as a result of the aggregate skeleton bulging (dilation) in mixture samples. To confirm this mechanism in the Tertiary stage, the TPL analysis of two sides of samples is presented in Figure 4-9.

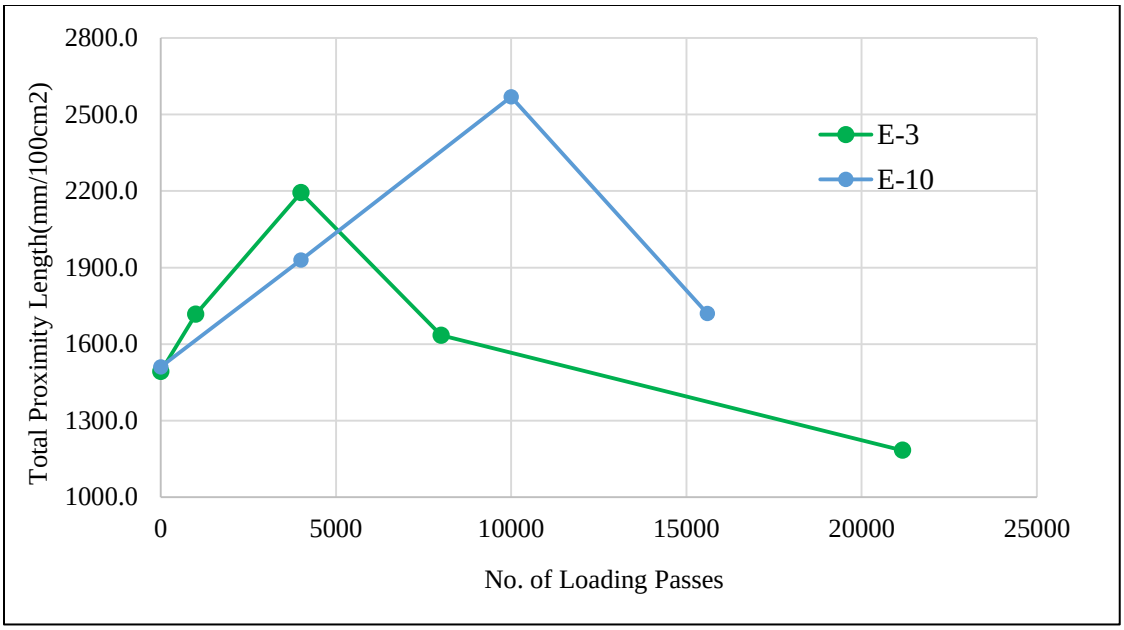

Figure 4-9. TPL vs Number of Loading Passes at Both Sides from the Wheel Track of Sample.

As can be seen in Figure 4.9, the TPLs shows increasing number of loading pass until the secondary zone and starts decreasing until failure. This is consistent with the hypothesis of Roohi (2012) that the failure in mixture and decrease in TPLs during secondary and tertiary zone is due to some localized deformation and discontinuities in the aggregate skeleton of mixes leading to failure of the whole sample and severe reduction in load-bearing capacity of mixture.

4.1.2.2 Shear Deformation Failure Analysis

The shear deformation failure can be also analyzed by the orientation analysis in IPAS2 software, since the shear failure is expected to reorient the aggregate skeleton. Therefore, in this study the IPAS2 is applied to evaluate the orientation of the aggregate before and after testing in the HWT at two sides of samples, as shown Figure 4-10. The orientation angle distribution is given as the results, as listed for the E-3 and E-10 mixes in Table 4-3 and Table 4-4, respectively. The tables present the percentage of the aggregate orientation angle in three ranges

as the combination of vertical and horizontal aggregate angle (0+90+180), the aggregates oriented at the angles of 10 to 80˚, and the aggregates oriented at the angles of 100 to 170˚.

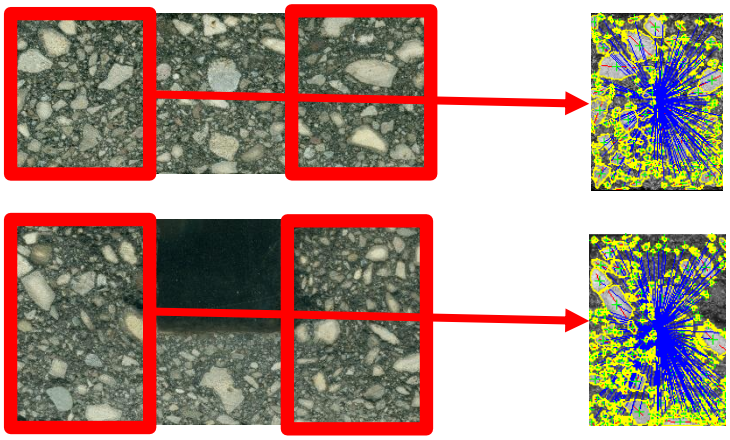

Figure 4-10. The Analysis of Aggregate Orientation using IPAS[2]

Table 4-3. The Orientation of Aggregate of Each Loading Pass in Left and Right Side of the Sample for E-3 Mixture.

Type	Passes	Left Side			Right Side		
		Angle Range			Angle		
		0+90+180	10-80	100-170	0+90+180	10-80	100-170
E-3	0	17%	43%	41%	11%	45%	44%
	4000	14%	47%	39%	12%	38%	49%
	8000	11%	52%	37%	13%	37%	50%
	20000	9%	65%	26%	13%	36%	51%
Orientation Change due to HWT loading		Decrease	Increase	Decrease	Minor Increase	Decrease	Increase

Table 4-4. The Orientation of Aggregate of Each Loading Pass in Left and Right Side of the Sample for E-10 Mixture.

Type	Passes	Left Side			Right Side		
		Angle			Angle		
		0+90+180	10-80	100-170	0+90+180	10-80	100-170
E-10	0	15%	47%	38%	14%	36%	50%
	4,000	15%	48%	37%	13%	35%	52%
	20000	14%	50%	36%	11%	34%	55%
	50,000	14%	56%	30%	10%	30%	60%
Orientation Change due to HWT Loading		Decrease	Increase	Decrease	Decrease	Decrease	Increase

Left side and right side are analyzed separately since the aggregates angle should be oriented differently due to the position of the wheel being to the right of the left sample side and to the left of the right sample side. Results show that the orientation in both mixtures is changed with number of loading pass. On the left side of the sample, the percentage of oriented aggregate angle for 0˚, 90˚ and 180˚ as well as 100˚ to 170˚ decreases with number of passes, while the percentage of the angle of 10˚ to 80˚ keep increasing with number of passes for both E-3 and E-10 mixtures. In an E-3 mix, from 0 passes to 20000 passes the percentage of the angle of 10˚-80˚

increase from 43% to 65%, while E-10 mix is showing change from 47% to 50% in 0 to 20,000 passes. In the right side of the sample, the aggregate orientation is also changing; however, the percentage increase in the range of 100˚-170˚ is form 44% before testing to 51% after 20,000 passes in E-3, and from 50% to 55% in the E-10 mix. These results indicate that significant reorientation of aggregates occurs with increasing number of passes. In the left side of the sample, aggregates show increasing in percentage on 10˚-80˚, and 100˚-170˚ in the right side.

Results of aggregates orientation imply that shear failure occurs in the secondary stage of rutting, which is the main cause of reduction in the TPL.

4.2 Correlation between Dry Hamburg Wheel Tracking Test and Confined Flow Number Test

Since confined flow number is the prevalent testing method that many national research studies in the United States have used, comparing results in confined flow number and dry Hamburg Wheel Tracking test to verify the trends is needed to justify the used of the HWT.

In this study, a few mixed were prepared to determine the relationship between HWT and Confined Flow Number. The objective is to validate the results from the HWT. The target air void for test samples was 7%±0.5%. Two replicate samples were tested for each performance test to determine the tertiary point (flow number) in HWT and Confined axial test, respectively. The testing temperature in HWT used was the same as in the previous study. For confined flow number, the test was controlled by the stable temperature of 50°C which is the 50 % reliability high-performance grade temperature from LTPPBind3.1 at a depth of 20 mm in pavement for the climate of Madison, Wisconsin. The testing conditions of confined flow number were followed NCHRP Project 30A in the development of an improved rutting model for asphalt concrete. This

test uses a confining pressure of 69 kPa and a repeated deviator stress of 600 kPa. The Project 9-30A researchers believe that confining pressure is needed to differentiate the difference in rutting resistance for various mixture types. It should be mentioned that the HWT is considered a self-confined test in the sense that sample is approximately 3 times (150-mm) wide while only the center 50-mm is loaded. Also, the effective stress applied from the wheel is 730 kPa.

4.2.1 Confined Flow Number and HWT Results

As explained in the previous sections, Tertiary Point can be determined by the second derivative of the Francken model method. The model was fitted for both test results and the Flow numbers and Tertiary Points from the confined testing are summarized in Table 4-5. The results show that the tertiary point in HWT testing is in general lower than the flow number from the Confined FN testing by approximately 8,000 cycles. This can be explained by the increased stress conditions that are used in the two tests. The average contact stress of 730 kPa (105psi) for HWT is higher than the deviator stress of flow number testing of 600 kPa (87psi); therefore, the sample in Confined flow number test is expected to fail at higher cycles than the HWT.

Table 4-5. Tertiary Point and Flow Number for E-3 and E-10 Mixtures

Mix Type	Tertiary Point	
	HWT (Passes)	Confined FN (Cycles)
E-3	8800	12670
E-10	15,600	>20,000

4.2.2 Equivalent Cycles Correlation

In addition to comparing the tertiary point or flow number, strain accumulation in the flow number test and converted strain in HWT can be taken into account to correlate the two

methods. The objective is to verify that the mechanisms of rutting are similar and equivalent in both tests. Although the rate of loading is different in the two tests, comparisons of results can be summarized by plotting the relationship per cycle of both tests as shown in Figures 4-11 and 4-12.

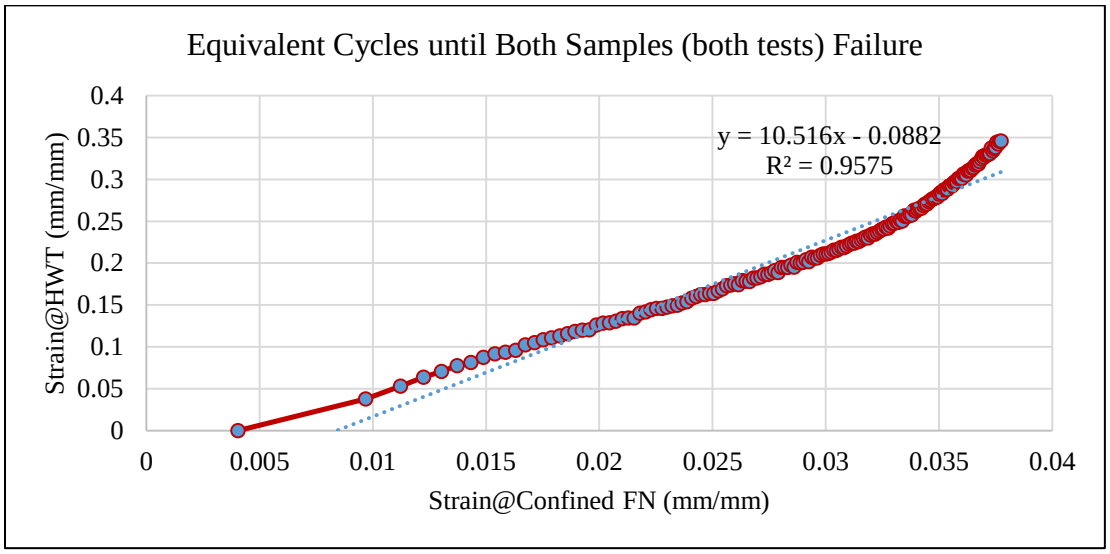

Figure 4-11. Correlation of Equivalent Cycle between Strain of Dry HWT and Confined FN until Both Samples Fail.

Figure 4-11 shows the accumulated strain in the HWT and confined FN until both samples are at a failure stage. Results show strain at confined FN from 0.004 until 0.038 and strain in Dry HWT from 0 until 0.35. The result of the regression analysis indicates that a strong relationship can be established between the strains of the Dry HWT and confined FN with R^2 of 0.958. This shows that the strain rate is linearly correlated of both tests within the secondary creep stage. Nevertheless, it can be seen that there are some differences in the initial as well as the tertiary zones of the testing. Therefore the relationship in the tertiary zone is plotted separately as presented in Figures 4-12 and 4-13.

Considering to the cycle at which tertiary flow starts, the strain in confined flow number up to 0.035 and for HWT up to 0.24 can be considered as the pre-tertiary zones, as presented in Figure 4-12. The linear regression relationship (R^2) improves to 0.997.

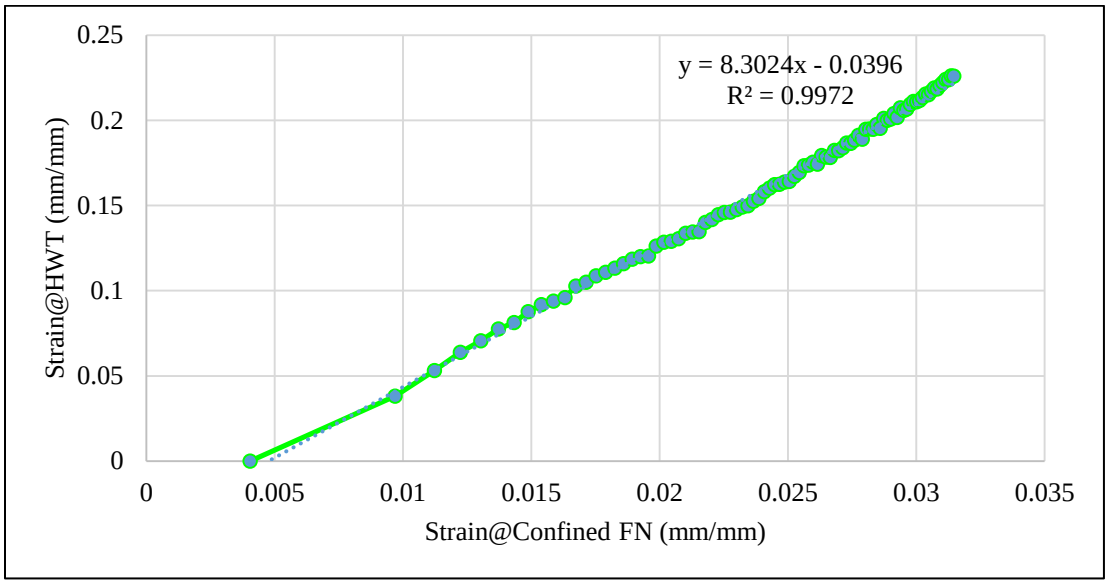

Figure 4-12. Correlation of Equivalent Cycle between Strain of Dry HWT and Confined FN to Tertiary Point of Dry HWT Test.

In addition, if the strain relationship is considered post the tertiary point of HWT, the linear regression shown in Figure 4-13 can be plotted and it is observed that the relationship is also linear and R^2 is at 0.9858.

The results show that before and after the tertiary point, the relationships between both tests are in excellent agreement. This clearly confirms that the mechanisms of failures are similar and despite the difference in the loading rate, stress, and confining conditions.

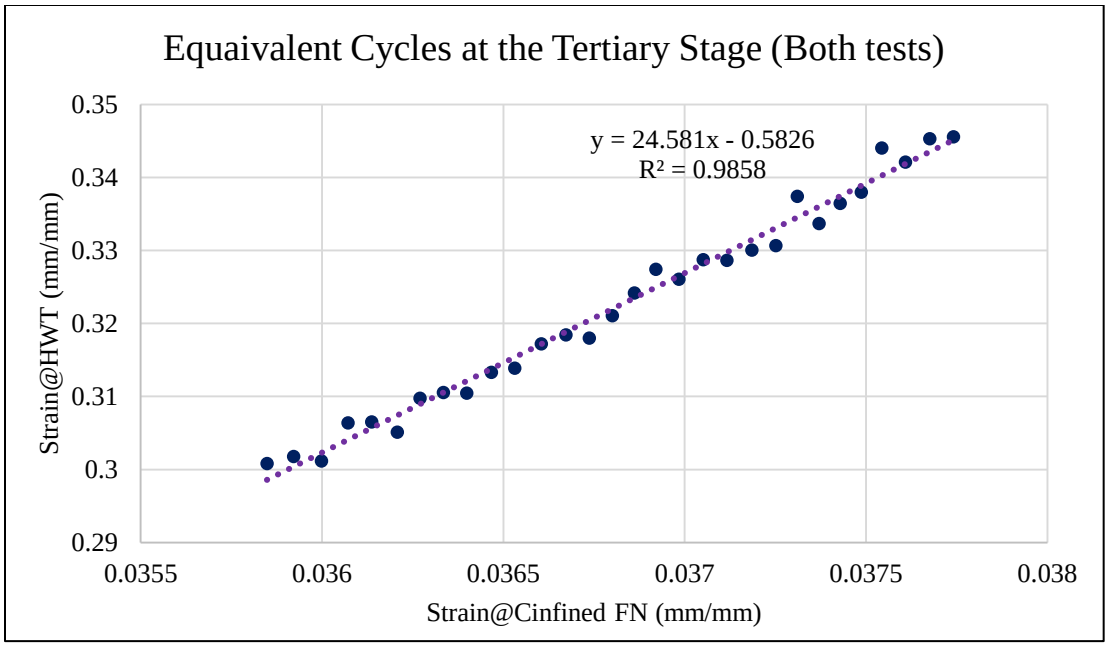

Figure 4-13. Correlation of Equivalent Cycle between Strain of HWT and Confined FN at Tertiary Stage of Both Tests.

It should be noted that the slope in tertiary stage is 24.58, while the slope value of secondary stage for these two tests is approximately 9. This shows that after the tertiary point, the strain relationship between both tests is changed, which could be attributed to the difference in the confinement. More examples of Flow Number versus dry Hamburg are shown in Figures 4-14 and 4-15 for other mixes tested in this study.

Figures 4-14 and 4-15 show the correlations of equivalent cycle between Strain at dry HWT and Confined FN to the tertiary point of Dry HWT test for four mixes. These correlations show excellent linear relationship with R2 in range of 0.970-0.996. However as shown by the correlation lines, the slopes and intercepts of relationships vary among mixes; Therefore, the specifications limits for Dry HWT need to be verified and selected independent of the limits used today for FN.

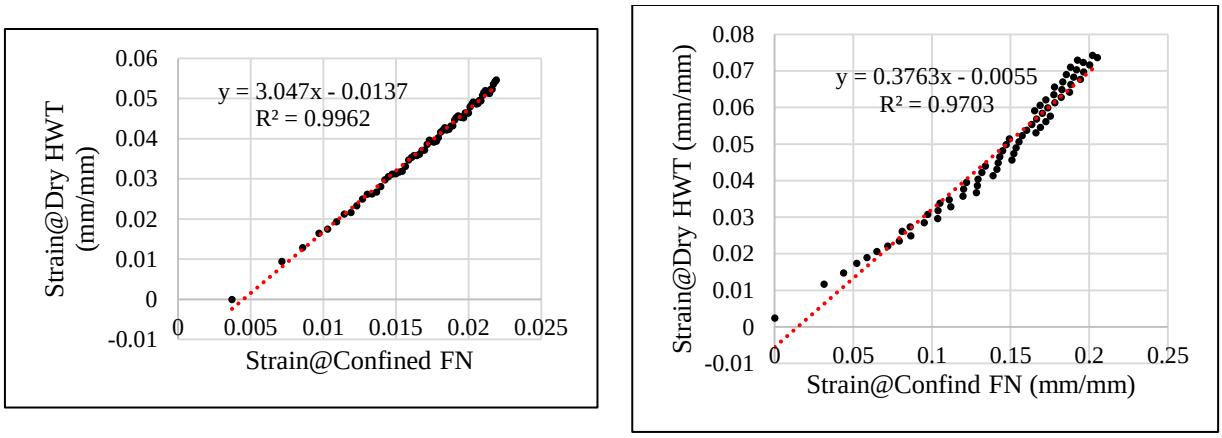

(a) (b)

Figure 4-14. Correlation of Equivalent Cycle between Strain of HWT and Confined FN to Tertiary Point of Dry HWT Test for (a) Cisler-HT-V-28 (b) Cisler-MT-S-28

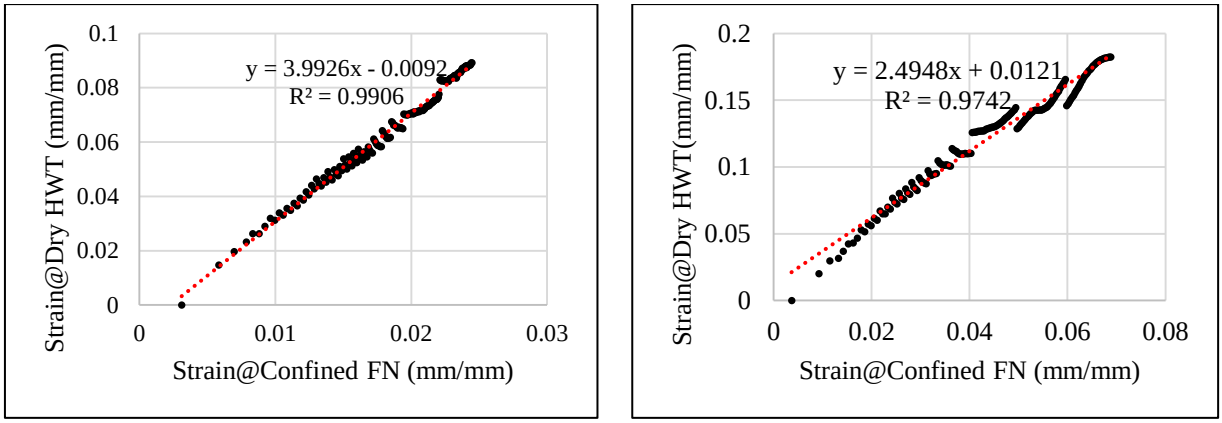

(a) (b)

Figure 4-15. Correlation of Equivalent Cycle between Strain of HWT and Confined FN to Tertiary Point of Dry HWT Test for (a) Waukesha-MT-V-28 (b) Waukesha-MT-S-28

4.2.3 The Creep Slope of Dry HWT and Confined FN

Another method used widely today to model rutting of asphalt pavement is the use of the Power Law. The power law is therefore used for verification if the dry HWT can substitute the confined FN based on determining the creep slope. As explained earlier, the slope acquired from the Francken model is calculated by a minimum value from the first derivative equation as shown in Equation 4-2, while the Power Law can be determined by the power factor (b) in the equation of $\varepsilon = aN^b$. The creep slopes of Confined FN and Dry HWT by Francken model are shown in Figure 4-16 which illustrates the change in strain (mm) as a function of the number of cycles for all asphalt mixtures.

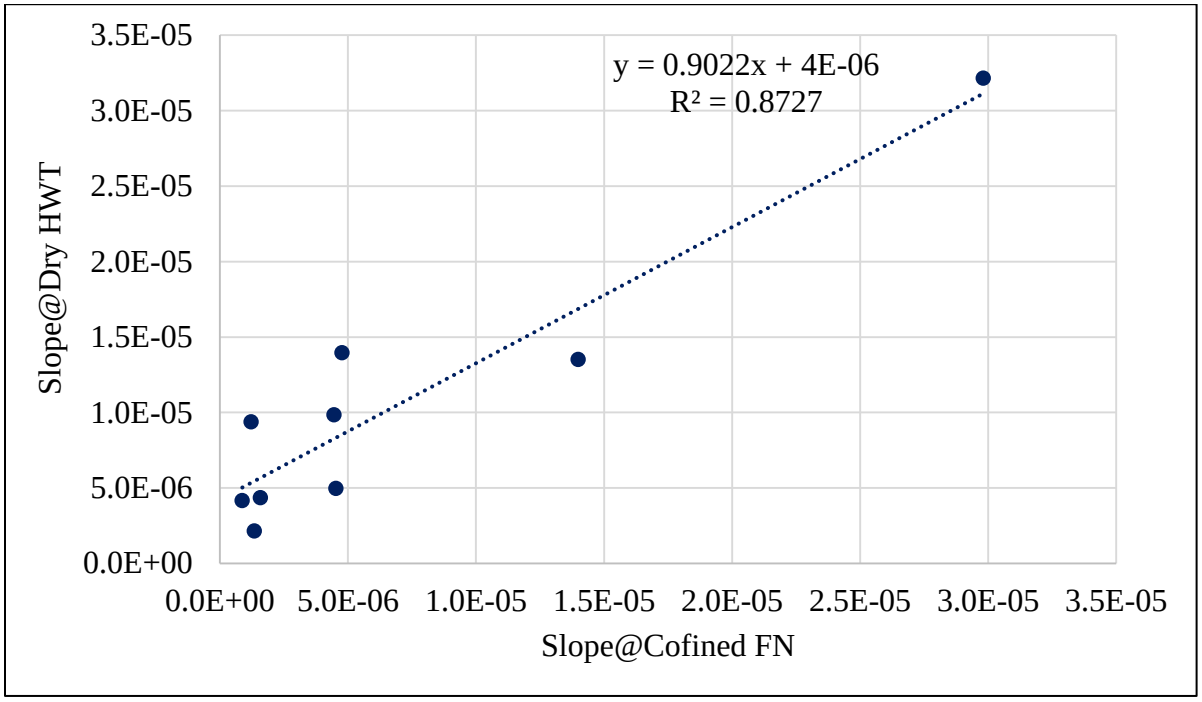

(a)

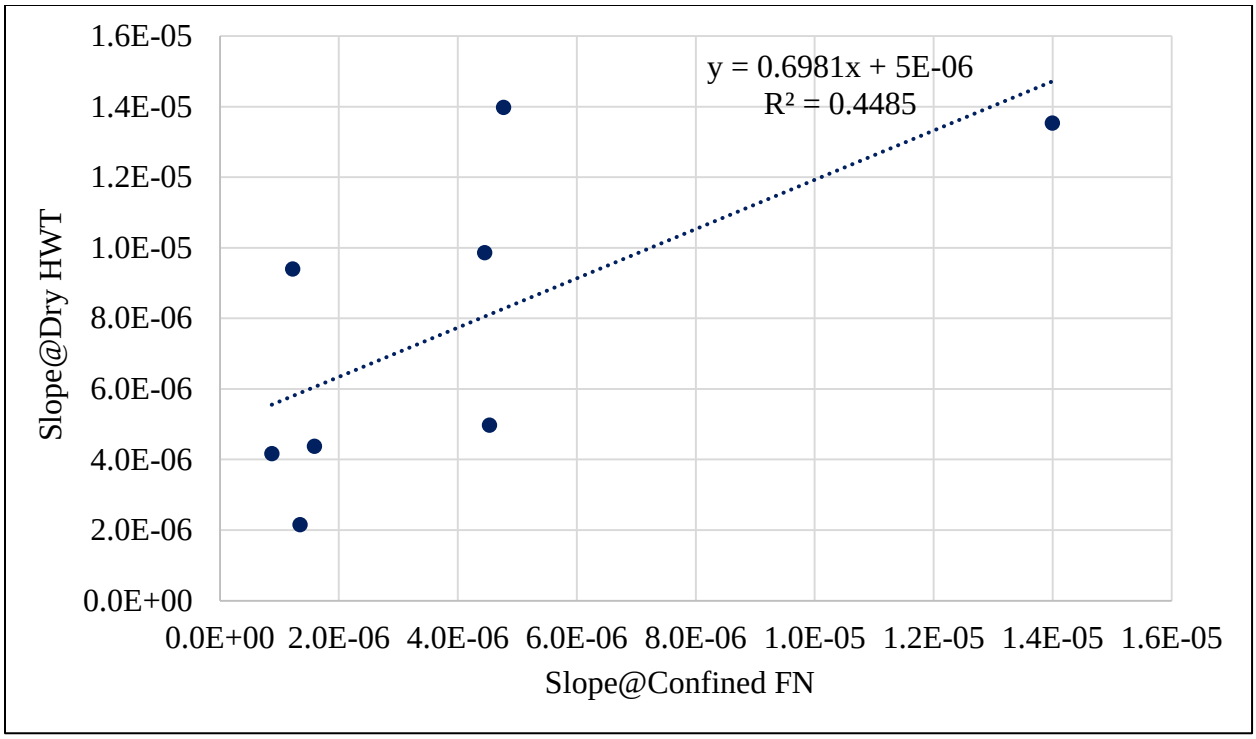

(b)

Figure 4-16. The Correlation of Slope between Dry HWT and Confined FN for (a) All Mixes (b) All Mixes without Cisler MT S-28 by Minimum Value by Francken Model.

Results indicate that a good linear relationship exists between Confined FN slope and Dry HWT slope for all mixtures with a correlation of 87% as shown in Figure 4-16(a). However, the linear regression decreases the correlation to 45% when Cisler MT S-28 mix is removed, as shown in Figure 4-16(b). Since in some mixtures, the tertiart point (FN) did not show in confined FN test, the minimum values from first derivative are selected at the last observed cycle. As a result, the results are not accurate to plot Confined FN against Dry HWT correlation. Hence, the Francken model cannot be considered suitable to determine the creep slope.

For these mixtures that do not show a clear tertiary transition, it could be a better choice to use the Power Law to determine a slope (b) from the Power Law fit. An example of the fit for the data in normal scale and in a log-log plot are shown in Figure 4-17.

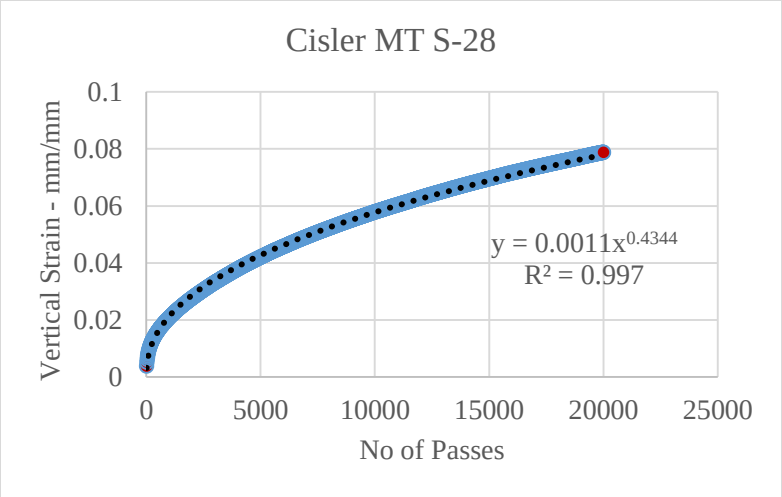

(a)

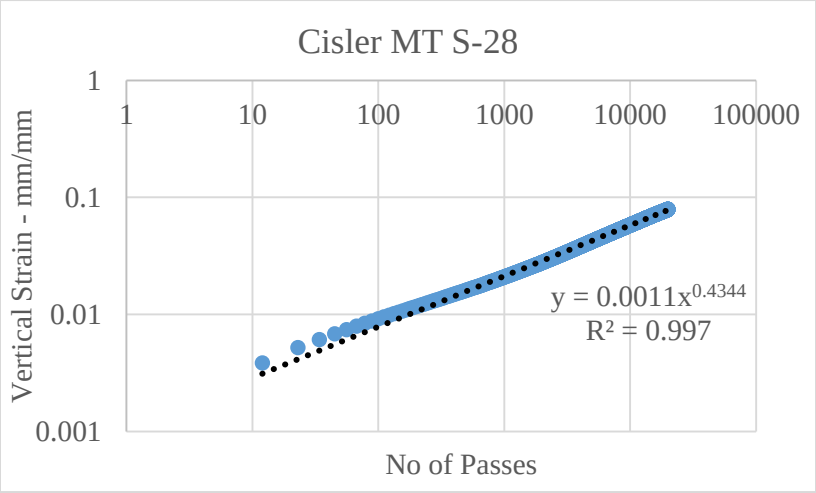

(b)

Figure 4-17. Power Law Fit for HWT results, (a) normal scale, and (b) log-log scale

The slope (b) values for Confined FN and Dry HWT are shown in Table 4-6. It should be noted that all the data points from the dry HWT test were used in fitting the power law without removing the data in the tertiary zone.

Table 4-6. The Slope for Dry HWT and Confined FN by Power Law.

Creep Slope (Power Model)	Confined FN	Dry HWT
Cisler MT S-28	0.52	0.50
Cisler MT V-28	0.43	0.47
Cisler HT S-28	0.43	0.43
Cisler HT V-28	0.28	0.42
Waukesha MT S-28	0.49	0.45
Waukesha MT V-28	0.29	0.41
Waukesha HT S-28	0.17	0.39
Waukesha HT V-28	0.14	0.34

The relationship of the slope values of Confined FN and Dry HWT by Power Law are shown in Figure 4-18 which illustrates that there is no equality between the two tests, but there is a very strong linear relationship.

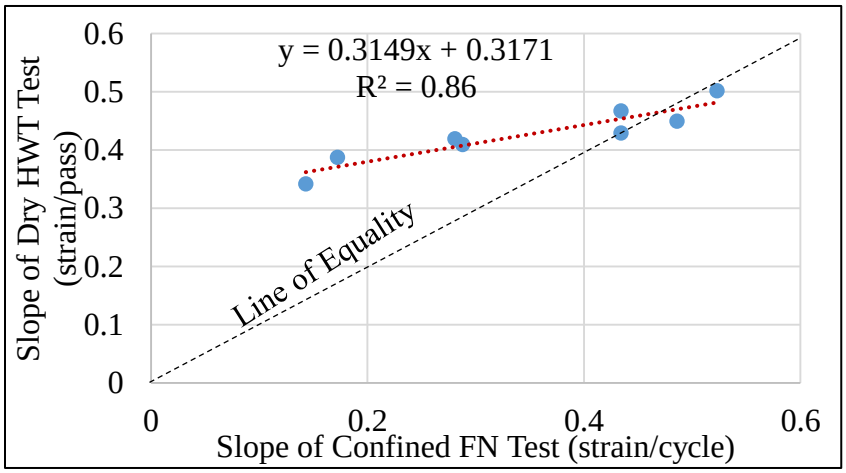

Figure 4-18. The Correlation of Slope between Dry HWT and Confined FN by the Power Law Method.

The results shown indicate that the slope parameters of Dry HWT show a positive and rational relationship with those of Confined FN. A good significant slope relationship can be established between Dry HWT and Confined FN with R^2 of 0.86 as shown in Figure 4-18. Most

of the HT mixes are above the line of equality. These results are logical since the contact stress of Confined FN (87 psi) is lower than that of Dry HWT (105 psi). This is in agreement with previous research from Quintus et.al, 2012 in which it is shown that higher stress resulted in higher strain slope, as shown in Figure 4-19. Therefore, using Power Law to determine creep slope is a suitable method. For the Confined FN at 10 psi confining pressure, it can be shown that the prediction model is as shown in Equation 4-4.

$$Y = 0.3149X + 0.3171, R^2 = 0.8559 \qquad 4\text{-}4$$

Where: Y= Slope at Dry HWT (strain/passes)

X= Slope at Confined FN (strain/cycles)

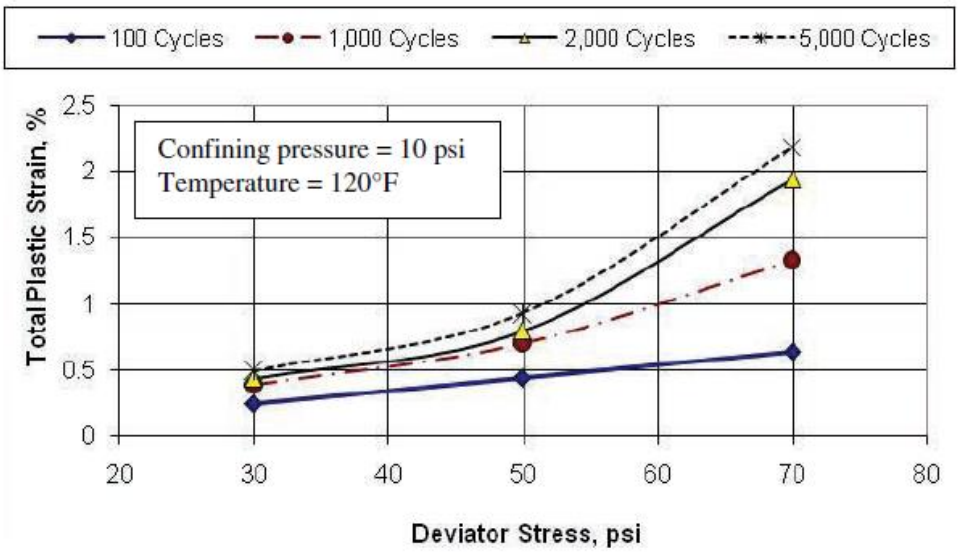

Figure 4-19. Influence of Deviator Stress on Plastic Strain. (Quintus et.al, 2012)

To verify the effect of confinement on the relationship between Dry HWT and FN, unconfined FN test was conducted with the same mixes. Five mixes were selected to evaluate the

Unconfined FN test. The other test condition of Unconfined FN were kept the same as the Confined FN test (same test temperature, and deviator stress), but without confining pressure. The results were plotted as shown in Figure 4-20.

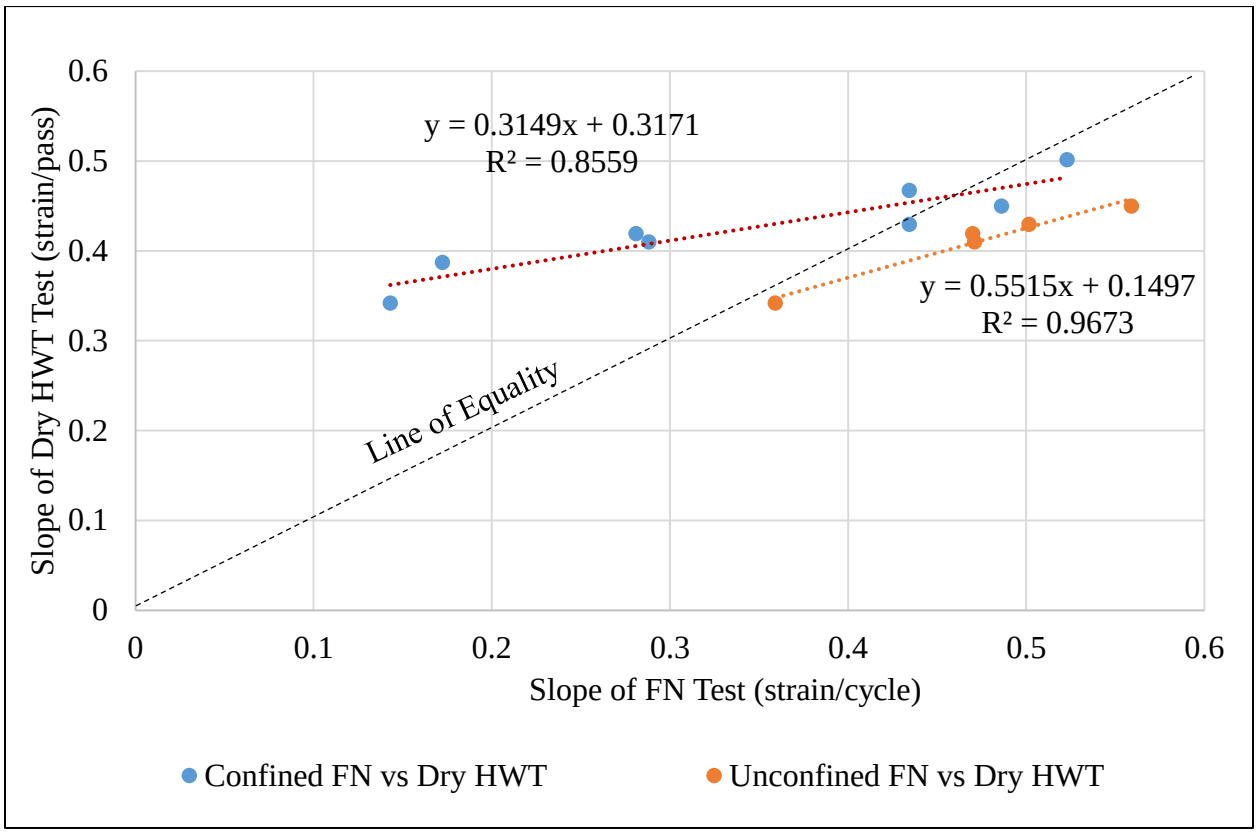

Figure 4-20. The Correlation of Slope between Dry HWT and Flow Number test by the Power Law Method.

Results indicate that the slope parameters of Unconfined FN mixes are under the line of equality. These results are logical since the confining pressure of (10 psi) is expected to reduce the rutting rate (lower value of the slope) as compared the unconfined test. These results are also in agreement with the previous study from Quintus et.al, 2012 in which lower confining pressure resulted in higher creep slope as shown in Figure 4-21. Figure 4-20 also shows that the slope of Confined FN mixtures can be well shifted to Unconfined FN slope in the same trend.

With the significant linear relationship between Dry HWT and Unconfined FN, a simple linear relations as shown in Equation 4-5 can be used.

$$Y = 0.5515X + 0.1497, R^2 = 0.9673 \quad (4\text{-}5)$$

Where: Y= Slope at Dry HWT (strain/passes)

X= Slope at Unconfined FN (strain/cycles)

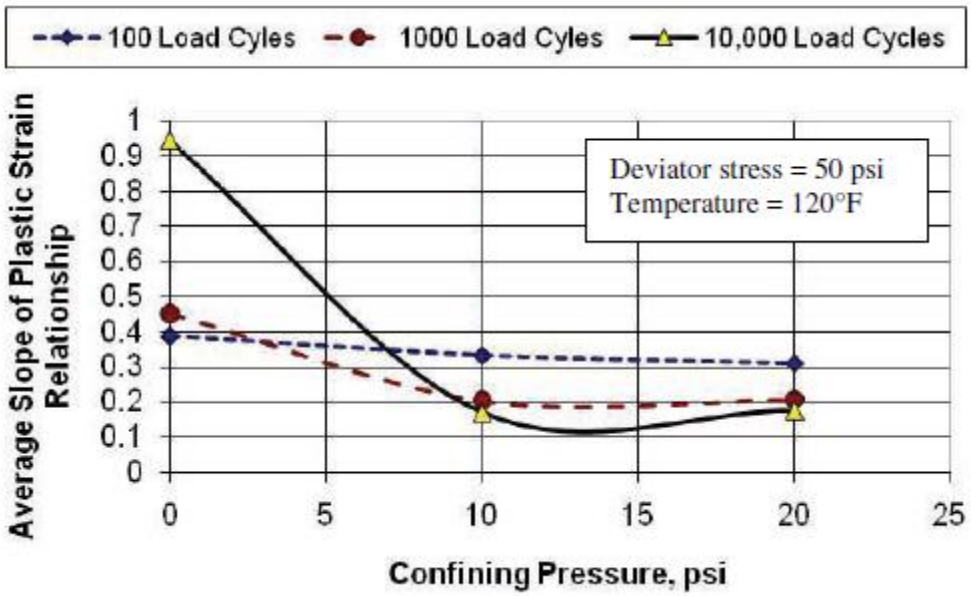

Figure 4-21. Influence of Confining Pressure on Slope from Repeated-Load Triaxial Test. (Quintus et.al, 2012)

In addition, another parameter that can be potentially considered in permanent deformation resistance is an intercept (a). The correlation between the intercepts of Dry HWT and Confined FN is shown in Figure 4-22.

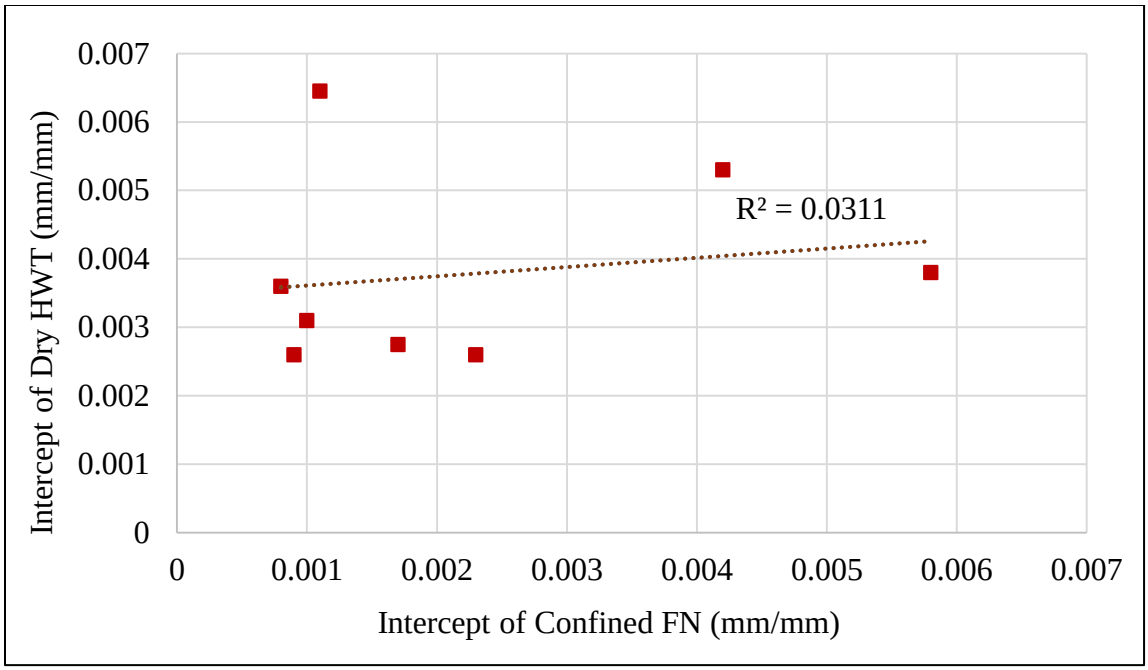

Figure 4-22. The correlation between the Intercepts of Dry HWT and Confined FN by Power Law.

Results show the intercept parameter (a) of Dry HWT show a rational relationship with the Confined FN intercept, but it has a poor measure of correlation. These results are consistent with the results in Witczak, 2002 which indicated that no correlation between the intercept parameter and the rut depth in lab or field tests could be found. Also, it is noted that the intercept effect is very minor on rutting prediction due the small magnitude of intercept as compared to the total rutting with passes. As shown in Figure 4-23, assuming a total strain of 10% to be hardly measurable for a typical layer of 50-mm, all values of the intercepts for mixture tested are in a group at the corner of zero strain. This indicates that the small magnitudes cannot represent field characteristics with a large number of passes of truck loadings. Hence, the intercept (a) parameter is not a good indicator for rutting and thus its relationship between Dry HWT and Confined FN is not significant.

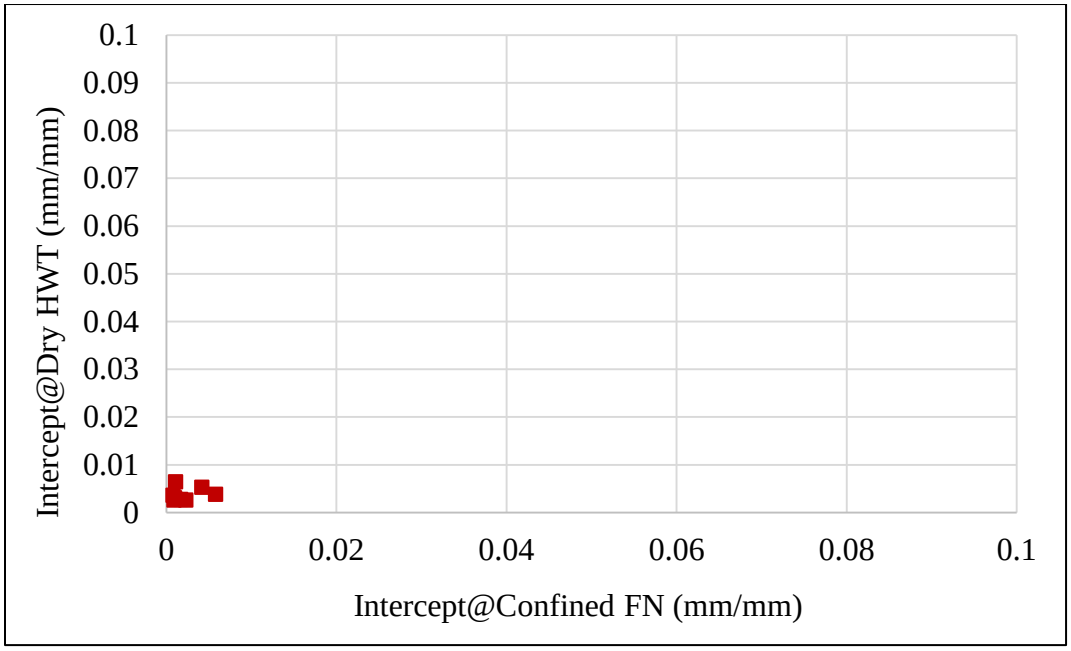

Figure 4-23. The correlation between the Intercepts of Dry HWT and Confined FN by Power Law with Extending the Maximum Limit on Both Axes.

4.3 The Comparison between Confined FN and Unconfined FN

According to above results, the correlations of creep slope between Dry HWT and FN are relatively strong. Because the FN is still in use to determine rutting resistance in some states, the relationship of both tests intrigue researchers to ensure that unconfined FN and confined FN with the confining pressure of 10 psi can be interchangeably used. The plot shown in Figure 4-24 shows the cumulative strain against number of cycles for confined and unconfined FN. These two methods use the same conditions of the deviator stress (87 psi) and the test temperature (52 ˚C).

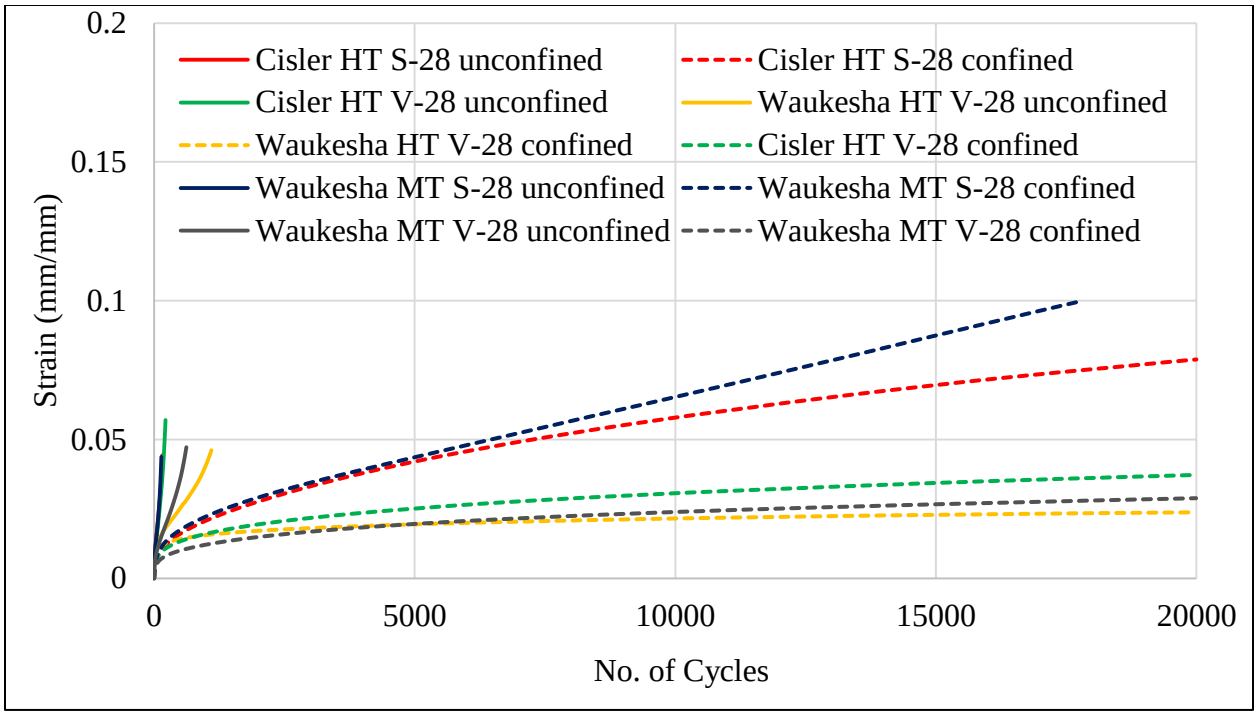

Figure 4-24. The Plot of Strain VS. Number of Cycles for Unconfined and Confined FN

Results show that the ranking in rutting resistance of confined FN and unconfined FN are of the same order, however the rate of strain accumulation is significantly different. In fact the confined test do not show the tertiary creep zone for any of the mixtures. These results can confirm that test methods can be used to determine rutting resistance in terms of mixture ranking, although some mixtures of unconfined FN show premature failure and have very smaller number of cycles to tertiary stage. Since the Unconfined condition is not a good simulation of actual field conditions, the use of the confined is preferred, but the limits should be reestablishment for using confined FN.

4.4 The Analysis of Outputs between Wet HWT and Dry HWT

The typical slope of permanent deformation versus wheel passes in the HWT is shown in Figure 4-25, which indicates there are two main inflection points: consolidation and stripping points. Between these points the slope is called the creep slope, and after the stripping point the

slope is called stripping slope. Although these terms are used widely, there is no clear evidence reported that in fact the stripping point is the passes at which moisture damage begins. The results for the wet and dry HWT tests reported in the previous sections are compared to determine if the creep slope is the same in the wet and dry conditions and what is the cause of the stripping point. Obviously the results in the dry condition do not show the stripping point or the stripping slope. However in the dry condition a mild tertiary point is seen after which the slope of the rutting curve increases marginally in some mixes, which can be called tertiary zone.

The creep slope is calculated as the inverse (absolute value) of the deformation rate within the linear region of the deformation curve post densification point and prior to stripping point (if stripping occurs). The creep slope measures rutting susceptibility and is assumed as a measure of the accumulation of permanent deformation primarily due to a mechanism other than moisture damage (Yildirim, 2006). This slope is expect to be similar to the slope of the secondary stage in dry HWT or FN testing. However, there is no evidence to verify whether the presence of moisture deteriorates the bonding between asphalt and aggregate, or the cohesion of the binder, which may make the slope in creep of wet HWT samples different than that in the dry HWT test. Therefore, the correlation between wet and dry results of HWT was investigated to verify whether the slopes before the stripping point stage for both conditions are equal or related.

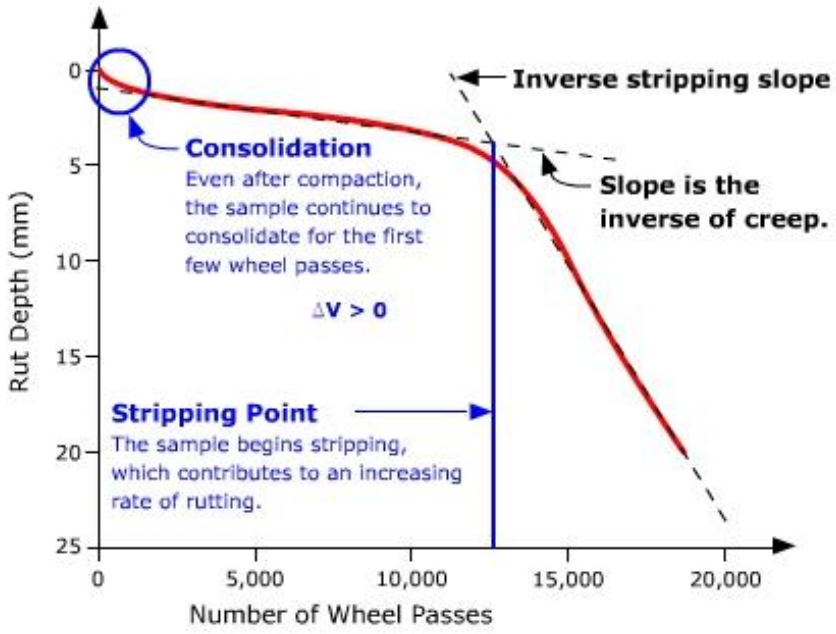

Figure 4-25. Typical Output of HWT Testing.

4.4.1 Results

As indicated earlier, the Francken model can well fit the HWT curves in the wet and dry conditions. In this analysis, the wet and dry HWT results were used to determine the stripping and tertiary points by means of estimating the cycles at which the first derivative of the Francken model reaches the minimum. The minimum value is selected since it indicates a change in strain accumulation from a decreasing trend to increasing trend. The results are shown in Table 4-7.

Table 4-7. Stripping and Tertiary Points of the Wet and Dry HWT Results estimated by the Francken Model Method.

Mixture Type	Stripping / Tertiary Point (Passes)					
	Ave. Wet HWT	SD.	COV.	Ave. Dry HWT	SD.	COV.
Cisler MT S-28	1,900	141.42	7.4%	9,300	282.84	3.0%
Cisler MT V-28	5,620	169.71	3.0%	10,150	212.13	2.1%
Cisler HT S-28	2,050	70.71	3.4%	3,400	70.71	2.1%

Cisler HT V-28	5,120	254.56	5.0%	18,000	494.97	2.7%
Waukesha MT S-28	1,500	183.85	12.3%	9,200	141.42	1.5%
Waukesha MT V-28	2,650	141.42	5.3%	9,100	141.42	1.6%
Waukesha HT S-28	2,150	155.56	7.2%	8,800	0.00	0.0%
Waukesha HT V-28	3,500	14.14	0.4%	26,650	1909.19	7.2%

In 8 mixes, the results show that the stripping points in wet HWT test present the values in range of 1,500 to 5,620 passes, while the tertiary points in dry HWT test are greater than those in wet HWT by at least two times, except for the Cisler HT S-28 mix in which they are closer than the ratio of 2.

According to the Wisconsin specification, a critical rut depth to identify the HWT testing is 12.5 mm at 20,000 passes. Therefore, in this section, wet and dry HWT outputs are compared to distinguish whether the passes of both are equivalent. All tests were conducted through 12.5 mm with the same conditions of temperature and tire. Figures 4-26 to 4-33 show the rut depth in dry and wet HWT measured for different mix designs.

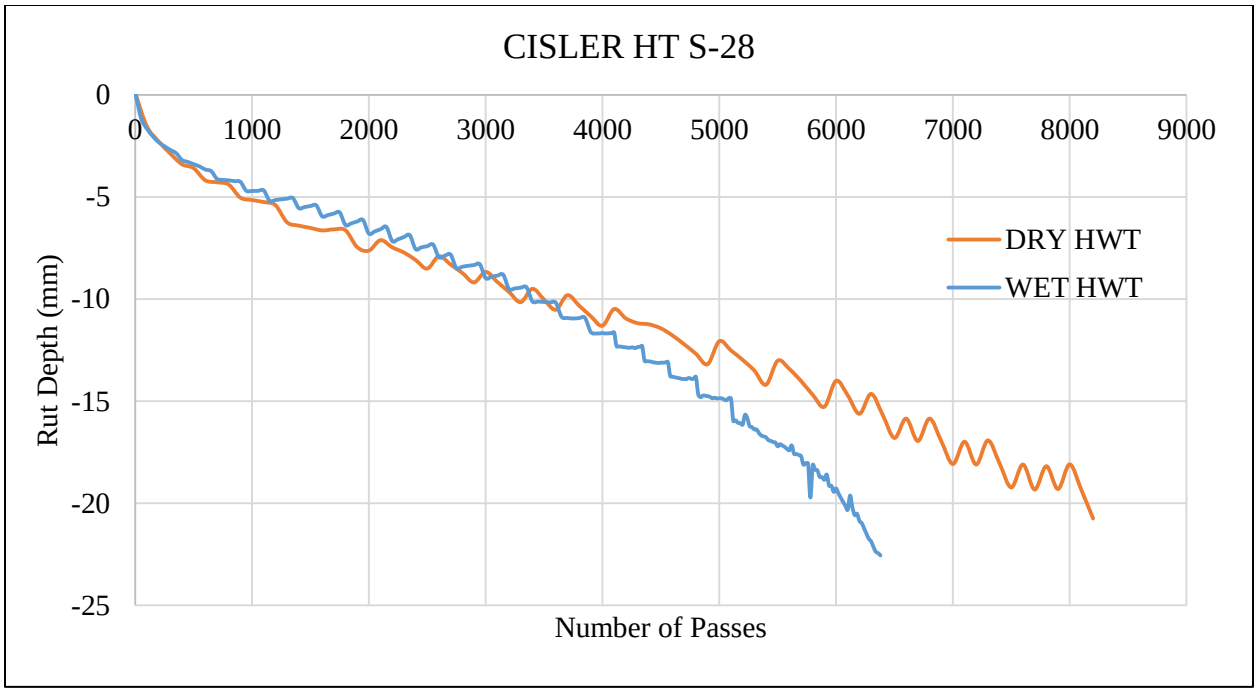

Figure 4-26. Rut Depth in Dry and Wet HWT of Cisler HT S-28.

Figure 4-26 shows two slopes of wet and dry HWT of Cisler HT S-28. The slope of wet and dry are identical at the primary stage and the beginning of the secondary stage. Nevertheless, after the middle point of the secondary stage of wet HWT at rut depth of 10 mm, the slope of wet continues steeper than the dry. The slope for the dry HWT still maintains constant slope through 25 mm. At the critical rut depth of 12.5-mm for both wet and dry HWT, the number of passes of dry condition sample is greater than that of wet condition sample (approximately 4500 passes) by approximately 700 passes.

Figure 4-27 shows the two slopes of wet and dry HWT of Cisler HT V-28, which is the exact same mix as the one shown in Figure 4-26 but the binder is modified to achieve the V-28 grade using an elastomer. Similar to the mix with the S-28 binder, the slope of wet and dry are close at both the primary stage and some of the secondary stage.

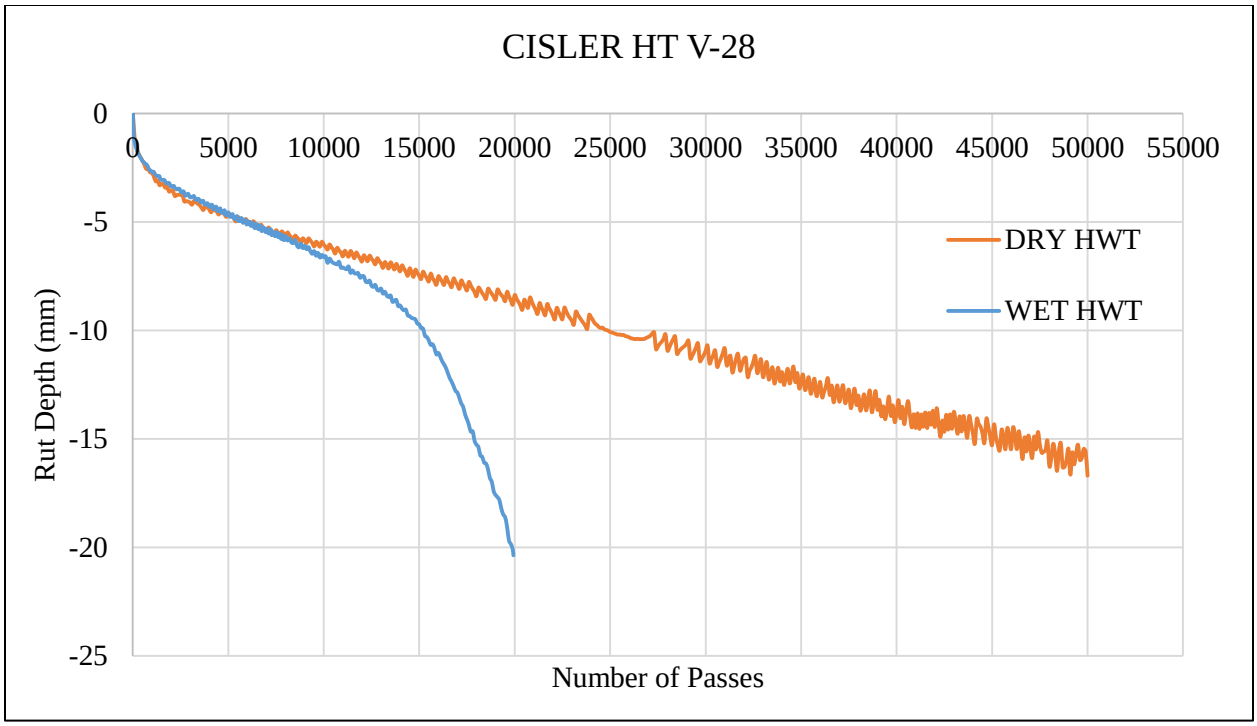

Figure 4-27. Rut Depth in Dry and Wet HWT of Cisler HT V-28.

It appears that due to the moisture, the stripping occurs in this mix before 10 mm. The slope of wet condition becomes much steeper reaching the limit of 12.5-mm at much lower passes than the dry condition, while the slope of the dry HWT maintains constant slope through 25 mm. At the critical rut depth (12.5 mm) the number of passes of wet and dry condition sample are equal to 16,800 and 34,400 passes, respectively. It should be noted that the V-28 grade is increasing the passes to stripping point significantly when compared to the S-28 binder in both the wet and dry conditions. The passes to 12.5-mm increased from 4,500 to 16,800 in the wet condition and from 5200 to 34400 in the dry condition.

All other mixes showed very similar trends in terms of changes from wet to dry conditions as shown in Figures 4-28 through 4-33 which include the plots for the remaining 6 mixtures. Also Table 4-8 includes comparison of the number of passes to 12.5 mm rut depth of

the wet and dry condition. As can be seen in the table the value of passes and the relative change between wet and dry is highly variable and is significantly related to the grade of the binder.

Table 4-8. Number of Passes to 12.5-mm rut depth

Mixture Type	Number of Passes to 12.5 mm rut depth					
	Ave. Wet HWT	SD.	COV.	Ave. Dry HWT	SD.	COV.
Cisler MT S-28	4,050	212.13	5%	4,625	530.33	11%
Cisler MT V-28	11,750	1343.50	11%	12,625	106.07	1%
Cisler HT S-28	4,840	0	0%	5,800	989.95	17%
Cisler HT V-28	16,100	848.53	5%	33,200	2969.85	9%
Waukesha MT S-28	4,750	70.71	1%	11,000	2687.01	24%
Waukesha MT V-28	10,100	707.11	7%	29,150	7141.78	25%
Waukesha HT S-28	5,680	1640.49	29%	14,525	2368.80	16%
Waukesha HT V-28	13,000	424.26	3%	-	-	-

Based on the results shown in Tables 4-7 and 4-8, it is clear that effect of wet conditioning starts at the stripping point. Also it is clear that using the 12.5-mm limit in the wet Hamburg is not related to the rutting behavior only, but also to the moisture confounding in the sample.

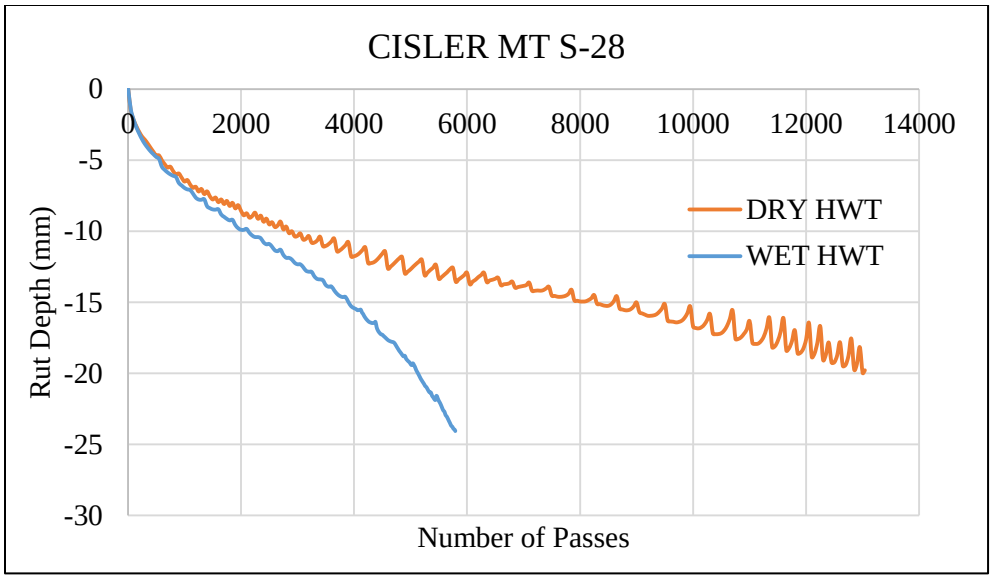

Figure 4-28. Rut Depth in Dry and Wet HWT of Cisler MT S-28.

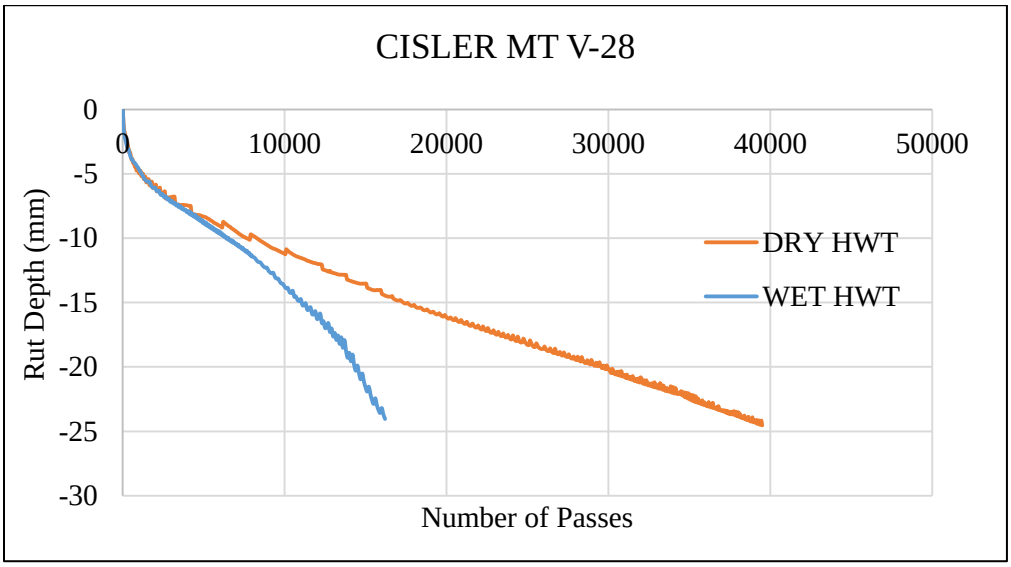

Figure 4-29. Rut Depth in Dry and Wet HWT of Cisler MT V-28.

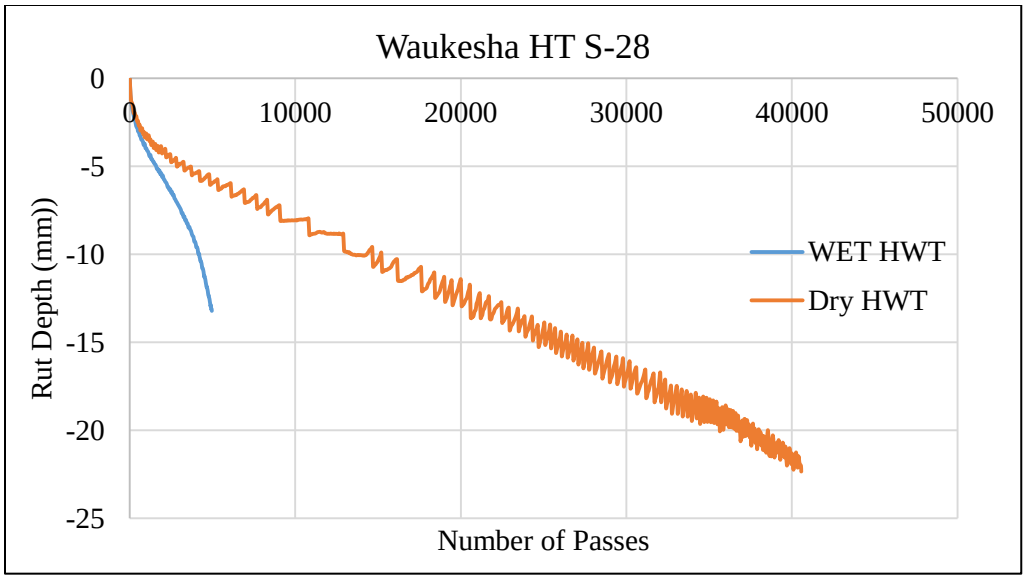

Figure 4-30. Rut Depth in Dry and Wet HWT of Waukesha HT S-28.

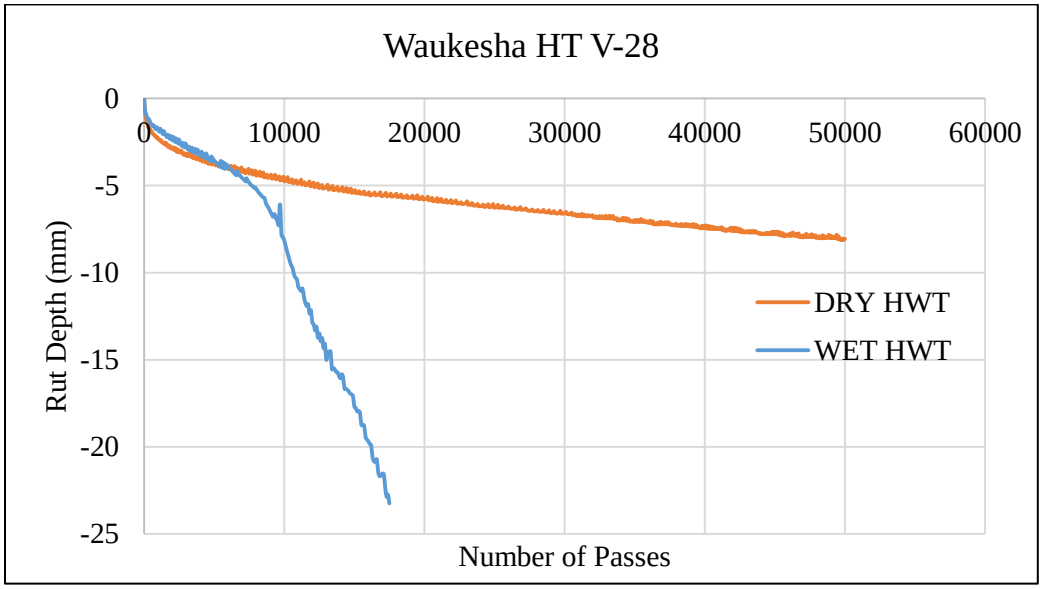

Figure 4-31. Rut Depth in Dry and Wet HWT of Waukesha HT V-28.

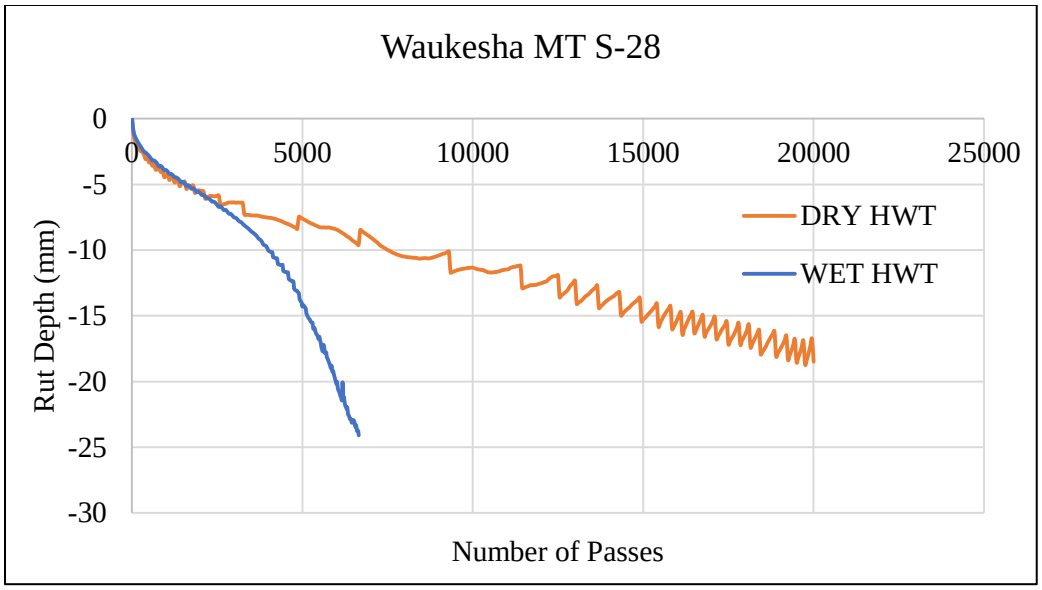

Figure 4-32. Rut Depth in Dry and Wet HWT of Waukesha MT S-28.

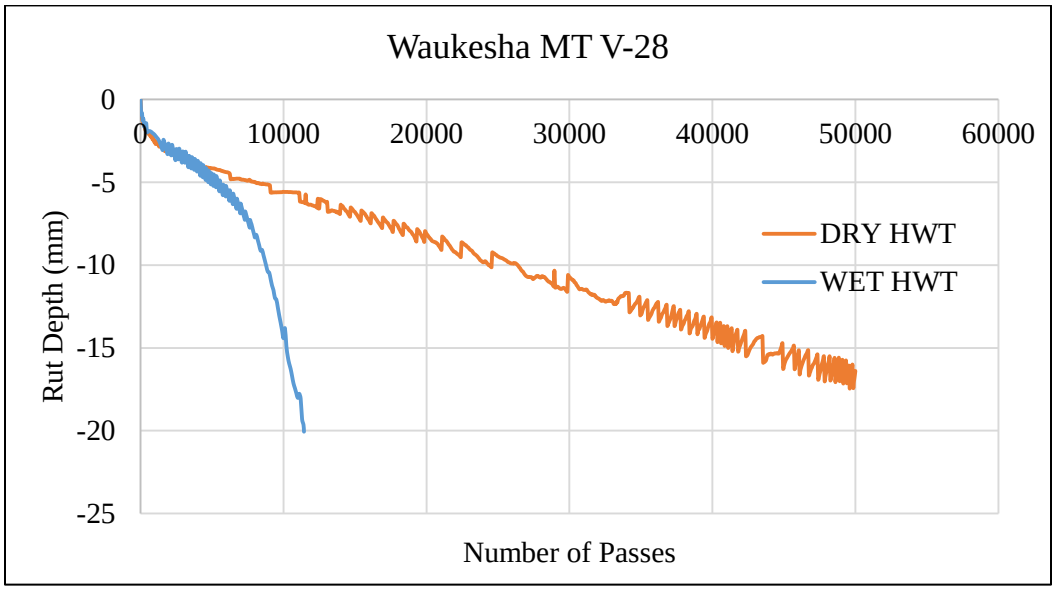

Figure 4-33. Rut Depth in Dry and Wet HWT of Waukesha MT V-28.

4.4.2 Creep Slope and Stripping Slope Results

According to the specification of Iowa and Wisconsin, to determine the ratio of stripping slope to creep slope should be equal or larger than 2.0 in the wet HWT test (Mohammad, 2015); otherwise, no stripping has occurred. Since the most important part of the rutting modeling is the

creep slope, the power law model was used to verify the effect of the moisture conditioning in wet HWT on the creep stage as shown in Tables 4-8. It is noted that the data after tertiary points for the dry testing and after the stripping point for the wet testing were removed in the fitting to avoid an confounding of the moisture damage effects.

Table 4-8. Creep Slope for 8 Mixes of Wet and Dry HWT.

Mixture Type	Wet	SD.	COV.	Dry	SD.	COV.	Sensitivity
Cisler MT S-28	0.51	3.54E-03	1%	0.50	1.13E-02	2%	2%
Cisler HT V-28	0.37	3.71E-02	10%	0.35	1.32E-02	4%	4%
Cisler HT S-28	0.47	1.46E-02	3%	0.42	7.07E-05	0%	9%
Cisler MT V-28	0.42	3.42E-02	8%	0.38	9.05E-03	2%	10%
Waukesha HT S-28	0.45	7.35E-03	2%	0.39	3.10E-02	8%	15%
Waukesha HT V-28	0.37	1.90E-02	5%	0.36	2.18E-02	6%	2%
Waukesha MT S-28	0.47	3.78E-02	8%	0.45	1.80E-02	4%	4%
Waukesha MT V-28	0.37	3.81E-02	10%	0.33	3.96E-03	1%	10%

The creep slopes in wet and dry condition are used to calculate the slope sensitivity which is equal to (wet creep slope – dry creep slope)/wet creep * 100 as shown in Table 4-8. The sensitivity to wet conditioning ranges from 2% to 15% of the wet slope. All mixtures shows relatively low values of sensitivity that can be considered to be within the experimental error of the HWT results.

The results indicate that within the creep stage, rut depth is increasing with very marginal confounding effect of moisture damage. This is logical since moisture damage is unlikely to happen in the first few hours in HWT testing. Creep slope relates to rutting primarily due to plastic flow (Aschenbrener. 1995). Also the ranks of creep slope for wet and dry HWT are in the same rank in which the V-28 mixtures are more resistant to permanent deformation than S-28 mixtures. However, it is not clear what is the mechanism of the moisture damage after the creep stage and beyond the stripping inflection point. Therefore in the next section the asphalt mastic bonding test is used to explain the difference of sensitivity between the mixtures for moisture damage.

After the striping inflection point, the slopes of the wet conditioned samples get even steeper while the dry condition can hardly show any changes. The Wet HWT creep and stripping slopes were analyzed by the method proposed by Iowa DOT as listed in Table 4-9. The analysis method involves fitting a sixth degree polynomial to the wheel passes vs. deflection curve, and inserting a tangent line at the location where the first derivative of the polynomial is at a minimum near the end of the test; the slope of this tangent is referred to as the stripping slope. A tangent line is also inserted at a point where the second derivative of the polynomial is zero prior to the stripping initiation point; the slope of this tangent is the creep slope.

Table 4-9. The Creep Slopes and Stripping Slopes of Wet HWT.

Name of the mixture	Creep Slope	SD.	COV.	Stripping Slope	SD.	COV.
Cisler-MT-S-28	-0.00226	0.0001	4.1%	-0.0055	0.0007	12.7%
Cisler-MT-V-28	-0.00069	0.0001	16.3%	-0.00164	0.0001	4.6%
Cisler-HT-S-28	-0.0012	0.0001	8.6%	-0.0051	0.0003	6.5%
Cisler-HT-V-28	-0.00038	0.0000	6.0%	-0.00228	0.0004	16.3%
Waukesha-MT-S-28	-0.00164	0.0000	1.6%	-0.00582	0.0006	9.8%
Waukesha-MT-V-28	-0.00052	0.0000	3.7%	-0.00323	0.0003	9.0%
Waukesha-HT-S-28	-0.00113	0.0002	20.5%	-0.00522	0.0001	1.2%
Waukesha-HT-V-28	-0.00045	0.0000	4.7%	-0.00179	0.0000	1.9%

As mentioned earlier the ratio of stripping slope and creep slope in Wisconsin and Iowa specification should be equal to or greater than 2 in wet HWT test. The results show that the ratio in the wet condition is greater than 2 for all the mixtures as shown in Table 4-10.

Table 4-10. The Ratio of Stripping Slope to Creep Slope for the Wet Condition

Name of the mixture	Stripping/Creep Slope Ratio		
	Average	SD.	COV.
Cisler-MT-S-28	2.43	0.21	8.5%
Cisler-MT-V-28	2.38	0.28	11.9%
Cisler-HT-S-28	4.25	0.09	2.1%
Cisler-HT-V-28	6.02	0.62	10.3%
Waukesha-MT-S-28	3.56	0.29	8.3%
Waukesha-MT-V-28	6.21	0.33	5.3%
Waukesha-HT-S-28	4.6	1.02	22.2%
Waukesha-HT-V-28	3.93	0.26	6.6%

The results indicate that all mixtures that were tested in wet HWT test are moisture susceptibility. It can be visually observed the difference between dry and wet HWT test by the dislodgement of the aggregate as shown in Figure 4-34.

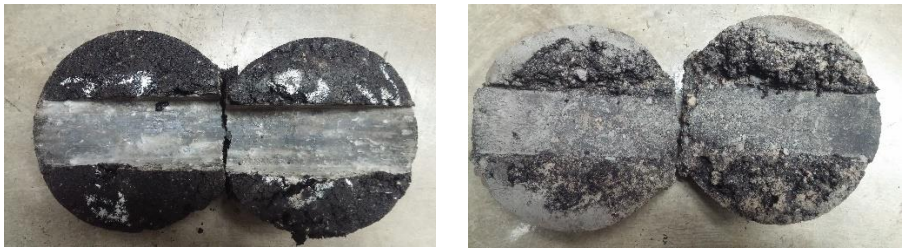

(a) **(b)**

Figure 4-34. Failure of HWT Samples on Running in (a) Dry Condition (b) Wet Condition

The results of comparing the wet and dry testing trends lead to conclude that these two tests (dry and wet) are interchangeable tests in creep stage; the wet HWT test can substitute the dry HWT to determine the permanent deformation.

4.4.3 Verification of the Cause of Moisture Damage

To explain the cause of this variation between dry and wet HWT, it is hypothesized that moisture damage for the mixtures is the main cause. Moisture damage can be caused either by an adhesion loss between asphalt binder and aggregate surface or by a cohesion strength weakening of asphalt mastic caused by the interaction with moisture. Some researchers have studied the mechanism of adhesion loss between asphalt binder and aggregate surface. Cheng et al. (2002) stated that the strength loss can predict when the dry adhesive bond compares the wet adhesive bond strength between the asphalt and the aggregate. Recently, Moraes et al. (2011) used the Bitumen Bond Strength test (BBS) to verify the effect of moisture on asphalt-aggregate adhesive bond. This study indicated that bonding between asphalt and aggregate under wet conditions was greatly dependent on binder modification type and conditioning time.

Cohesive failure of asphalt mastic bond is one cause of moisture damage in HMA. This damage may be due to two factors: the diffusion of water into bitumen weakening of the mastic and the migration of water through mastic to interface of mastic and aggregate. Kim et al. (2002) stated that the cohesive strength of the asphalt mastic is not only controlled by the asphalt cement, but also by the combination and interaction of the asphalt cement and the mineral filler. Terrel and Al-Swailmi (1994) presented that water can affect cohesion of mastic and bond to aggregates by reducing the strength of the mastic due to moisture saturation and void swelling or expansion.

Airey et.al (2007) showed that mineralogical and chemical composition of aggregate might play a fundamental role in moisture damage in HMA. In addition, Apeagyei et.al (2013) applied the dog bone-shaped tensile specimens to determine the cohesion (tensile strength) of the mastics. Results showed a good correlation between moisture condition time and adhesion strength. However, the test could not provide the result of the effect on physico-chemical and physical mineral fillers. Therefore, the moisture confounding effect can be verified by the Bitumen Bond Strength testing (BBS), which is standardized in the AASHTP TP-91 procedure.

4.4.3.1 Materials

To select the materials for verifying the mechanism affecting the moisture damage, the tertiary point slopes in Francken model method were used in the analysis. The reason of using tertiary point slope from Francken model is the stripping and the tertiary stage occur after this point. Therefore this point is deemed to be the starting point of having the moisture effect leading to the stripping stage. The slopes at the tertiary point for dry and wet HWT are shown in Table 4-11.

Table 4-11. The Slope at the Tertiary Point for Dry and Wet HWT by Francken Model.

Mixture type	DRY	SD	COV	WET	SD	COV	Sensitivity
Cisler MT S-28	0.0008	2.9E-05	4%	0.0023	3.5E-04	15%	68%
Cisler MT V-28	0.0005	2.1E-05	4%	0.0007	1.0E-04	16%	26%
Cisler HT S-28	0.0016	2.6E-04	17%	0.0019	3.0E-04	16%	18%
Cisler HT V-28	0.0002	6.6E-06	3%	0.0004	3.1E-05	9%	30%
Waukesha MT S-28	0.0006	5.9E-05	9%	0.0018	9.5E-05	5%	65%
Waukesha MT V-28	0.0003	5.6E-05	19%	0.0005	9.1E-05	17%	43%
Waukesha HT S-28	0.0004	1.5E-05	3%	0.0013	1.3E-04	10%	65%
Waukesha HT V-28	0.0002	4.9E-05	23%	0.0004	3.3E-05	9%	41%

Since the Cisler-HT-S-28 mixture as shown in Table 4-11 shows different dry/wet sensitivity in creep slope than others. To verify the mechanism affecting moisture damage and

the sensitivity of creep slope, four mixtures need to be considered including Cisler MT S-28, Cisler MT V-28, Waukesha MT S-28 and Waukesha HT S-28. However, the amount of the filler in MT and HT of Waukesha are similar, and they do not show the difference in the sensitivity. Therefore, three types of mineral fillers and two aggregate substrates (Waukesha Limestone and Cisler Granite) which are consistent with the aggregate used for the HWT test were selected to create asphalt mastic for testing Bitumen Bond Strength: limestone, granite, and blended sand. The filler use for each test was consistent with HWT test mixture: Cisler HT-S-28 used Cisler Filler, Waukesha HT-V-28 used Waukesha Filler, and Cisler MT-S-28 used Cisler+Blended Sand Filler.

4.4.3.2 Bitumen Bond Strength Test (BBS)

Bitumen Bond Strength test is developed from the Pneumatic Adhesive Tensile Testing Instrument (PATTI) test as shown in Figure 4.35(a) to evaluate the bitumen-aggregate bond strength. As shown in Figure 4-35, the BBS device is comprised of a portable pneumatic adhesion tester, pressure hose, piston, reaction plate and a metal pull-off stub. During the test, a pulling force is applied on the specimen by the metal stub. Raquel et al. (2011) found that BBS test is feasible for assessing moisture susceptibility of aggregate and asphalt binder. Bahia and coworkers (2012) developed the test to account for the stiffness of the binder on BBS measurements. The test can be conducted with samples curing in both the dry and wet condition. In the study by Raquel et al. (2011), it is shown that the pull off strength in the wet condition was highly dependent on conditioning time. To confirm that moisture fully infiltrates between asphalt mastic and aggregate, longer conditioning time of 96 hours was used for wet condition measurement.

After preparing the asphalt mastics, all samples were setup on substrate as shown in Figure 4-35(b). Two set of samples were cured in dry condition at room temperature for 24 h and in the wet condition samples are first left at room temperature for 1 hour to allow for the aggregate-bitumen-stub system to reach a stable temperature, then samples are submerged into a water bath at 40°C for 96 h. After curing, samples were taken out of water and kept at room temperature for 1 h before testing. The parameter that needs to be calculated and recorded is POTS, which is calculated using the following equation:

$$POTS = \frac{(BP - A_g) - C}{A_{ps}} \qquad (6)$$

Where:

POTS = Pull off tensile strength (kPa)

BP = Burst pressure (kPa)

A_g = Contact Area of Gasket with Reaction Plate (mm2)

C = Piston Constant (Provided by manufacturer)

A_{PS} = Area of pull-off stub (mm2)

(a) **(b)**

Figure 4-35. The photograph of (a) Bitumen Bond Strength Test Device (BBS) and (b) Sample Preparation.

4.4.3.3 Iso-Stiffness Temperature Test

Before testing bonding strength between asphalt mastic and aggregate, obtaining the same stiffness in asphalt mastic is necessary to avoid the confusion of the pull-off tensile strength in different stiffness. Bahia and co-workers (2012) proposed the method for determining binder stiffness by interpolating among three DSR test temperatures (20, 25, and 30°C) to calculate the temperature at which the |G*| is equal to 1 MPa. Table 4-12 shows the determined iso-stiffness temperature of the selected asphalt mastics. All concentration of fillers in asphalt binder are kept at 40% by volume.

Table 4-12. Asphalt Mastics Iso-Stiffness Temperature.

Asphalt Mastic Sample	**Iso-Stiffness Temperature (°C)**
S-28 + Cisler (Granite)	27.9
S-28 + Waukesha (Limestone)	28.4
S-28 + Cisler (Granite) + Blended Sand	27.3

These temperatures were adjusted to cure the sample for 5 minutes to maintain test temperature before BBS testing. The equipment to control temperature is shown in Figure 4-36.

Figure 4-36. The Equipment to Control Temperature of the BBS Samples.

4.4.3.4 Result and Analysis

By verifying the moisture damage in the wet HWT test using the BBS testing, it is possible that the filler can affect cohesion of the mastic and possibly the bonding of asphalt to aggregates. These effects change the moisture susceptibility of mixtures as observed in this study and as reported before by other reserachers (Terrel and Al-Swailmi ,1994). Three types of filler corresponding to the mixture test were added in asphalt binder at 40% by volume of mastic, which is a typical concentration in asphalt mixtures. Figure 4-37 shows three types of mastic with the corresponding substrate aggregates to asphalt mixtures. The results are shown in the dry and wet condition. Results show that in the dry and wet condition for Cisler_S-28 mastic have pull-off tensile strength of 1.78 MPa and 1.48 MPa, respectively, while for Waukesha_S-28 and Cisler+Blened Sand_S-28 mastics, lower pull-off tensile strengths are measured of 1.65 MPa, 1.11 MPa (dry, wet) and 1.20 MPa, 0.83 MPa (dry, wet), respectively. These trends indicate that pull off strength is dependent on filler type more than only the stiffness of asphalt mastic,

because even at the same stiffness, different pull-off strength values are measured. This confirms earlier findings made by Bahia and coworkers (2012). Therefore, the BBS test should be conducted in a temperature-controlled environment, and at a temperature that reflects field conditions, rather than at room temperature.

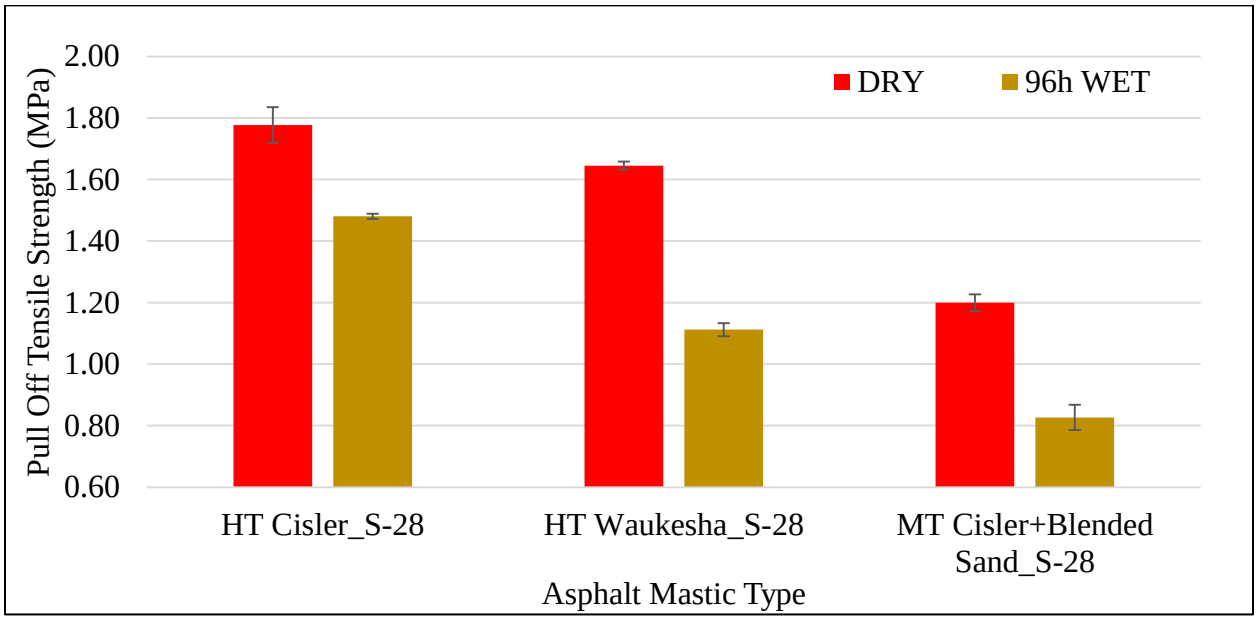

Figure 4-37. Pull-Off Tensile Strength of Dry and Wet condition on Cisler S-28 and Waukesha S-28 Asphalt Mastic.

In order to identify the potential effect of mastic on moisture damage resistance, loss of strength is calculated as indicator from the BBS testing. The calculation of loss of pull-off tensile strength is shown in Equation 4-7.

$$\%\ \text{loss of pull-off tensile strength} = \frac{\text{POTS}_{\text{dry}} - \text{POTS}_{\text{wet}}}{\text{POTS}_{\text{dry}}} \times 100 \qquad (7)$$

Figure 4-38 shows percent loss of pull-off tensile strength after wet conditioning. Results show that percent loss of pull-off strength for Waukesha_S-28 and the combination of Cisler and Blended Sand fillers are in a range of 31.1-32.4%, which is higher than the value for Cisler_S-28

filler (16.7%). This indicates that the loss of pull-off tensile strength is dependent on mineral filler sources.

It should be noted however that the absolute % loss value of the strength after wet conditioning (wet strength) is also a very critical factor since moisture damage is dependent not only on % change but also on the wet value of strength. In this case, values shown for the wet strength in Figure 4-37 indicates that wet strengths for the Waukesha and the combination of Cisler and Blended Sand fillers are lower than those for the Cisler filler. Therefore, the verification from BBS test confirmed the moisture damage occurring in the HWT testing.

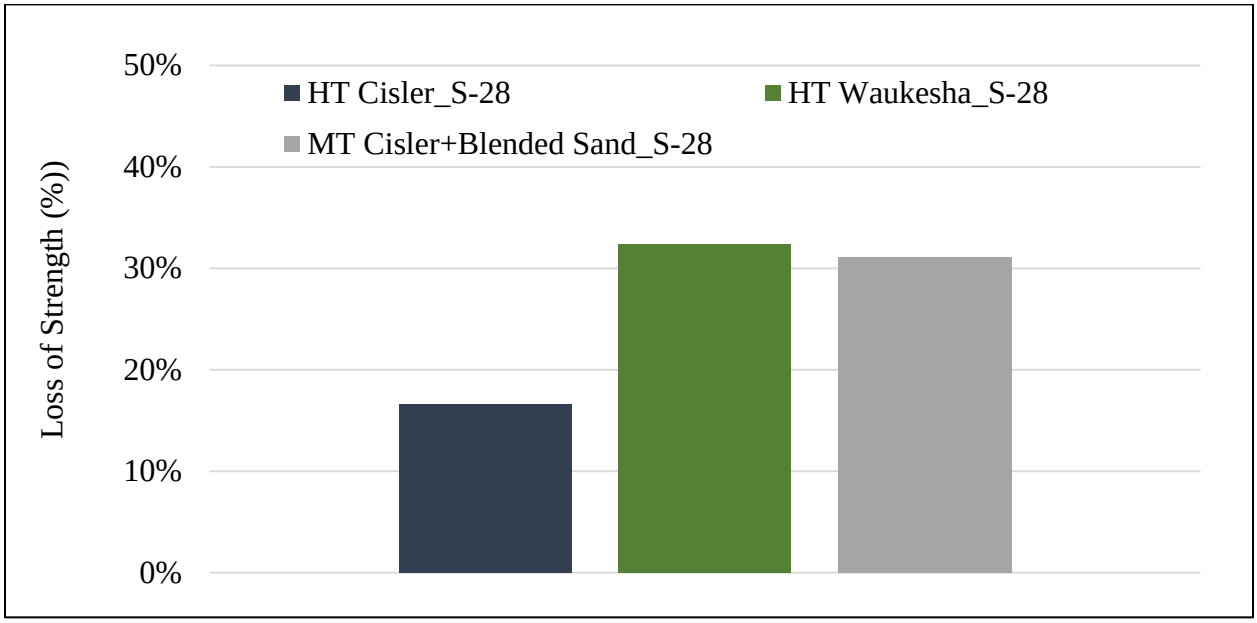

Figure 4-38. Percent Loss of Pull-Off Tensile Strength after Moisture.

4.4.3.5 Mode of Failure

As shown in Figure 4-38, water conditioning resulted in a reduction in the pull off strength of mastic. However the total strength cannot explain if the failure is Cohesive (within the mastic), or Adhesive (at the interface with the aggregate surface). The mode of failure can only be detected visually by inspecting the surface of the aggregate as shown in Figure 4-39,

which illustrates cohesive and adhesive failures form the BBS test. The modes of failure observed for all combinations are shown in Table 4-13, which shows that for all of the mastics the failure has been cohesive (Figure 4-40). Also, because the wet strengths are lower than the dry values, the effect is mostly weakening the mastic itself either by softening of binder or weakening the bond between the binder and the filler particles. These results are consistent with the cohesive failure (Displacement) mechanism affecting the moisture damage.

Table 4-13. Mode of Failure in 3 Mastic Types.

Asphalt Mastic Sample	Dry Condition Failure Type	Wet Condition Failure Type
S-28 + Waukesha	C	C
S-28 + Cisler	C	C
S-28 + Cisler + Blended Sand	C	C

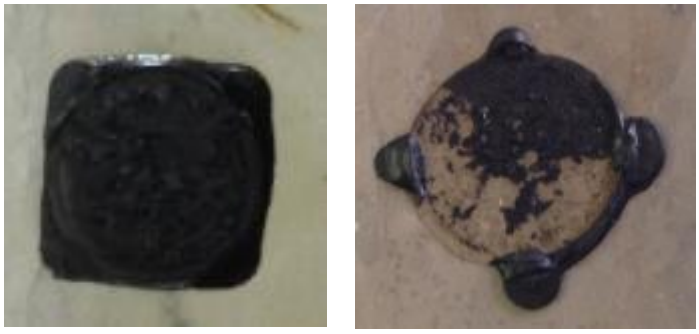

(a) **(b)**

Figure 4-39. Typical Failure Modes in the BBS (a) Cohesive Failure (b) Cohesive and Adhesive Failure.

(a) **(b)**

(c)

Figure 4-40. Failure Mode (a) S-28 + Cisler Dry (Left), Wet (Right) (b) S-28 + Waukesha Dry (Left), Wet (Right) (c) S-28 + Cisler + Blended Sand Dry (Left), Wet (Right)

5 SUMMMARY OF FINDINGS, CONCLUSION AND RECOMMENDATIONS

5.1 Overview

It is well recognized that resistance of asphalt mixtures for rutting can be measured using axial repeated loading of cylindrical samples in unconfined or confined mode, or using wheel tracking devices. Currently the most widely used method in the USA include the Hamburg Wheel Tracking (HWT) Test (AASHTO T324) and the unconfined axial load test, also called the Flow Number (FN) test as described in the AASHTO TP 79. The HWT is a much simpler device that allows using relatively thin samples from constructed pavements, which provides confinement similar to the pavement field conditions. The FN test, on the other hand, requires a cylindrical sample of 150-mm depth, which is not typically available from the field, and requires specifying confining pressure to simulate pavement field conditions. Currently the HWT is conducted in wet conditions, which could confound the effects of moisture and traffic loading, however it is known that HWT can be conducted in both wet and dry conditions. The overall objectives of this dissertation are to present the rationale for using the dry or wet HWT tests to determine the permanent deformation performance of asphalt mixtures in the laboratory as a more effective method than the FN test. In this chapter the main findings, conclusions and recommendations are listed.

5.2 Summary of Findings

This study focused on evaluating the potential of using the HWT device in the dry condition to quantifying permanent deformation resistance of asphalt mixtures. The Dry HWT test is examined by studying the mechanisms of permanent deformation, correlation with the

confined Flow Number (FN) standard test using tri-axial (Confined) loading, and by the analysis of outputs from the wet HWT, which is a standard test method, and the dry HWT test.

5.2.1 Evaluation of Rutting Mechanism by Hamburg Wheel Tracking Test

The rutting behavior of mixtures in the dry and wet HWT test is found to follow the model developed by Francken which can successfully define primary creep, secondary creep and tertiary creep. However, in the dry condition not all mixtures showed the tertiary behavior. Therefore, a simpler model (the power law model) was used to fit the dry condition results and compare them to the confined FN results. To understand the mechanisms in each creep stage, the change in aggregate packing during cyclic loading process until failure of the mixtures in HWT testing was determined by using IPAS2 software, which allows determining the orientation of aggregates and the contact or proximity zones. Based on the analysis of the results, the following findings can be stated:

1. Francken model can be used for appropriate fitting of the HWT data to analyze the creep stages and define the tertiary point. However, in the dry condition not all mixes can reach the tertiary creep stage within reasonable number of passes.
2. Rutting in the dry HWT testing is caused by different mechanism; during the initial (primary) creep, the aggregates are packed by the load applied from the steel wheel, thus aggregate skeleton shows increase in contact/proximity zones between aggregates. In the secondary stage, sample mixes are in the steady stage that the aggregate skeleton begins deforming along the loading directions and shifted to the sides of the sample mixes as observed by dilation of aggregate structure. Since the aggregate skeleton is still stable at most of the proximity zones, there is no rapid deformation or failure of the specimen. However, the aggregate skeleton deforms rapidly and moves to the sides of the samples

(dilation) within the tertiary stage. These mechanisms are confirmed by the observation that the two sides of the samples show reoriented aggregate skeleton, which is an indication of shear failure. The instability happens as a result of the dilation in mixture samples. In this case, the sides of samples appeared as upheavals with some aggregates dislodged which is consistent with typical rutting that can be observed in the field.

3. The failure in mixture and decrease in Total Proximity Lengths (TPLs) values during secondary and tertiary zone is due to some localized deformation and discontinuities in the aggregate skeleton of mixes leading to failure of the whole sample and severe reduction in load-bearing capacity of mixture. In this study, Angle Orientation Measurements was adopted to determine the possibility of shear failure of the samples. The results show that the angle orientation changed during secondary stage. Hence, this method may be one to identify the change in shear mode during loading passes in HWT test.

5.2.2 Correlation between Dry Hamburg Wheel Tracking Test and Confined Flow Number Test

Based on the results of correlating the dry HWT with FN, the following findings can be stated:

1. The correlations of cumulative strain in the Dry HWT and Confined FN with cycles up to the tertiary point of Dry HWT test showed excellent linear relationship with R^2 in the range of 0.970-0.996 for 8 different mixtures. However, the correlation between Dry HWT strain vs Confined strain in tertiary stage of both tests is not consistent for all mixtures. Therefore, the specifications limits for Dry HWT need to be verified and selected independent of the limits used today for FN.

2. With the Francken model, the linear regression analysis of secondary creep rate for 8 mixes shows a strong relationship with R^2 of 0.87. However, if the Cisler MT-S-28 was removed, the linear regression reduces the relationship with R^2 of 0.45. Hence, the Francken model is not a suitable method to determine the creep slope.
3. With the Power Law fit, Dry HWT test can be used as a surrogate for testing of confined FN since a good significant slope relationship can be established between Dry HWT and Confined FN with R^2 of 0.86. The slope parameters of Confined FN mixes are above the line of equality. These results are logical since the contact stress of Confined FN (87 psi) is lower than that of Dry HWT (105 psi). Also, the slope was verified by determining unconfined FN slopes with the same mixtures. The slope parameters of Unconfined FN mixes are under the line of equality. These results are logical since the confining pressure of Confined FN (10 psi) exists, while no confining pressure is applied in the HWT test.
4. Intercept parameters of Dry HWT show a rational relationship with the Confined FN intercept, however a very poor correlation could be found. The intercept is not considered an important parameter since it contributes very little to the critical rutting depth commonly used in specification. Hence, the lack of correlation for the intercept parameter can be ignored in regards to the relationship between Dry HWT and Confined FN.

5.2.3 The Analysis of Outputs between Wet HWT and Dry HWT

Mixtures with varying asphalt binders, aggregate types and mix designs are selected for testing to allow for evaluation of the distinction between the two conditions of wet and dry. The results showed that the creep slopes of wet HWT were very similar to those from the dry HWT within the creep stage before the stripping point. Therefore the creep rate measured in the dry HWT test, which represents rutting without confounding effects of moisture damage, can be

estimated from the wet HWT test. The effect of moisture damage in the wet test (stripping slope) can be explained by the Bitumen Bond Strength (BBS) test results which indicate that moisture can reduce the Pull-Off Tensile strength (POTs) of mastics, and the % loss of POTs are consistent with the difference in the sensitivity of creep slope to wet conditioning estimated from the HWT test.

5.3 Conclusions

Based on the findings of this study, it can be concluded that the rutting resistance measured in the Dry HWT can be successfully used to replace the FN test in measuring the rutting resistance of asphalt mixtures. The Dry HWT test shows strong correlation of creep stages observed for Confined and Unconfined FN. It is also concluded that the creep rate measured in the Wet HWT, before the stripping inflection point, can be used reliably to estimate the creep rate of the Dry HWT since the differences between wet and dry creep slopes are well within the experimental error, and the creep slope ranking is also similar.

5.4 Recommendations

1. The Hamburg Wheel Tracking test as defined in this report is shown as a suitable testing for use as a surrogate for the Flow Number and as a screening test for the public and private agency. However, the verification of more HMA mixtures which are both sensitive and in-sensitive to rutting performance is needed. Therefore, the development of the framework to establish the criteria for HMA testing is recommended for a further study.
2. As the tertiary point was rarely observed in Confined Flow Number test within 20,000 passes, a variety of temperature testing in the test is needed to investigate if it can expedite the occurrence of the tertiary point in stiffer mixture.

3. For HMA testing in the laboratory to provide equivalent performance to the field, there is a need to consider both wet HWT and field performance testing in verification of the effective laboratory testing for rutting performance.

REFERENCES

2011. *"Minitab Statistical Software Features - Minitab." Software for Statistics, Process Improvement,*. Six Sigma, Quality-Minitab. N.P., n.d. Web. April. http://www.minitab.com/en-US/products/minitab/features/.

Advanced Asphalt Technologies, LLC. 2011. *A Manual for Design of Hot Mix Asphalt with Commentary*. Washington D.C.: NCHRP Report 673, National Cooperative Highway Research Program.

Airey, G., E. Masad, A. Bhasin, S. Caro, and D. N. Little. 2007. "Asphalt Mixture Moisture Damage Assesment Combined with Srface Energy Characterization." *Advanced Characterization of Pavement and Soil Engineering Materials* 739-748.

Apeagyeia, A.K., J. R. A. Grenfella, and G.D. Airey. 2014. "Moisture-Induced Strength Degradation of Aggregate-Asphalt Mastic Bonds." *Road Materials and Pavement Design* 15 (sup 1): 239-262.

Aschenbrener, T. 1995. "Evaluation of Hamburg Wheel Tracking Device to Predict Moisture Damage in Hot-Mix Asphalt." *Transportation Research Record.*

Aschenbrener, T. 1995. "Evaluation of Hamburg Wheel-Tracking Device to Predict Moisture Damage in Hot Mix Asphalt." (Transportation Research Board) Transportation Research Record 1492.

Aschenbrener, Timothy, Ronald L. Terrel, and Richard A. Zamora. 1994. *COMP ARISON OF THE HAMBURG WHEEL-TRACKING DEVICE AND THE ENVIRONMENTAL CONDITIONING SYSTEM TO PAVEMENTS OF KNOWN STRIPPING*

PERFORMANCE. the U.S. Department of Transportation Federal Highway Administration.

Bahia, Hussain, Raquel Moraes, and Raul Velasquez. 2012. "The Effect of Bitumen Stiffness on The Adhesive Strength Measured by The Bitumen Bond Strength Test." *5th Eurasphalt and Eurobitume Congress.* Istanbul.

Biligiri, K.P., K.E. Kaloush, M.S. Mamlouk, and M.W. Witczak. 2007. "Rational Modeling of Tertiary Flow For Asphalt Mixtures." (Transportation Research Record) 2001.

Bonaquist, R. 2012. *Evaluation of Flow Number (Fn) as a Discriminating HMA Mixture Property*. WHRP 12-01.

Bonaquist, R. 2011. *Precision of the Dynamic Modulus and Flow Number Tests Conducted with the Asphalt Mixture Performance Tester.* Washington D.C.: NCHRP Report 702, National Cooperative Highway Research Program.

Bonaquist, R. 2008. *Refining the Simple Performance Tester for Use in Routine Practice.* Washington D.C.: NCHRP Report 614, National Cooperative Highway Research Program.

Bonaquist, R. 2008. *Ruggedness Testing of the Dynamic Modulus and Flow Number Tests with the Simple Performance Tester*. Washinton D.C.: NCHRP Report 629, National Cooperative Highway Research Program.

Bonaquist, R. 2010. *Wisconsin Mixture Characterization Using the Asphalt Mixture Performance Tester (AMPT) on Historical Aggregate Structures.* Wisconsin Highway Research Program.

BONAQUIST, R.F., and W. STUMP. 2003. *Simple Performance Tester for Superpave Mix Design: First-Article Development and Evaluation.* Washington, D.C.: NCHRP REPORT 513.

Bonaquist, R.F., D.W. Christensen, and W. Stump. 2003. *Simple Performance Tester for Superpave Mix Design: First Article Development and Evaluation.* Washington D.C.: NCHRP Report 513, National Cooperative Highway Research Program.

Brown, E. Ray, Prithvi S. Kandhal, and Jingna Zhang. 2001. *PERFORMANCE TESTING FOR HOT MIX ASPHALT.* Auburn: NCAT Report.

Brown, E.R., and Cross S.A. 1989. *A STUDY OF IN-PLACE RUTTING OF ASPHALT PAVEMENTS.* Auburn: NCAT Report 89-02.

Brown, E.R., and S.A. Cross. 1992. *A NATIONAL STUDY OF RUTTING IN HOT MIX(HMA) PAVEMENTS.* Auburn: NCAT Report 92-05.

Brown, E.R., P.S. Kandhal, and J. Zhan. 2001. *PERFORMANCE TESTING FOR HOT MIX ASPHALT* . Auburn: NCAT Report 01-05.

Canestrari, F., F. Cardone, A. Graziani, F. Santagata, and H. and Bahia. 2010. "Adhesive and Cohesive Properties of Asphalt-Aggreate Systems Subjected to Moisture Damage." *Road Materials and Pavement Design* 11: 11-32.

Cheng, D., D. N. Little, R. L. Lytton, and J. C. Holste. 2002. "Surface Energy Measurement of Asphalt and Its Application to Predicting Fatigue and Healing in Asphalt Mixtures." *Transportation Reserach Record: Journal of transportation Reserach Board* 1810: 44-53.

Coenen, A. 2011. *Image Analysis of Aggregate Structure Parameters as Performance Indicators of Rutting Resistance.* PhD. thesis of University of Wisconsin Madison.

Cooley Jr., L.A., Prithvi S., Buchanan, M.S. Kandhal, F. Fee, and A. Epps. 2000. "LOADED WHEEL TESTERS IN THE UNITED STATES: STATE OF THE PRACTICE." (Transportation Research E-circular) E-C016.

Epps, Jon A., Adam Hand, Steve Seeds, Todd Schulz, Sirous Alavi, and shmore Colin. 2002. *Recomended Performace-Related Specification for Hot-Mix Asphalt Construction: Results of Westrack Project.* Washington, D.C.: NATIONAL COOPERATIVE HIGHWAY RESEARCH PROGRAM (NCHRP Report 455).

Francken, L. 1977. "Permanent Deformation Law of Bituminous Road Mixes in repeated Triaxial Compression." Ann Arbor: Proceedings, Fourth International Conference on the Structural Design of Asphalt Pavements, University of Michigan, Ann Arbor.

Gierhart, D. 2013. "Tack Coat to Chip Seal." *Louisiana Transportation Conference.* Baton Rouge.

Gogula, A., M. Hossain, J. Boyer, and S. Romanoschi. 2003. "Effect of PG Binder Grade and Source on Performance of Superpave Mixtures under Hamburg Wheel Tester." *Proceedings of the 2003 Mid-Continent Transportation Research Symposium.* Ames, Iowa.

Hajj, Elie Y., Alvaro Ulloa, Raj Siddharthan, and Peter E. Sebaaly. 2010. "Estimation of Stress Conditions for the Flow Number Simple Performance Test." (Transportation Research Record: Journal of the Transportation Research Board) 2181.

Izzo, R.P., and M. Tahmoressi. 1999. "Use of the Hamburg Wheel Tracking Device for Evaluating Moisture Susceptibility of Hot-Mix Asphalt." *Transportation Research Record* 1681: 76-85.

Izzo, Richard P., and Maghsoud Tahmoressi. 1998. *EVALUATION OF THE USE OF THE HAMBURG WHEEL-TRACKING DEVICE FOR MOISTURE SUSCEPTIBILITY OF HOT MIX ASPHALT.* Austin: Texas Department of Transportation Research Report DHT-4s.

KanDhal, P.S. 2003. *Accelerated Laboratory Rutting Tests: Evaluation of the Asphalt Pavement Analyzer.* Washington D.C.: NCHRP Report 508, National Coopertive Highway Research Program.

Kanitpong, K., and H. Bahia. 2003. "Role of Adhesion and Thin Film Tackiness of Asphalt Binders in Moisture Damage." *Asphalt Paving Technology* 72: 502-528.

Little, D.N., and D.R. Jones IV. 2003. "Moisture Sensitivity of Asphalt Pavement." *Chemical and Mechanical Process of Moisture Damage in Hot-Mix Asphalt Pavements*, 37-74.

Lu, Q, and J.T. Harvey. 2006a. "Evaluation of Hamburg Wheel Tracking Device Test with Laboratory and Field Performance Data." *Transportation Research Record* 1970: 25-44.

Mclean, D.B., and C.L. Monismith. 1974. "Estimation of Permanent Deformation in Asphalt Concrete Layers Due to Repeated Traffic Loading." *Transportation Research Record* 510.

Mohammad, Louay. 2006. *Performance Tests for Hot Mix Asphalt (HMA) Including Fundamental and Empirical Procedures.* Vol. STP1469. Mayfield: ASTM International.

Moraes, R., R. Velasquez, and H. and Bahia. 2011. "Measuring Effect of Moisture on Asphalt-Aggregate Bond with The Bitumen Bond strength Test." *Journal of the Transportation Research Board* 2209: 70-81.

Powell, R. Buzz. 2008. "COMPARING RUTTING PERFORMANCE UNDER A HEAVY VEHICLE SIMULATOR TO RUTTING PERFORMANCE AT THE NCAT PAVEMENT TEST TRACK." *Third International Conference on Accelerated Pavement Testing.*

Quintus, H.L.V., Jagannath Mallela, Ramon Bonaquist, C.W. Schwartz, and R.L. Carvalho. 2012. *Calibration of Rutting Model for Sructural and Mix Design.* Washington D.C.: National Cooperative Highway Research Prgram.

R. L., Terrel, and Al-Swailmi S. 1994. *Water Sensitivity of Asphalt-Agregate Mixes: Test Selection.* Washington, D.C.: SHRP Report A-403. Strategeric Highway Research Program, National Reserach Council.

Rahman, F., and M. Hossain. 2014. *Review and Analysis of Hamburg Wheel Tracking Device Test Data.* Kansas: Kansas State University Transportation Center.

Reinke, Gerald, Scott Veglahn, Doug Herlitzka, Steve Engber, and Dave Tranberg. 2009. "Update on Study of Impact of Loose Mix Aging Time and Temperature on the Mechanistic Performace of Hot and Warm Bituminous Mixtures ." *Warm Mix Technical Working Group Meeting.* Seattle.

1991. *Report on the 1990 European Asphalt Study Tour.* Washington, D.C.: AASHTO.

Roberts, F. L., S. Prithvi, E. Kandhal, R. Brown, D-Y Lee, and Kennedy T. W. 1996. *Hot Mix Asphalt Materials, Mixture Design, and Construction.* Vol. 2. NAPA Education Foundation.

Robertson, R. E. 2000. "Chemical Properties of Asphalts and Their Effects on Pavement Performance." *Transportation Research Circular 499.*

Roohi Sefidmazgi, N., L. Tashman, and Bahia H.U. 2012. "Internal Structure haracterization of Asphalt Mixtures for Rutting Performance Using Imaging Analysis." (Association of Asphalt Pavement Technologies).

Roohi, N. 2014. *Hot Mix Asphalt Design to Optimize Construction and Rutting Performance Properties.* Madison: Ph.D thesis at University of Wisconsin Madison.

Solaimanian, M. 2003. "Test Methods to Predict Moisture Sensitivity of Hot-Mix Asphalt Pavements, Moisture Sensitivity of Asphalt Pavements." *a National Seminar.*

Sousa, J.B., J. Craus, and C.L. Monismith. 1991. *Sumary Report on Permanent Deformation in Asphalt Concrete.* Washington, D.C.: Strategic Highway Research Program (SHRP).

Team, WesTrack Forensic. June 1998. *Performance of Coarse-Graded Mixes at WesTrack – Premature Rutting.* Final Report.

Ulloa, C.A. 2013. *Development of a Mechanistic-Based Approach to Evaluate Critical Conditions of Hot Mix Asphalt Mixtures.* PhD. Thesis.

Williams, R.C. 2007. *Testing Wisconsin Asphalt Mixtures for the AASHTO 2002 Mechanistic Design Procedure.* Madison: WHRP Report 07-06, Wisconsin Department of Transportation.

Witczak, M.W., K. Kaloush, T. Pellinen, M. El-Basyouny, and H. Von Quintus. 2002. *Simple Performance Test for Superpave Mix Design.* Washington D.C.: NCHRP Report 465, National Cooperative Highway Research Program.

Yildirim, Y., P. W. Jayawickrama, M. S. Hossain, A. Alhabshi, C. Yildirim, A. F. Smit, and D. Little. 2007. "Hamburg Wheel Tracking Database Analysis." Texas Department of Transportation, Austin, Texas, FHWA/TX-05/0-1707-7.

Zhang, Jingna, E. Ray Brown, Prithvi S. Kandhal, and Randy West. May 2005. "An Overview of Fundamental and Simulative Performance Tests for Hot Mix Asphalt." (Journal of ASTM International) 2 (5).

Zhang, Jingna, Jr., L. Allen Cooley, and Prithvi S. Kandhal. 2002. *COMPARISON OF FUNDAMENTAL AND SIMULATIVE TEST METHODS FOR EVALUATING PERMANENT DEFORMATION OF HOT MIX ASPHALT.* Auburn: NCAT Report 02-07.

Zhou, F., S. Hu, and T. Scullion. 2005. *Integrated Asphalt (Overlay) Mixture Design, Balancing Rutting and Cracking Requirements.* Texas: FHWA/TX-06/0-5123-1, Texas Transportation Institute.

APPENDIX A: Detailed Mix Design Information

Table A-1. MT-S-28-Cisler.

Project: WHRP 0092-15-04		Spec. 12.5mm E3 Mix	Date:
Location:		TH#:	
Mix Type: MT-S-28-Cisler			

	%	Aggregate Description		Legal Description
1		#1 Stone	5/8x3/8 Bit Agg(3326)	
2		#2 Stone	3/8 Washed Chips(3237)	
3		#3 Stone	3/8 Bit Agg(3235)	
4		#4 Stone	3/16 Washed Man Sand(3403)	
5		#5 Stone	5/8 River Sand(5501)	
6		#6 Stone	STH 182 RAP(5%AC)	

Aggregate		A	B	C	D	E	6		Blend	
%Aggregate		15	10	10	20	25	20		MAS	
Sieve Size	mm	Percent Passing							NMAS	
1 1/2"	37.5	100	100	100	100	100	100		100.0	
1"	25	100	100	100	100	100	100		100.0	
3/4"	19	100.0	100	100	100	100	99		99.8	MAS
1/2"	12.5	77.0	100	100	100	99	93	NMAS	94.9	
3/8"	9.5	29.0	100.0	100	100	96	86		85.6	
#4	4.75	2.1	35.0	67.0	99.0	89.0	69.0		66.4	
#8	2.36	1.7	3.0	40.0	66.0	82.0	55.0		49.3	
#16	1.18	1.5	2.0	26.0	41.0	73.0	44.0		38.3	
#30	0.6	1.4	1.0	18.0	24.0	53.0	33.0		26.8	
#50	0.3	1.4	0.6	13.0	13.0	17.0	18.0		12.0	
#100	0.15	1.2	0.4	9.5	5.9	4.5	9.8		5.4	
#200	0.075	1.1	0.3	7.2	2.9	3.0	6.7		3.6	
	Gsb	2.691	2.691	2.683	2.671	2.624	2.624		2.656	
	Abs	0.4	0.4	0.4	0.5	0.3	0.4		0.4	
	F&E	2.6	1.8	1.8	1.8	1.3	0.9		1.6	
	#FF	100	100	100	100	30	83		79.1	

AC Content:			NMAS 12.5
Asphalt Source:		Grade:	

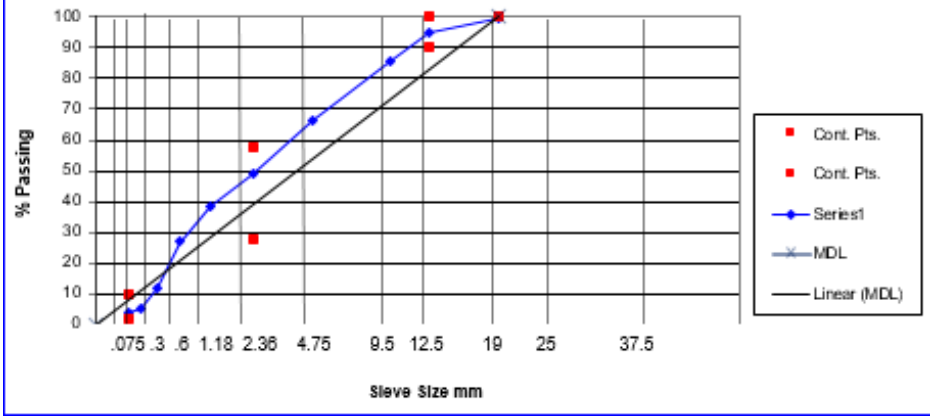

Table A-2. HT-S-28-Cisler.

Project: WHRP 0092-15-04		Spec. 12.5mm E30 Mix	Date:
Location:		TH#:	
Mix Type: HT-S-28-Cisler			

	%	Aggregate Description		Legal Description
1		#1 Stone	5/8x3/8 Bit Agg(3326)	
2		#2 Stone	3/8 Washed Chips(3237)	
3		#3 Stone	3/8 Bit Agg(3235)	
4		#4 Stone	3/16 Washed Man Sand(3403)	
5		#5 Stone	5/8 River Sand(5501)	
6		#6 Stone	STH 182 RAP(5%AC)	

Aggregate		A	B	C	D	E	6		Blend	
%Aggregate		13	8	31	32	8	8		MAS	
Sieve Size	mm	Percent Passing							NMAS	
1 1/2"	37.5	100	100	100	100	100	100		100.0	
1"	25	100	100	100	100	100	100		100.0	
3/4"	19	100.0	100	100	100	100	99		99.9	MAS
1/2"	12.5	77.0	100	100	100	99	93	NMAS	96.4	
3/8"	9.5	29.0	100.0	100	100	98	86		89.5	
#4	4.75	2.1	35.0	67.0	99.0	95.0	69.0		68.6	
#8	2.36	1.7	3.0	40.0	66.0	91.0	55.0		45.7	
#16	1.18	1.5	2.0	26.0	41.0	82.9	44.0		31.7	
#30	0.6	1.4	1.0	18.0	24.0	60.8	33.0		21.0	
#50	0.3	1.4	0.6	13.0	13.0	15.6	18.0		11.1	
#100	0.15	1.2	0.4	9.5	5.9	2.2	9.8		6.0	
#200	0.075	1.1	0.3	7.2	2.9	1.0	6.7		3.9	
Gsb		2.691	2.691	2.683	2.671	2.624	2.624		2.671	
Abs		0.4	0.4	0.4	0.5	0.3	0.4		0.4	
F&E		2.6	1.8	1.8	1.8	1.3	0.9		1.8	
#FF		100	100	100	100	30	83		93.0	

AC Content:			NMAS 12.5
Asphalt Source:		Grade:	

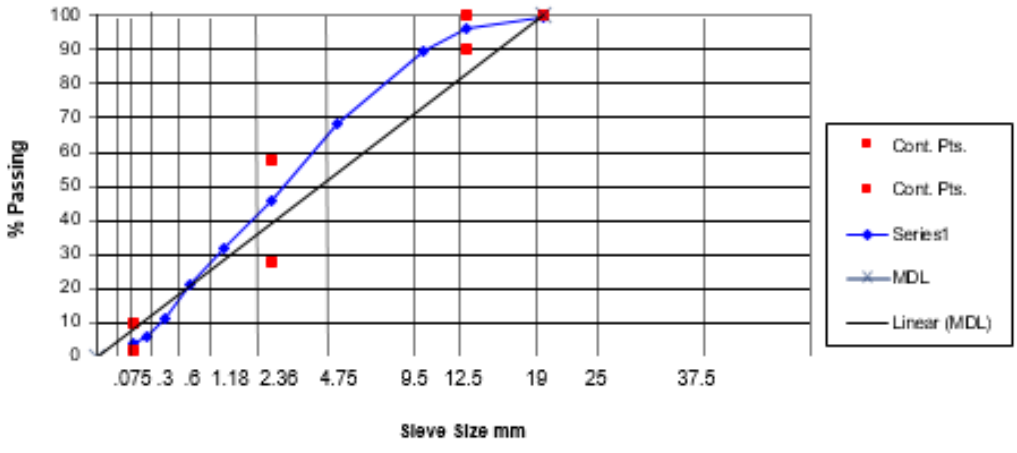

Table A-3. MT-V-28-Cisler.

Project: WHRP 0092-15-04		Spec. 12.5mm E3 Mix	Date:
Location:		TH#:	
Mix Type: MT-V-28-Cisler			

	%	Aggregate Description		Legal Description
1		#1 Stone	5/8x3/8 Bit Agg(3326)	
2		#2 Stone	3/8 Washed Chips(3237)	
3		#3 Stone	3/8 Bit Agg(3235)	
4		#4 Stone	3/16 Washed Man Sand(3403)	
5		#5 Stone	5/8 River Sand(5501)	
6		#6 Stone	STH 182 RAP(5%AC)	

Aggregate		A	B	C	D	E	6		Blend	
%Aggregate		15	10	10	20	25	20		MAS	
Sieve Size	mm	Percent Passing							NMAS	
1 1/2"	37.5	100	100	100	100	100	100		100.0	
1"	25	100	100	100	100	100	100		100.0	
3/4"	19	100.0	100	100	100	100	99		99.8	MAS
1/2"	12.5	77.0	100	100	100	99	93	NMAS	94.9	
3/8"	9.5	29.0	100.0	100	100	96	86		85.6	
#4	4.75	2.1	35.0	67.0	99.0	89.0	69.0		66.4	
#8	2.36	1.7	3.0	40.0	66.0	82.0	55.0		49.3	
#16	1.18	1.5	2.0	26.0	41.0	73.0	44.0		38.3	
#30	0.6	1.4	1.0	18.0	24.0	53.0	33.0		26.8	
#50	0.3	1.4	0.6	13.0	13.0	17.0	18.0		12.0	
#100	0.15	1.2	0.4	9.5	5.9	4.5	9.8		5.4	
#200	0.075	1.1	0.3	7.2	2.9	3.0	6.7		3.6	
Gsb		2.691	2.691	2.683	2.671	2.624	2.624		2.656	
Abs		0.4	0.4	0.4	0.5	0.3	0.4		0.4	
F&E		2.6	1.8	1.8	1.8	1.3	0.9		1.6	
#FF		100	100	100	100	30	83		79.1	

AC Content:			
		NMAS	12.5
Asphalt Source:	Grade:		

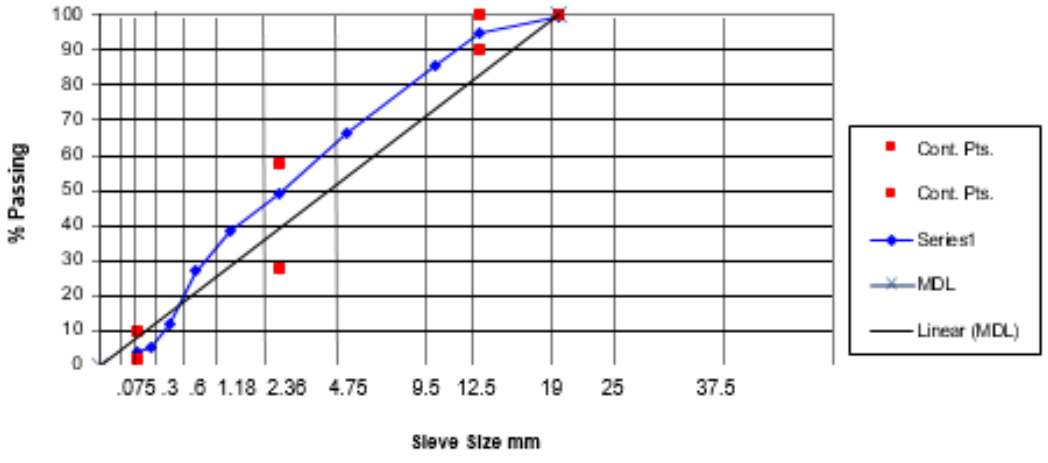

Table A-4. HT-V-28-Cisler.

Project: WHRP 0092-15-04		Spec. 12.5mm E30 Mix		Date:
Location:		TH#:		
Mix Type: HT-V-28-Cisler				

	%	Aggregate Description		Legal Description
1		#1 Stone	5/8x3/8 Bit Agg(3326)	
2		#2 Stone	3/8 Washed Chips(3237)	
3		#3 Stone	3/8 Bit Agg(3235)	
4		#4 Stone	3/16 Washed Man Sand(3403)	
5		#5 Stone	5/8 River Sand(5501)	
6		#6 Stone	STH 182 RAP(5%AC)	

Aggregate		A	B	C	D	E	6		Blend
%Aggregate		13	8	31	32	8	8		MAS
Sieve Size	mm	Percent Passing							NMAS
1 1/2"	37.5	100	100	100	100	100	100		100.0
1"	25	100	100	100	100	100	100		100.0
3/4"	19	100.0	100	100	100	100	99		99.9 MAS
1/2"	12.5	77.0	100	100	100	99	93	NMAS	96.4
3/8"	9.5	29.0	100.0	100	100	98	86		89.5
#4	4.75	2.1	35.0	67.0	99.0	95.0	69.0		68.6
#8	2.36	1.7	3.0	40.0	66.0	91.0	55.0		45.7
#16	1.18	1.5	2.0	26.0	41.0	82.9	44.0		31.7
#30	0.6	1.4	1.0	18.0	24.0	60.8	33.0		21.0
#50	0.3	1.4	0.6	13.0	13.0	15.6	18.0		11.1
#100	0.15	1.2	0.4	9.5	5.9	2.2	9.8		6.0
#200	0.075	1.1	0.3	7.2	2.9	1.0	6.7		3.9
	Gsb	2.691	2.691	2.683	2.671	2.624	2.624		2.671
	Abs	0.4	0.4	0.4	0.5	0.3	0.4		0.4
	F&E	2.6	1.8	1.8	1.8	1.3	0.9		1.8
	#FF	100	100	100	100	30	83		93.0

AC Content:		NMAS	12.5
Asphalt Source:	Grade:		

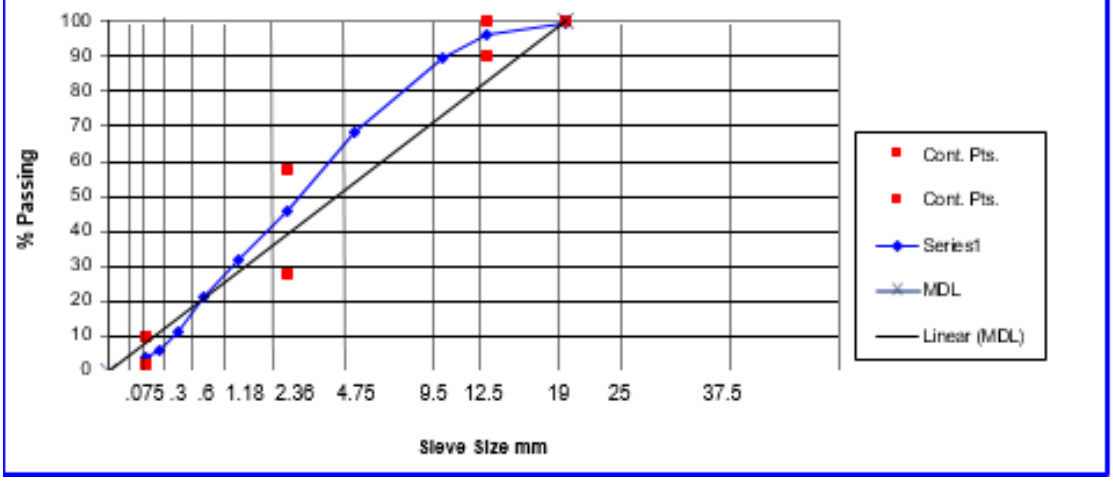

Table A-5. MT-S-28-Waukesha.

Project: WHRP 0092-15-04		Spec. 12.5mm E3 Mix	Date:
Location:		TH#:	
Mix Type: MT-S-28-Waukesha			

	%	Aggregate Description		Legal Description
1		#1 Stone	**5/8" Chips**	
2		#2 Stone	**3/8" Chips**	
3		#3 Stone	**MFG'D Sand**	
4		#4 Stone	**Natural Sand**	
5		#5 Stone	**DEG**	
6		#6 Stone	**FRAP**	

Aggregate		A	B	C	D	E	6		Blend
%Aggregate		11	9	20	40	2	18		MAS
Sieve Size	mm	Percent Passing							NMAS
1 1/2"	37.5	100	100	100	100	100	100		100.0
1"	25	100	100	100	100	100	100		100.0
3/4"	19	100.0	100	100	100	100	100		100.0 MAS
1/2"	12.5	84.9	100	100	100	100	100	NMAS	98.3
3/8"	9.5	16.0	92.6	100	100	100	96.3		89.4
#4	4.75	2.1	5.8	88.3	96.5	100	72.6		72.1
#8	2.36	1.5	1.8	50.4	86.3	100	53.6		56.6
#16	1.18	1.3	1.6	32.8	73.8	100	41.3		45.8
#30	0.6	1.2	1.4	15.7	61.7	100	29.2		35.3
#50	0.3	1.2	1.3	9.5	22.1	100	20.1		16.6
#100	0.15	1.1	1.2	5.4	3.9	100	14.9		7.6
#200	0.075	1.0	1.1	3.3	1.8	100	12.4		5.8
Gsb		2.777	2.764	2.733	2.668	2.697	2.697		2.707
Abs		0.4	0.4	0.4	0.5	0.3	0.4		0.4
F&E		2.6	1.8	1.8	1.8	1.3	0.9		1.7
#FF		100	100	100	100	30	83		95.5

AC Content:			NMAS 12.5
Asphalt Source:		Grade:	

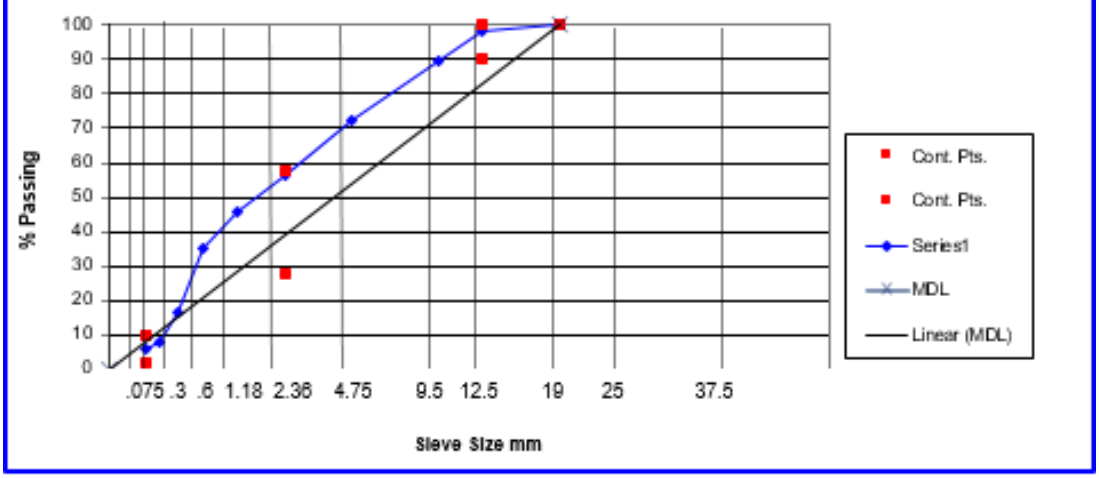

Table A-6. HT-S-28-Waukesha.

Project: WHRP 0092-15-04	Spec. 12.5mm E30 Mix	Date:
Location:	TH#:	
Mix Type: HT-S-28-Waukesha		

	%	Aggregate Description		Legal Description
1		#1 Stone	5/8" Chips	
2		#2 Stone	3/8" Chips	
3		#3 Stone	MFG'D Sand	
4		#4 Stone	Natural Sand	
5		#5 Stone	DEG	
6		#6 Stone	STH 182 RAP(5%AC)	

Aggregate		A	B	C	D	E	6	Blend	
%Aggregate		11	11	43	24	1	10	MAS	
Sieve Size	mm	Percent Passing						NMAS	
1 1/2"	37.5	100	100	100	100	100		90.0	
1"	25	100	100	100	100	100		90.0	MAS
3/4"	19	100.0	100	100	100	100		90.0	
1/2"	12.5	81.5	100	100	100	100		88.0	
3/8"	9.5	16.0	91.6	100	100	100		79.8	
#4	4.75	2.3	3.9	88.3	92.4	100		61.8	
#8	2.36	1.6	2.2	50.4	77.1	100		41.6	
#16	1.18	1.2	1.8	28.1	63.6	100		28.7	
#30	0.6	1.2	1.6	15.7	47.2	100		19.4	
#50	0.3	1.2	1.4	9.5	15.9	100		9.2	
#100	0.15	1.1	1.3	5.4	1.6	100		4.0	
#200	0.075	1.0	1.2	3.3	7.0	100		4.3	
Gsb		2.763	2.756	2.733	2.671	2.671	2.68	2.718	
Abs		0.4	0.4	0.4	0.5	0.3	0.4	0.4	
F&E		2.6	1.8	1.8	1.8	1.3	0.9	1.8	
#FF		100	100	100	100	30	83	97.6	

NMAS

AC Content:			NMAS	12.5
Asphalt Source:		Grade:		

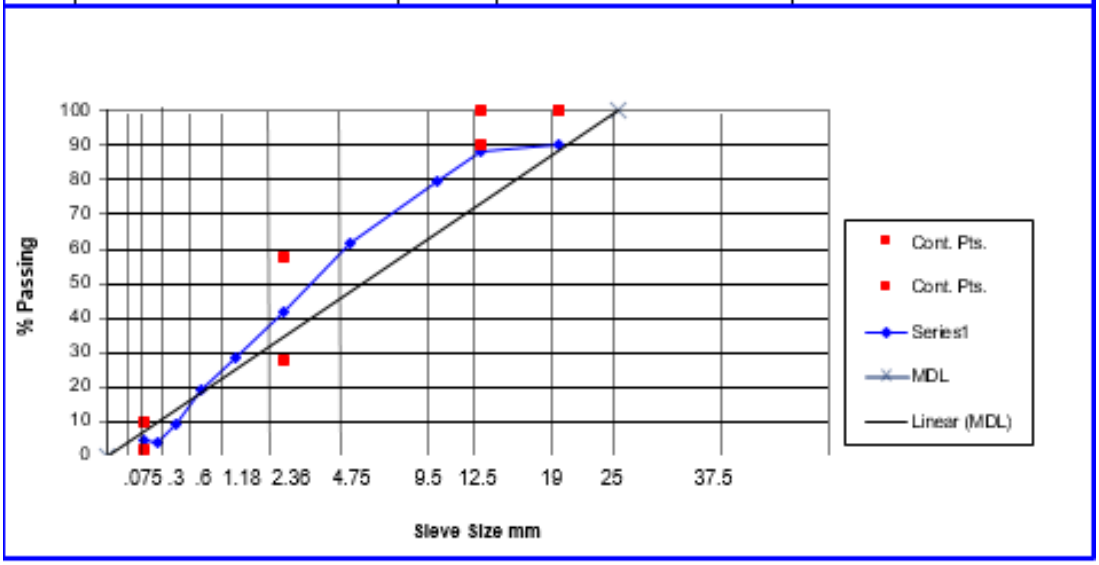

Table A-7. MT-V-28-Waukesha.

Project: WHRP 0092-15-04	Spec. 12.5mm E3 Mix	Date:
Location:	TH#:	
Mix Type: MT-V-28-Waukesha		

	%	Aggregate Description		Legal Description
1		#1 Stone	5/8" Chips	
2		#2 Stone	3/8" Chips	
3		#3 Stone	MFG'D Sand	
4		#4 Stone	Natural Sand	
5		#5 Stone	DEG	
6		#6 Stone	FRAP	

Aggregate		A	B	C	D	E	6		Blend
%Aggregate		11	9	20	40	2	18		MAS
Sieve Size	mm	Percent Passing							NMAS
1 1/2"	37.5	100	100	100	100	100	100		100.0
1"	25	100	100	100	100	100	100		100.0
3/4"	19	100.0	100	100	100	100	100		100.0
1/2"	12.5	84.9	100	100	100	100	100	NMAS	98.3
3/8"	9.5	16.0	92.6	100	100	100	96.3		89.4
#4	4.75	2.1	5.8	88.3	96.5	100	72.6		72.1
#8	2.36	1.5	1.8	50.4	86.3	100	53.6		56.6
#16	1.18	1.3	1.6	32.8	73.8	100	41.3		45.8
#30	0.6	1.2	1.4	15.7	61.7	100	29.2		35.3
#50	0.3	1.2	1.3	9.5	22.1	100	20.1		16.6
#100	0.15	1.1	1.2	5.4	3.9	100	14.9		7.6
#200	0.075	1.0	1.1	3.3	1.8	100	12.4		5.8
Gsb		2.777	2.764	2.733	2.668	2.697	2.697		2.707
Abs		0.4	0.4	0.4	0.5	0.3	0.4		0.4
F&E		2.6	1.8	1.8	1.8	1.3	0.9		1.7
#FF		100	100	100	100	30	83		95.5

MAS

AC Content:		NMAS	12.5
Asphalt Source:	Grade:		

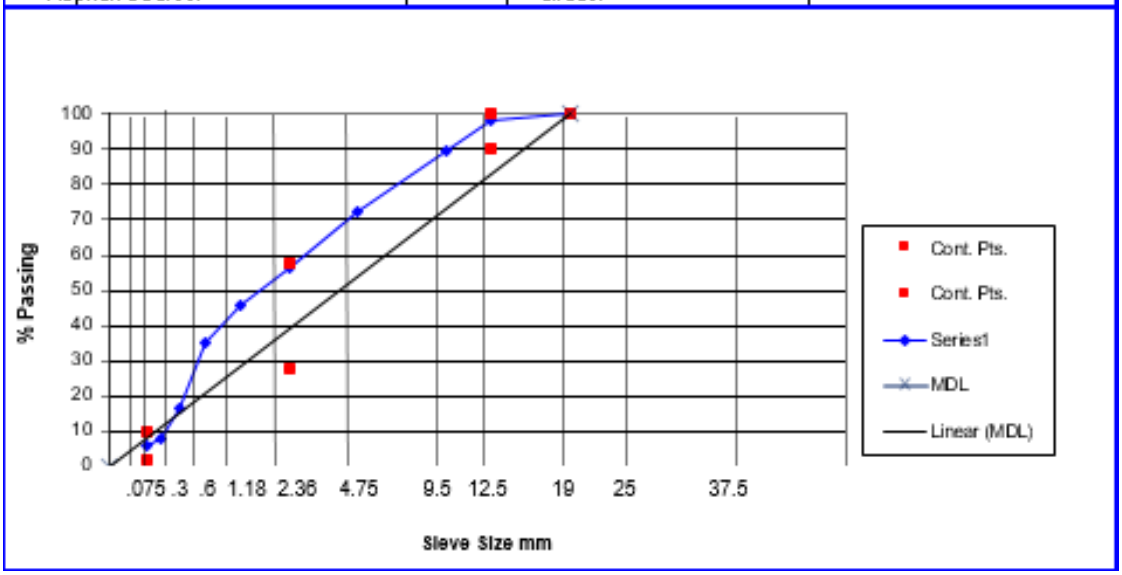

Table A-8. HT-V-28-Waukesha.

Project: WHRP 0092-15-04	Spec. 12.5mm E30 Mix	Date:
Location:	TH#:	
Mix Type: HT-V-28-Waukesha		

	%	Aggregate Description		Legal Description
1		#1 Stone	5/8" Chips	
2		#2 Stone	3/8" Chips	
3		#3 Stone	MFG'D Sand	
4		#4 Stone	Natural Sand	
5		#5 Stone	DEG	
6		#6 Stone	STH 182 RAP(5%AC)	

Aggregate		A	B	C	D	E	6	Blend	
%Aggregate		11	11	43	24	1	10	MAS	
Sieve Size	mm	Percent Passing						NMAS	
1 1/2"	37.5	100	100	100	100	100		90.0	
1"	25	100	100	100	100	100		90.0	MAS
3/4"	19	100.0	100	100	100	100		90.0	
1/2"	12.5	81.5	100	100	100	100		88.0	
3/8"	9.5	16.0	91.6	100	100	100		79.8	
#4	4.75	2.3	3.9	88.3	92.4	100		61.8	
#8	2.36	1.6	2.2	50.4	77.1	100		41.6	
#16	1.18	1.2	1.8	28.1	63.6	100		28.7	
#30	0.6	1.2	1.6	15.7	47.2	100		19.4	
#50	0.3	1.2	1.4	9.5	15.9	100		9.2	
#100	0.15	1.1	1.3	5.4	1.6	100		4.0	
#200	0.075	1.0	1.2	3.3	7.0	100		4.3	
	Gsb	2.763	2.756	2.733	2.671	2.671	2.68	2.718	
	Abs	0.4	0.4	0.4	0.5	0.3	0.4	0.4	
	F&E	2.6	1.8	1.8	1.8	1.3	0.9	1.8	
	#FF	100	100	100	100	30	83	97.6	

NMAS (Blend): 90.0 / 90.0 / 90.0 / 88.0 / 79.8 / 61.8 / 41.6 / 28.7 / 19.4 / 9.2 / 4.0 / 4.3

AC Content:		NMAS	12.5
Asphalt Source:	Grade:		

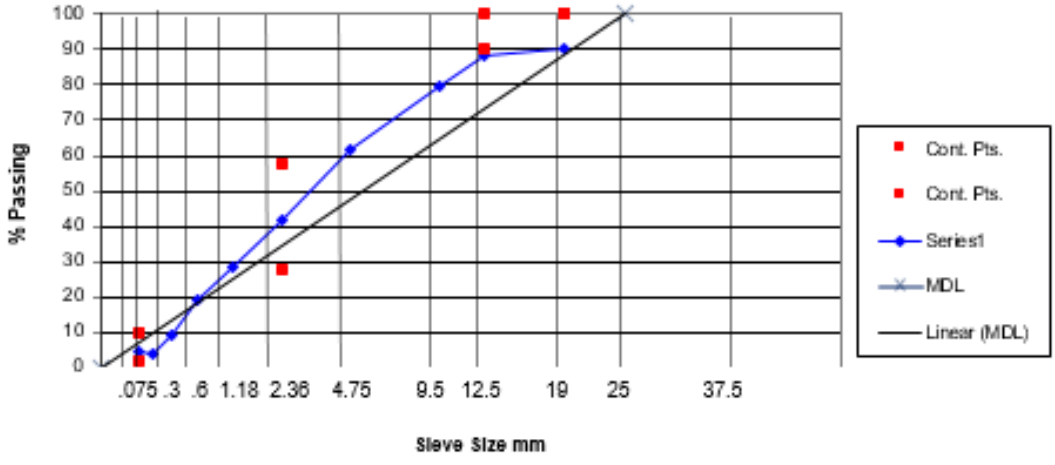

APPENDIX B: Image of Hamburg Wheel Tracking Test Samples

Figure B-1. The E-3 Mix in Experiment 1 and 2 after Dry HWT Testing.

Figure B-2. The E-10 Mix in Experiment 1 and 2 after Dry HWT Testing.

Figure B-3. The Example of Cisler Mixes after Dry HWT Testing.

APPENDIX C: The HWT Curve Fitted by Francken Model.

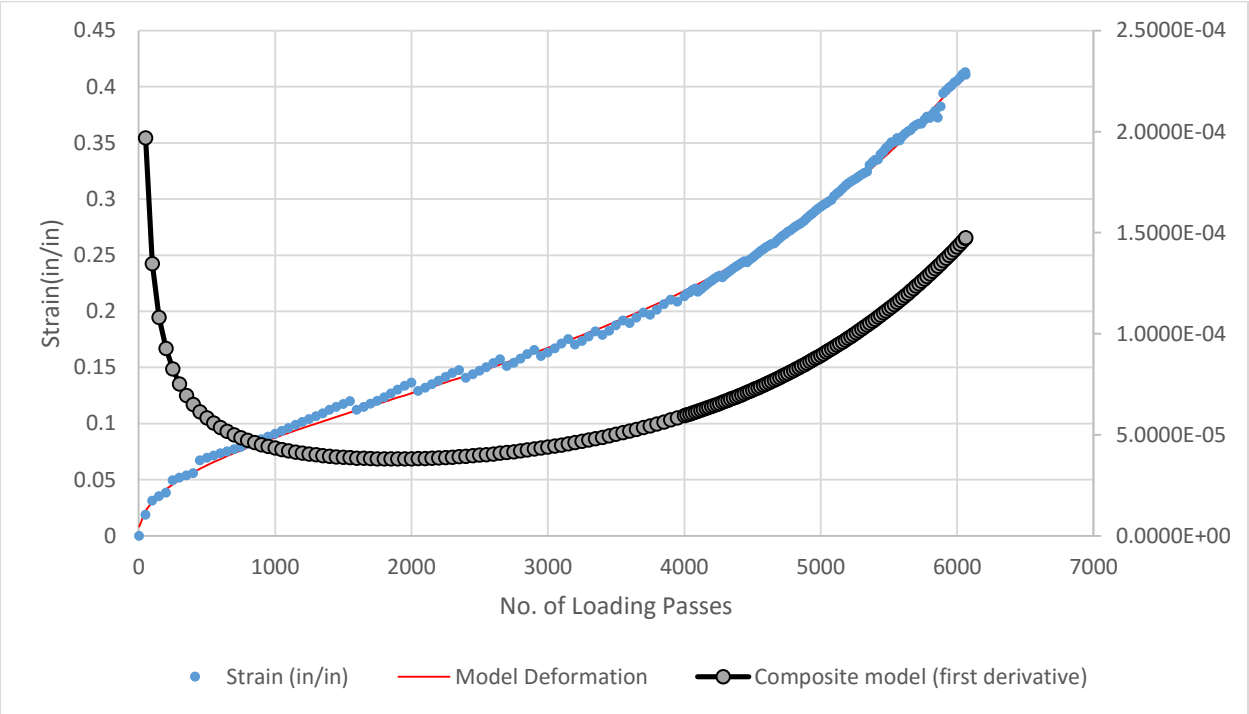

Figure C-1. MT-S-28-Cisler Wet Condition

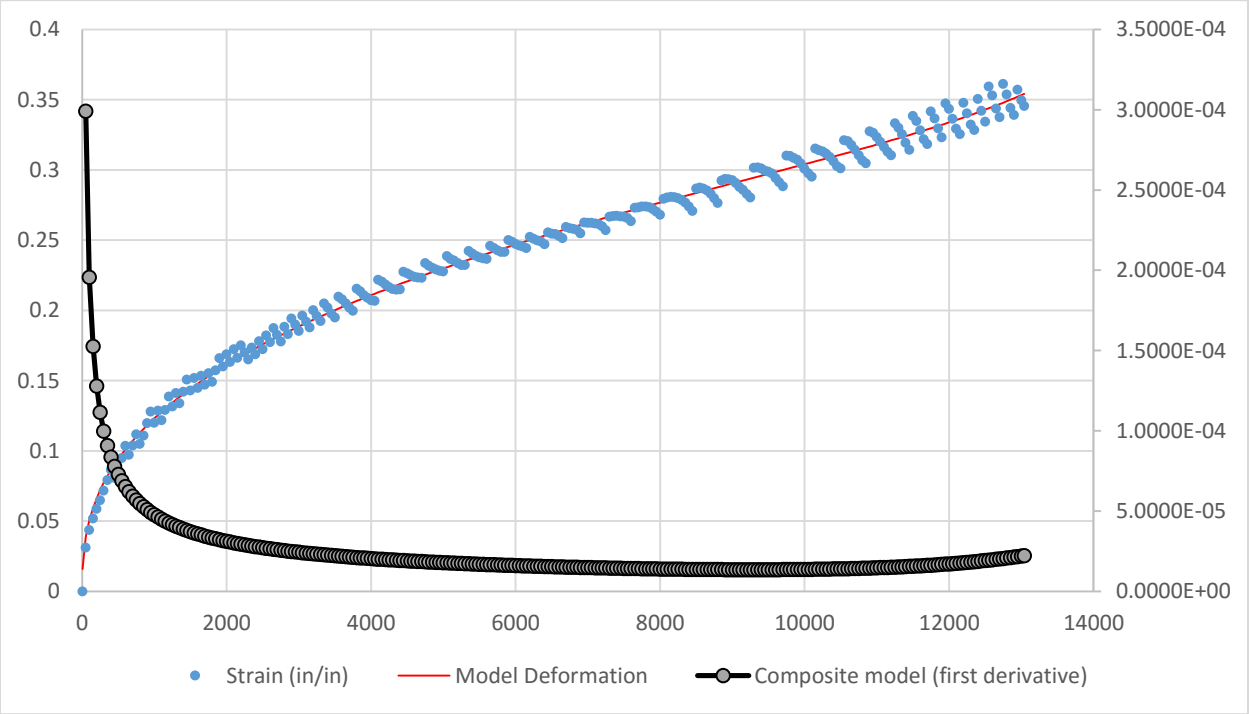

Figure C-2. MT-S-28-Cisler Dry Condition

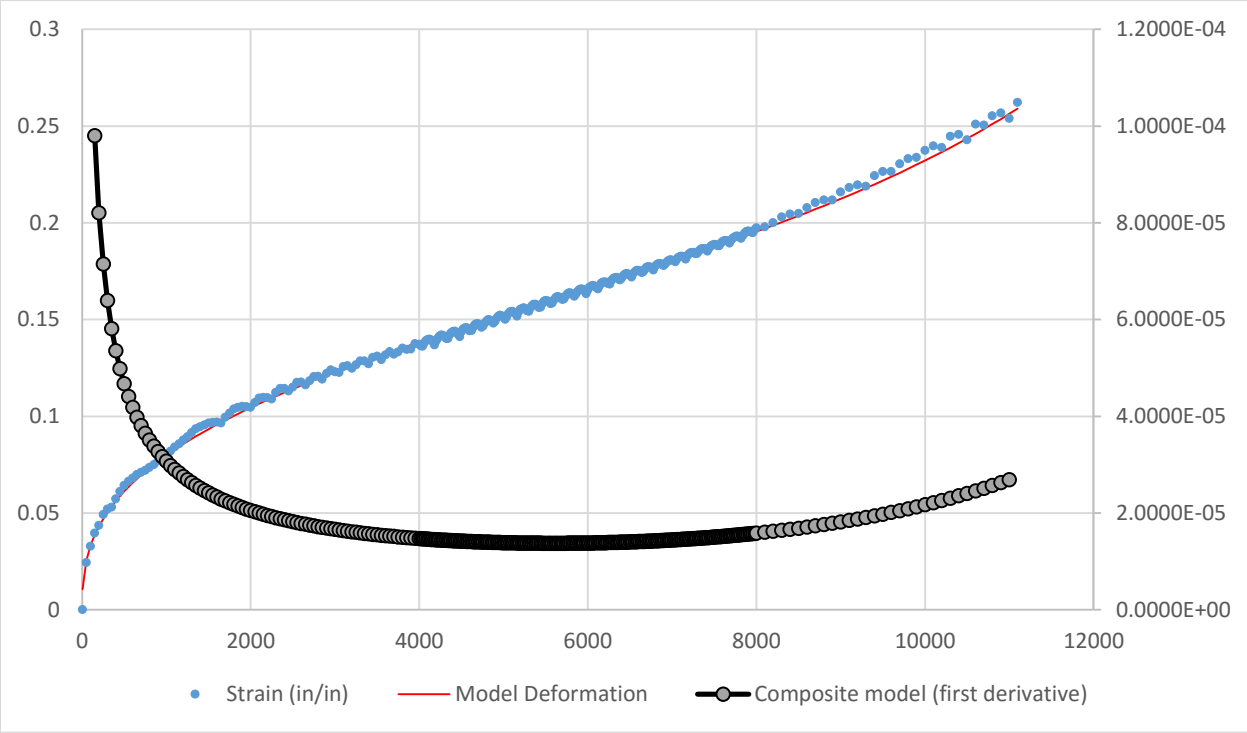

Figure C-3. MT-V-28-Cisler Wet Condition

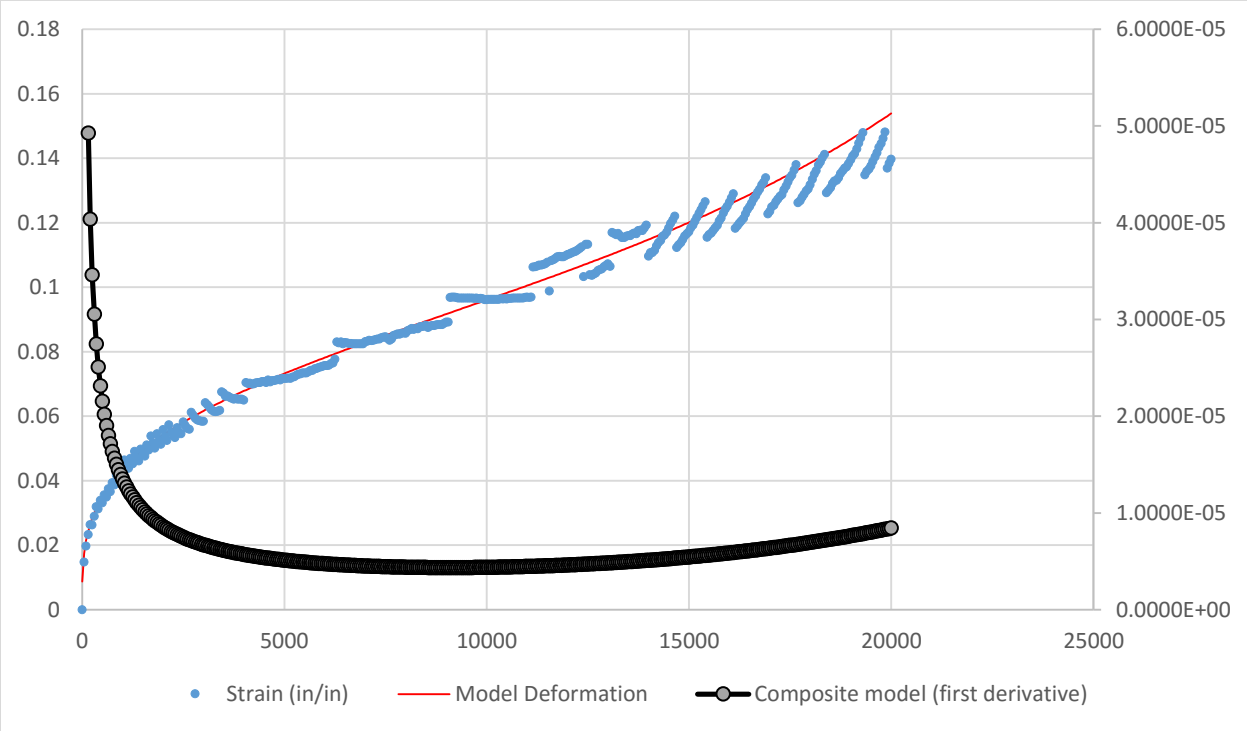

Figure C-4. MT-V-28-Cisler Dry Condition

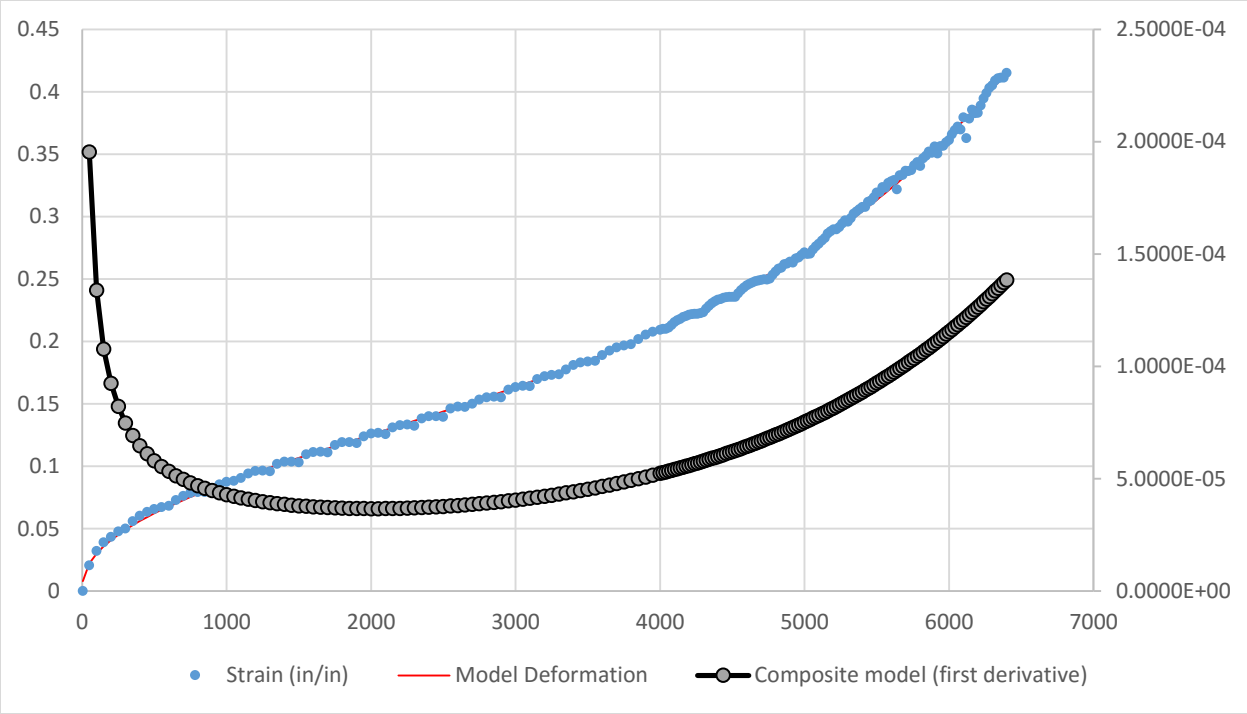

Figure C-5. HT-S-28-Cisler Wet Condition

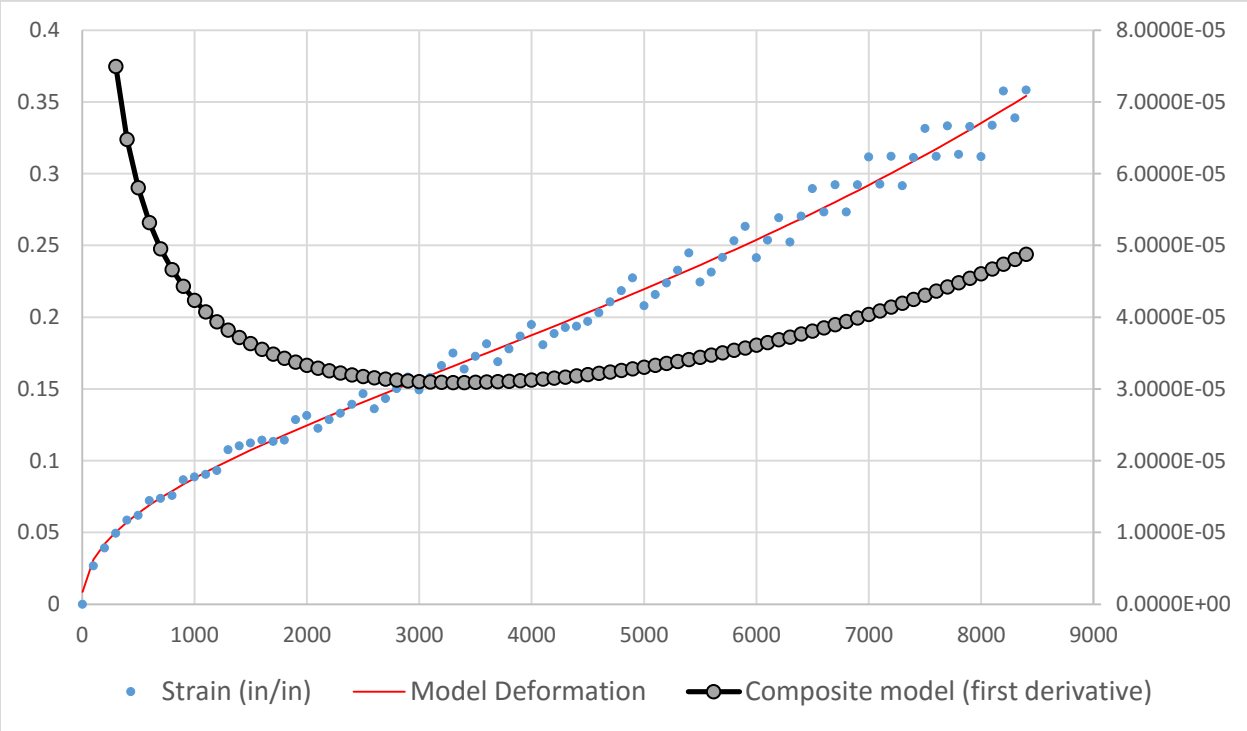

Figure C-6. HT-S-28-Cisler Dry Condition

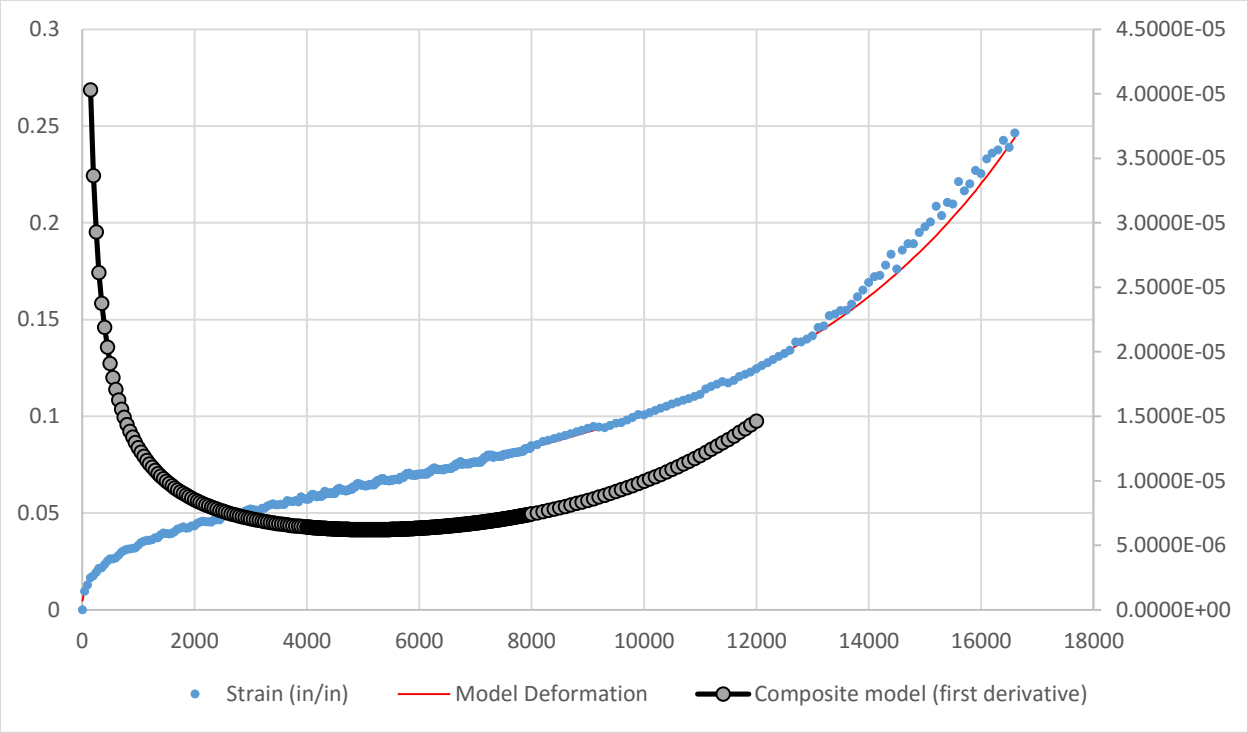

Figure C-7. HT-V-28-Cisler Wet Condition

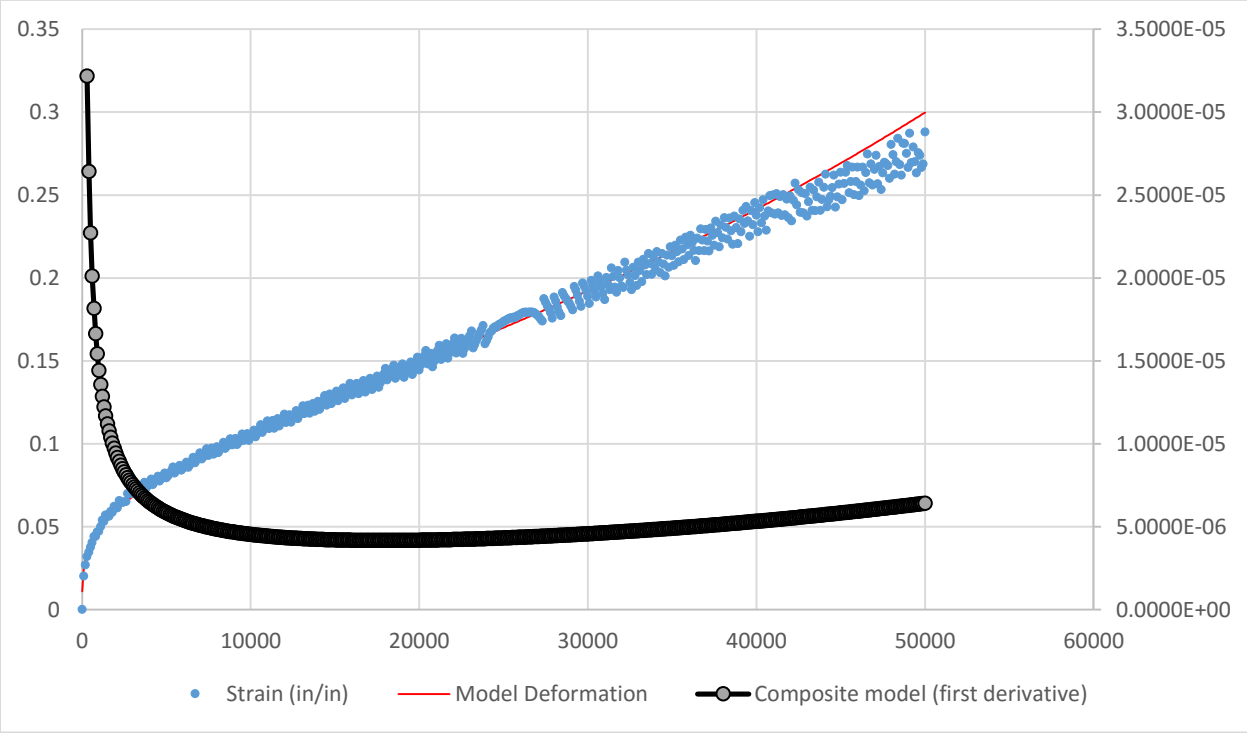

Figure C-8 HT-V-28-Cisler Dry Condition

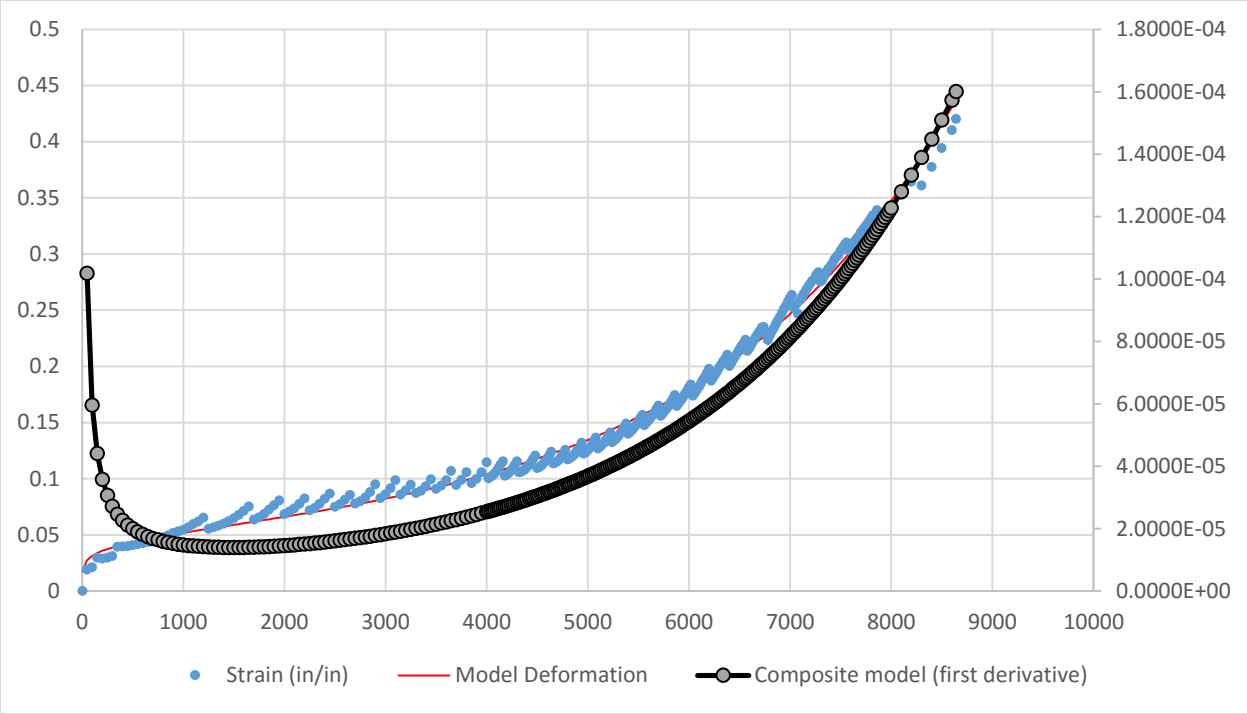

Figure C-9. MT-S-28-Waukesha Wet Condition

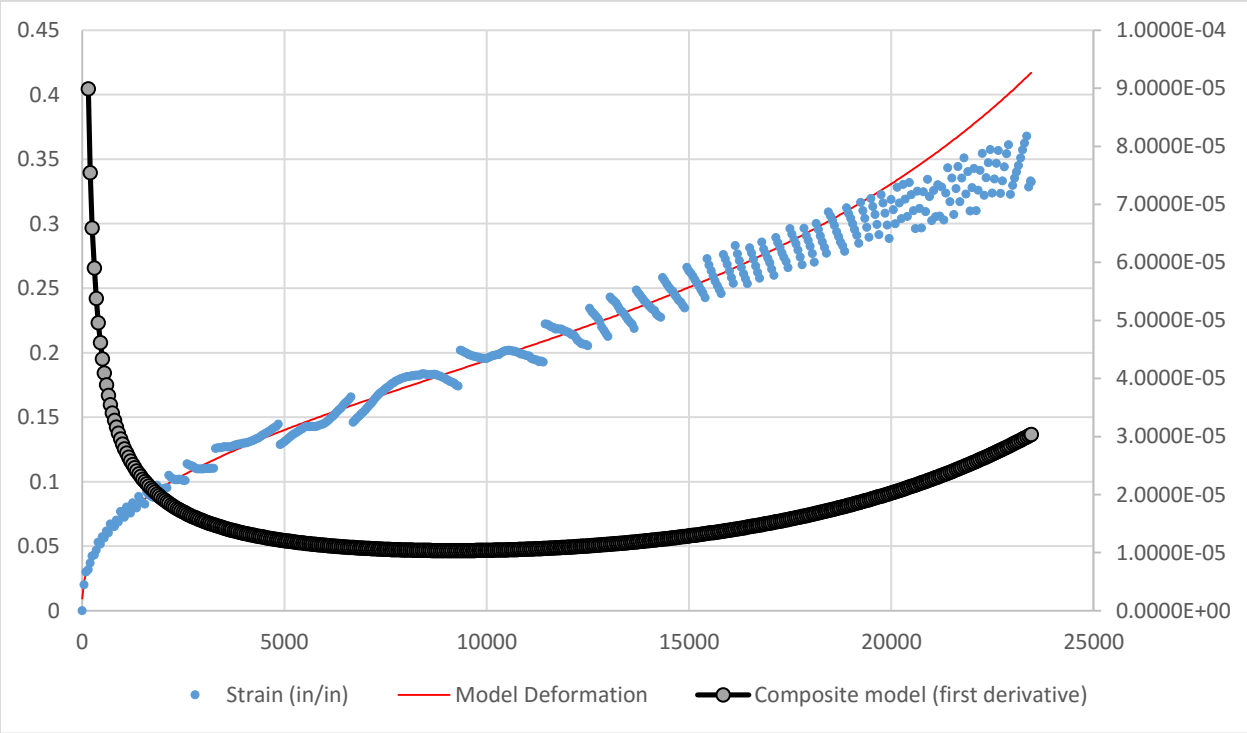

Figure C-10. MT-S-28-Waukesha Dry Condition

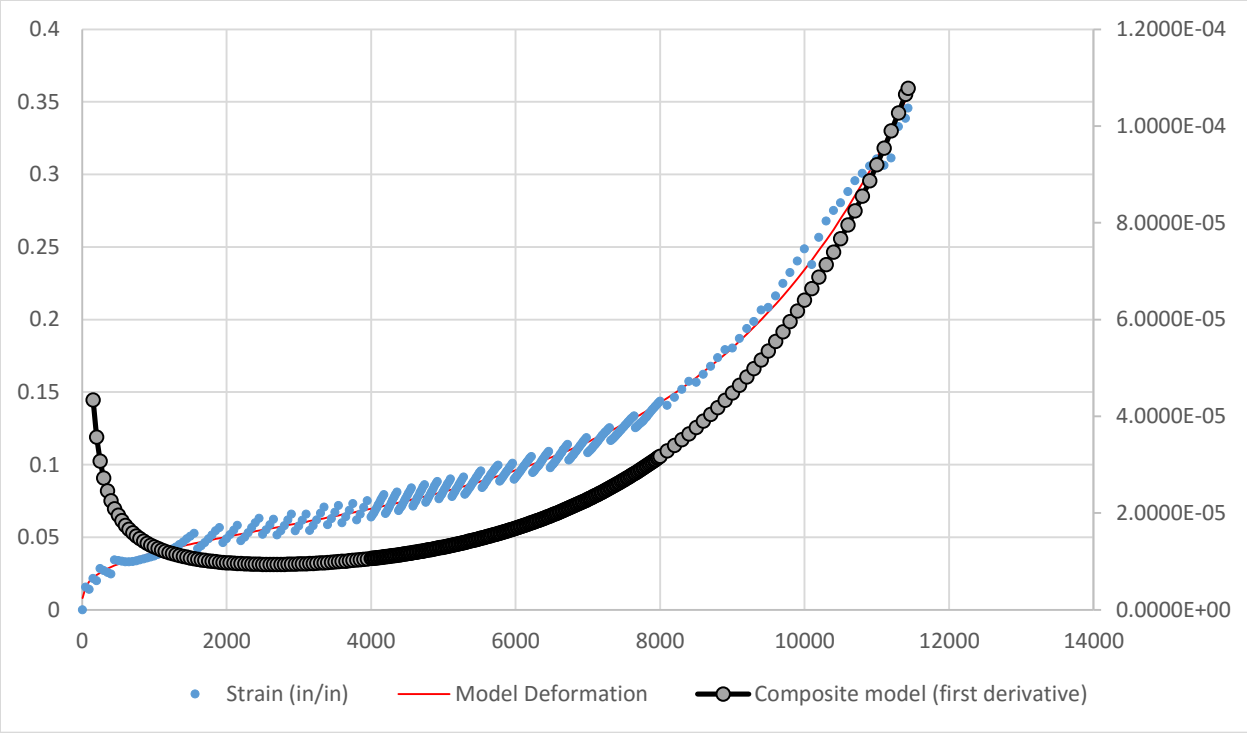

Figure C-11. MT-V-28-Waukesha Wet Condition

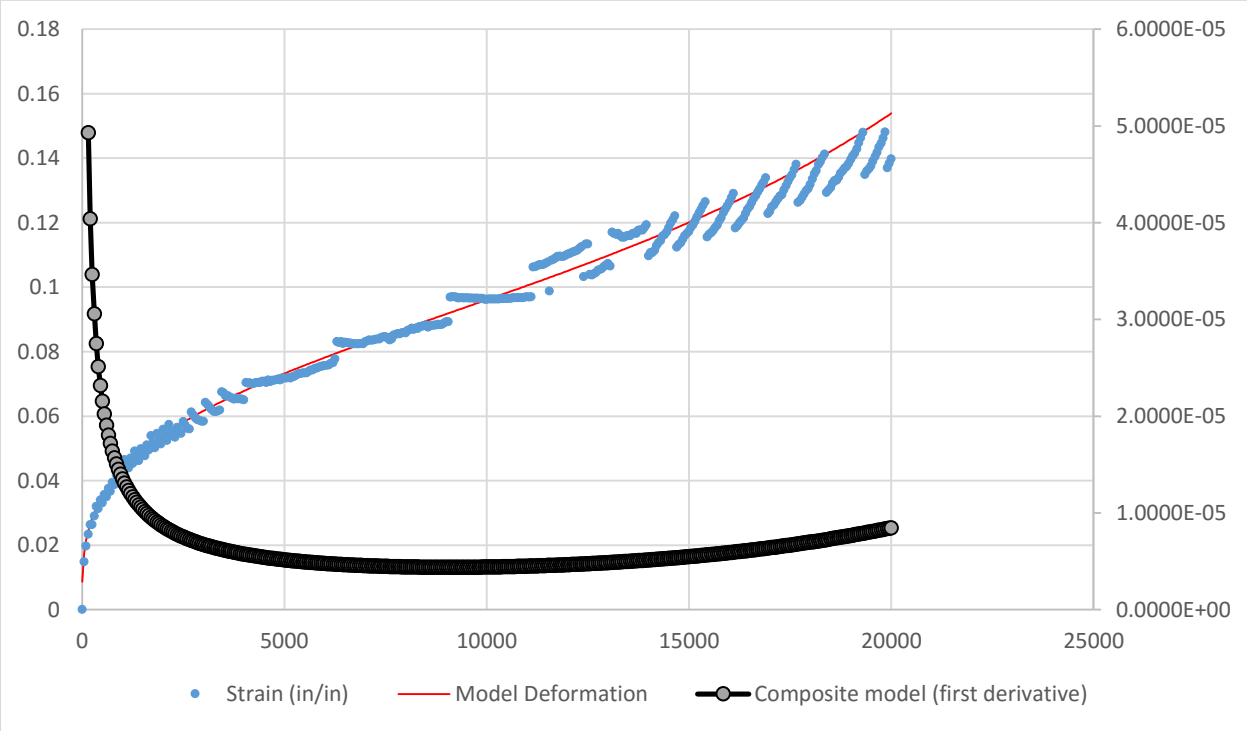

Figure C-12. MT-V-28-Waukesha Dry Condition

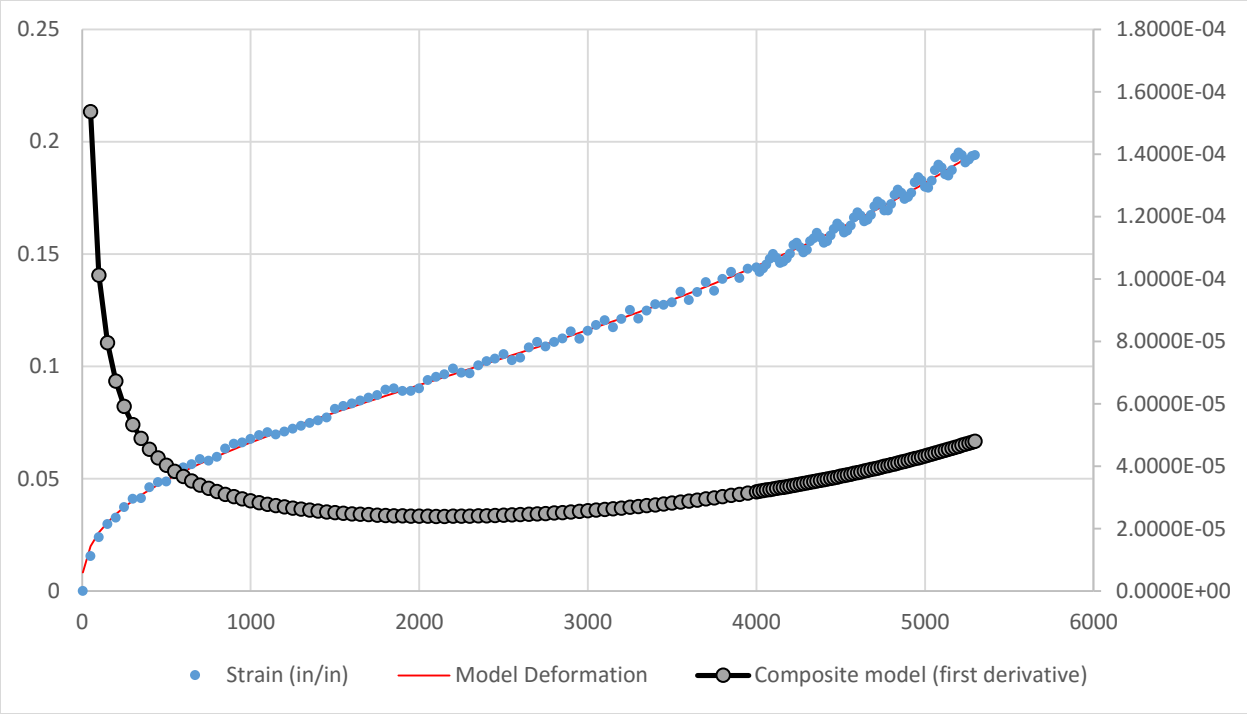

Figure C-13. HT-S-28-Waukesha Wet Condition

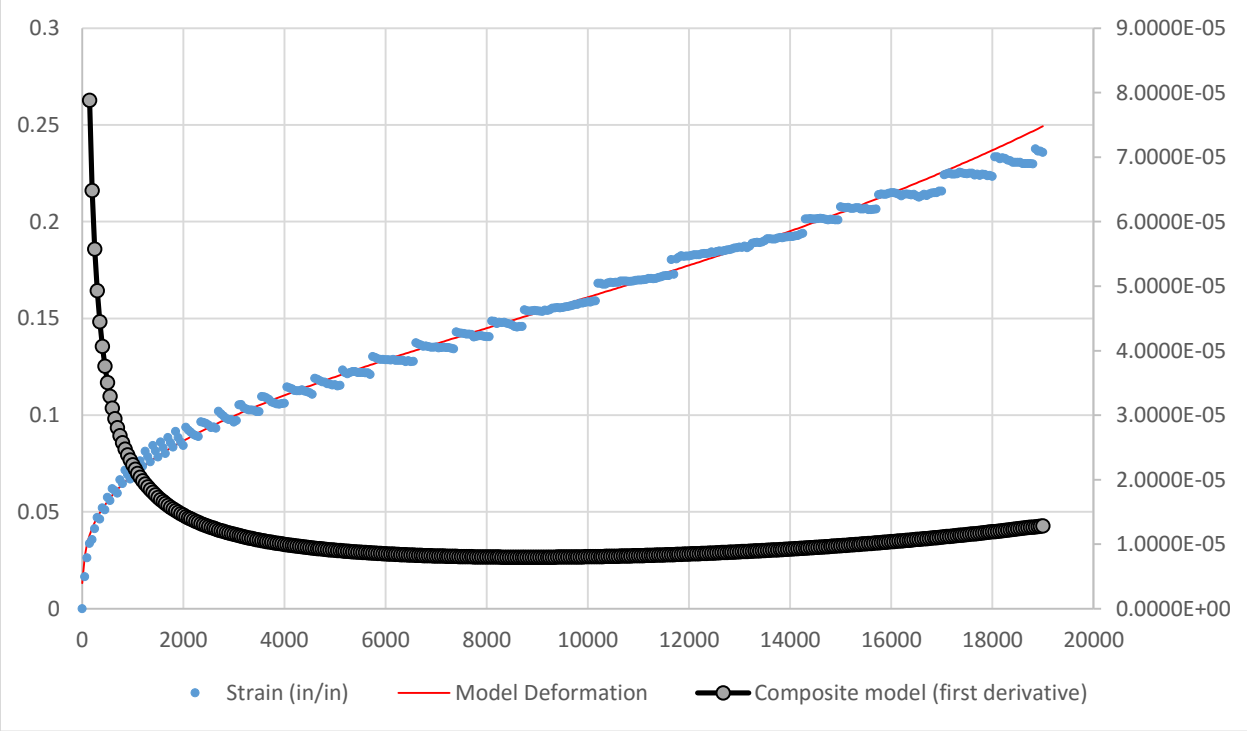

Figure C-14. HT-S-28-Waukesha Dry Condition

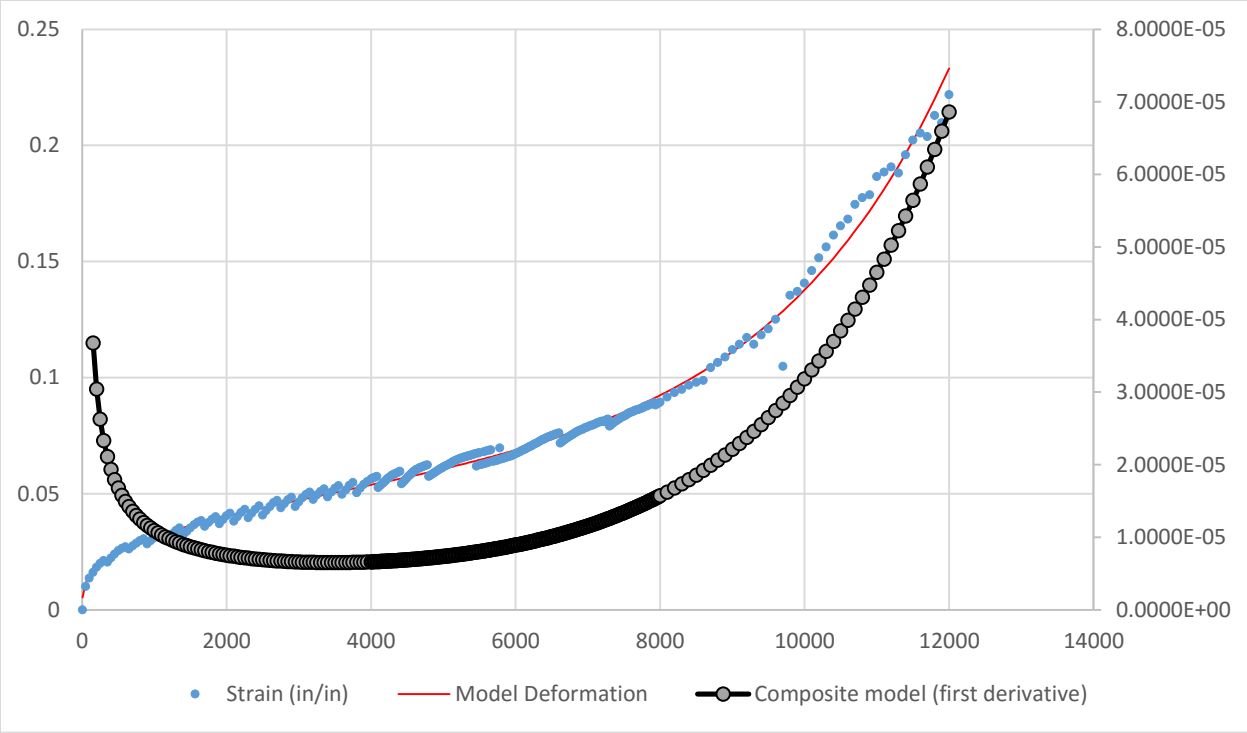

Figure C-15. HT-V-28-Waukesha Wet Condition

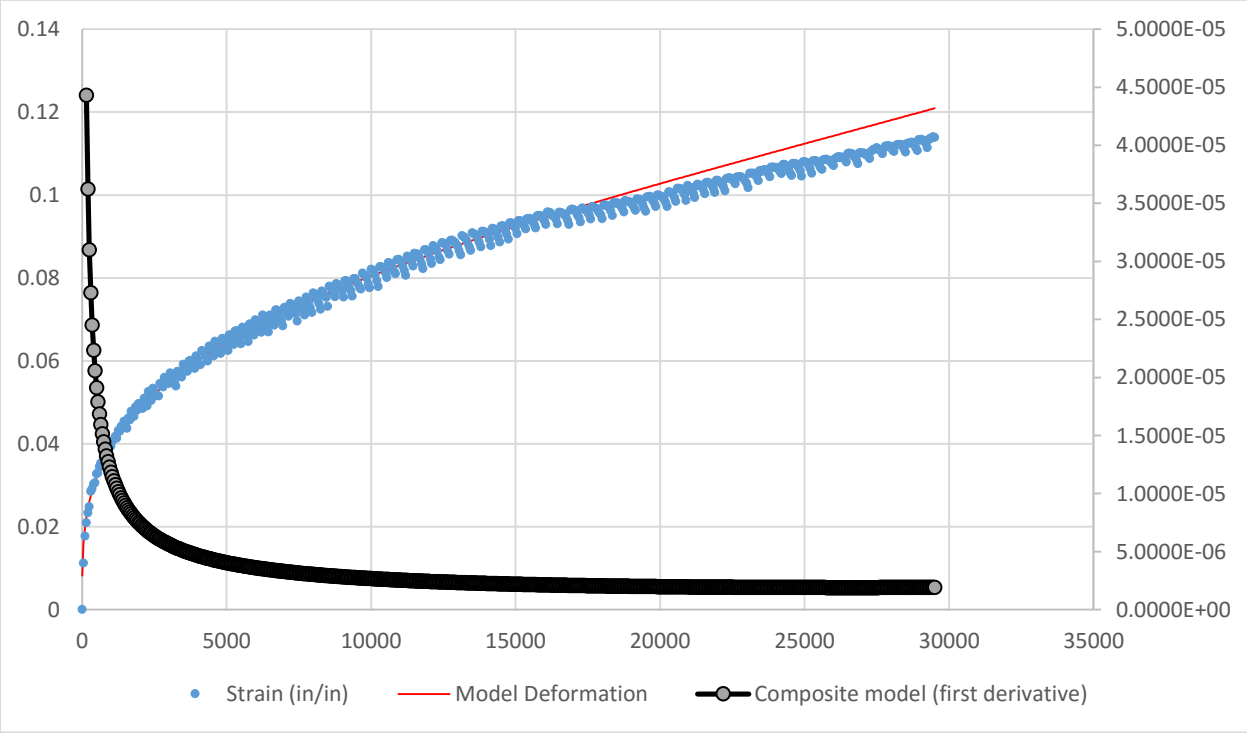

Figure C-16. HT-V-28-Waukesha Dry Conditio